

Channel Characterization of Radio Links in the Southern Region of Saudi Arabia

by

Usamah M. Adnan Al-Naser

A Thesis Presented to the

FACULTY OF THE COLLEGE OF GRADUATE STUDIES

KING FAHD UNIVERSITY OF PETROLEUM & MINERALS

DHAHRAN, SAUDI ARABIA

In Partial Fulfillment of the
Requirements for the Degree of

MASTER OF SCIENCE

In

ELECTRICAL ENGINEERING

January, 1993

INFORMATION TO USERS

This manuscript has been reproduced from the microfilm master. UMI films the text directly from the original or copy submitted. Thus, some thesis and dissertation copies are in typewriter face, while others may be from any type of computer printer.

The quality of this reproduction is dependent upon the quality of the copy submitted. Broken or indistinct print, colored or poor quality illustrations and photographs, print bleedthrough, substandard margins, and improper alignment can adversely affect reproduction.

In the unlikely event that the author did not send UMI a complete manuscript and there are missing pages, these will be noted. Also, if unauthorized copyright material had to be removed, a note will indicate the deletion.

Oversize materials (e.g., maps, drawings, charts) are reproduced by sectioning the original, beginning at the upper left-hand corner and continuing from left to right in equal sections with small overlaps. Each original is also photographed in one exposure and is included in reduced form at the back of the book.

Photographs included in the original manuscript have been reproduced xerographically in this copy. Higher quality 6" x 9" black and white photographic prints are available for any photographs or illustrations appearing in this copy for an additional charge. Contact UMI directly to order.

U·M·I

University Microfilms International
A Bell & Howell Information Company
300 North Zeeb Road, Ann Arbor, MI 48106-1346 USA
313/761-4700 800/521-0600

Order Number 1354073

**Channel characterization of radio links in the southern region of
Saudi Arabia**

Al-Naser, Usamah M. Adnan, M.S.

King Fahd University of Petroleum and Minerals (Saudi Arabia), 1993

U·M·I
300 N. Zeeb Rd.
Ann Arbor, MI 48106

**CHANNEL CHARACTERIZATION
OF RADIO LINKS IN THE
SOUTHERN REGION OF SAUDI
ARABIA**

BY

USAMAH M. ADNAN AL-NASER

ELECTRICAL ENGINEERING

JULY 1993

KING FAHD UNIVERSITY OF PETROLEUM & MINERALS

DHAHARAN, SAUDI ARABIA

This thesis, was written by USAMAN M. A. AL-NASER under the direction of his Thesis Advisor, and approved by his Thesis Committee, has been presented and accepted by the College of Graduate studies, in partial fulfillment of the requirements for the degree of

MASTER OF SCIENCE IN ELECTRICAL ENGINEERING

Thesis Committee


Chairman (Dr. K. M. Biyari)


Co-chairman (Dr. T. Halawani)


Member (Dr. M. Dawoud)

23.6.93

Member (Dr. S. Abdul-Jawad)


Member (Dr. M. S. El-Hennawy)


Department Chairman


Dean College of Graduate Studies

Date : 26.6.93



***To my beloved parants, brothers, and sisters;
to those who shared their care and concern***

ACKNOWLEDGMENT

First of all, praise be to **ALLAH** whose help made it possible to complete this study.

Acknowledgment is due to King Fahd University of Petroleum and Minerals for support of this research. Also, we appreciate the cooperation and the facilities provided by the Saudi Arabian Ministry of PTT and by the Detatsad company.

I gratefully acknowledge the help given to me by Dr. Khaled Biyari. Without his careful and inspired criticism and his wise patience, this project would have lacked such merit as it now possesses. I wish to express my deep appreciation to Dr. Abdallah Al-Shehri for his generous support during the course of this work. Also, I would like to express my sincere gratitude and appreciation to Dr. Talal Halawani, my thesis co-advisor, and to the other committee members, Dr. Mahmoud Dowoud, Dr. Samir Abdul-Jauwad, and Dr. M. Samy El-Hennawey, for their valuable suggestions and helpful remarks.

Thanks to all my friends and colleagues for their encouragement and help. Special thanks to Eng. Ali Al-Sahrahi, Eng. Raed Al-Naser, Mr. Hamoud Al-Obaid, and Mr. Muhammed Mimesh, for their practical and technical support.

خلاصة الرسالة

اسم الطالب : أسامة محمد محمد علي النصور
عنوان الرسالة : تصنيف قوت لبث الميكرويفي في المنطقة الجنوبية من المملكة العربية السعودية
التخصص : الهندسة الكهربائية
تاريخ الدرجة : المحرم من ١٤١٤ هـ الموافق يوليو ١٩٩٣ م

إن تصنيف قوت لبث الميكرويفي التي تتميز بشوقية التغيرات الزمنية هام جدا لصلابت نتيج أداء وتصميم هذه القوت . ومن المعروف أن غالب قوت لبث الميكرويفي تعاني من ظاهرة تضلزل الموجات بسبب تشتتها واختلاف التغيرات الحاصلة لها في الزمن والتردد بسبب تغيرات التضاريس والمناخ لمناطق التراسل والتي تؤدي في بعض الاحيان لتلاشي الموجات تملأا.

ويكمن الهدف الاساسي من هذه الدراسة في إيجاد نموذج إحصائي مناسب لقوت لبث في المنطقة الجنوبية من السعودية ، وذلك لتصين أداء بث هذه القوت. ومن النتائج التي تتوصل اليها هذه الدراسة تقدير الزمن الحقيقي لتواجد هذه القوت في الخدمة وحساب مقدار احتمال تضلزل الموجات. كما تعطي الدراسة بعض التطبيقات العملية والعلمية لهذه النتائج.

مدرجة الماجستير في العلوم
جامعة الملك فهد للبترول والمعادن
الظهران - المملكة العربية السعودية
المحرم من ١٤١٤ هـ / يوليو ١٩٩٣ م

THESIS ABSTRACT

NAME : Usamah M. Adnan Al-Naser

**TITLE : Channel Characterization of Radio Links in
the Southern Region of Saudi Arabia**

MAJOR : Electrical Engineering

Date : July 1993

The characterization of channels having randomly time varying response is important for system performance analysis and design. In particular, such characterization is needed for the performance evaluation over many radio fading channels. Those channels exhibit a multipath nature of signal propagation causing destructive or constructive interference to the signal which leads at some instances to the loss of the signal completely.

The main objective of this thesis is to find a suitable statistical model of some radio channels in the Southern Region of Saudi Arabia. When incorporated into the system design, these models should help in improving the performance of the system. The appropriate statistical models, the fade depth statistics, and the fading characteristics are found for some links in the region. Moreover, discussions regarding the physical interpretation of these results are presented.

MASTER OF SCIENCE DEGREE

KING FAHD UNIVERSITY OF PETROLEUM AND MINERALS

Dhahran, Saudi Arabia

July 1993

TABLE OF CONTENTS

Abstract (Arabic)	v
Abstract (English)	vi
List of Tables	x
List of Figures	xi
List of Acronyms	xiii
1. INTRODUCTION	1
1.1 Overview	1
1.2 Thesis Objectives	2
1.3 Literature Review	4
1.4 Thesis Organization	10
1.4.1 Test Path Parameters	10
1.4.2 Equipments and Experiments	11
1.4.3 Data Analysis and Modeling	12
1.5 Summary	15
2. Models of Fading Channels	16
2.1 Introduction	16
2.2 Channel Classification	17
2.2.1 Paths with Weak Reflectors	20
2.2.2 Paths with Strong Reflectors	23
2.2.3 Paths with Rain and Storms	24
2.2.4 Propagation Losses	26
2.2.4.1 Free Space Losses	27
2.2.4.2 Atmospheric Gases Losses	27
2.2.4.3 Diffraction Losses	28
PART I. Paths with weak reflectors	29
A. Fade Depth Statistics for small Percentage of Time	29
B. Fade Depth Statistics for various Percentage of time	32
C. Statistics of Number and Duration	36

of Fades	
D. Statistics of the Rate of Change in Signal Level	37
PART II. Paths with Strong reflectors	38
A. Fade Depth Statistics	38
B. The Statistics of Number and Duration of Fades	39
2.2.4.4 The Rain Losses	39
2.3 The Mathematical Models	40
2.4 The Effects of Fading	43
2.4.1 On Analogue Systems	44
2.4.2 On Digital Systems	45
2.5 Fading Countermeasures	49
2.5.1 Diversity Techniques	49
2.5.2 Channel Equalization	51
2.5.3 Coding and Error Correction	53
2.6 Summary	55
3. Measurements & Experimental Work	56
3.1 Introduction	56
3.2 Test One	57
3.2.1 Introduction	57
3.2.2 Nahran to NJ1 Link	60
3.2.3 Jizan to Atuwai Link	61
3.2.4 Experimental Procedures	62
3.3 Results and Comments	63
3.3.1 Analysis of Nahran Path	64
3.3.2 Analysis of Jizan Path	68
3.4 Test Two	71
3.4.1 Link Available Time	71
3.4.2 Available Time of Nahran	73
3.4.3 Available time of Jizan	75
3.5 Summary	86

4. Data Analysis and Interpretation	87
4.1 Introduction	87
4.2 Nahran to NJ1 Link	88
4.2.1 Data Analysis	88
4.2.2 Model Fitting	89
4.2.3 Data interpretation	103
4.3 Jizan to Atuwai Link	105
4.3.1 Data Analysis	105
4.3.2 Model Fitting	106
4.3.3 Data interpretation	113
4.4 Summary	113
5. Conclusions and Suggestions	115
for Further Work	
5.1 Summary & Conclusions	115
5.2 Future Work	120
Appendix A	122
Appendix B	133
References and Bibliography	146

LIST OF TABLES

Table	page
1 : Empirical values of parameters for equation(3)	32
2 : Time percentage of different AGC levels during our testing period	74
3 : Time percentage of different AGC levels during both testing periods	74
4 : Time percentage of different BER values during testing period	78
5 : Results of system monitoring of Jizan to Atuwat link using the Hp device	85
6 : The statistical models of Nahran path	97
7 : Time percentage of AGC levels	98
8 : The statistical models of Jizan path	107
9 : Time percentage of AGC levels on Jizan path	107

LIST OF FIGURES

Figure	page
1 : Fade margin vs. Distance	9
2 : Fade margin and Reliability	9
3 : Noise limits and Distance	9
4 : The block diagram of the system used during the measurements	12
5 : The data acquisition computer system used for recording the data	13
6 : Atmospheric reflection due to refractive index discontinuities	20
7 : Diffraction loss for obstructed LOS microwave radio paths	30
8 : Worst month atmospheric multipath fading for an average rolling treeian $f=4$ GHz temperate climate	34
9 : Calculations of fade margin as a function of flat fade margin for 8-PSK system with $BER=10^{-3}$ over 40-60 Km paths from 11-13 Ghz without diversity or equalization	47
10 : Sample drawing of the receiver AGC recorded during this test.	65
11 : Block diagram of The HA-8S microwave system	69
12 : Drawing sample of the measured data from the RX-1 antenna of Jizan link.	71
13 : The operator interface display and panel keys of the (Hp 37721A).	80
14 : The End-to-End testing setup.	81
15 : The Loopback testing setup.	82
16 : The block diagram of System Monitoring test.	84
17 : Sample of the new data after filtering out the non-fading periods	91
18 : The PDF's of channel RX-1 with the best fitted distribution	92
19 : The PDF's of channel RX-2 with its best fitted distribution	93
20 : The PDF's of channel RX-3 with its best fitted distribution	94
21-A : The CDF of channel Rx-1	95
21-B : The CDF's of channels Rx-2 and RX-3	96
22 : The fade depth statistics for RX-1.	98
23 : The fade depth statistics for RX-2 & RX-3.	99
24 : The time correlation function of Nahran.	102
25 : The spectrum for Nahran path.	103
26 : The PDF's of channel RX-1 with its best fitted distribution	108
27 : The PDF's of channel RX-2 with its best fitted distribution	109

28 :	The CDF's of channels Rx-1 and RX-2	110
29 :	The fade depth statistics for RX-1 & RX-2	111
30 :	The time correlation function of Jizan	112
31 :	The spectrum for Jizan path	114

LIST OF ACRONYMS

AGC	Automatic Gain Control
FDM	Frequency Division Multiplex
A/D	Analogue to Digital Converter
CDF	Cumulative Distribution Function
PDF	Propability Distribution Function
LOS	Line-Of-Sight
L	Free Space Loss
EFS	Error-Free Second
ISI	Inter-Symbol Interference
FM	Frequency Modulation
PSK	Phase Shift Keying
DFE	Decision Feedback Equalizer
BER	Bit Error Rate
FEC	Forward Error Correction
TMC	Trellis-Coded Modulation
MSK	Minimum Shift Keying
HDB3	High Density Binary-3
EC	Errors Count
ER	Error Ratio
ES	Error Second
EFS	Error Free Second
UNS	Unavailable Second
DM	Degrade Minute
TAF	Time-Autocorrelation Function

CHAPTER ONE

INTRODUCTION

1.1 Overview

The characterization of channels having randomly time varying impulse responses is important for system performance analysis. Such characterization is important for the transmission over many radio channels such as shortwave ionospheric channels, tropospheric scatter and ionospheric forward scatter. The treatment of such channels is statistical in nature.

Those multipath fading channels which exhibit the multipath nature of signal propagation at relatively long distances, cause the transmitted signal to arrive at a distant receiver by a multiplicity of propagation paths

having, in general, different path delays. This, in turn, produces destructive and constructive interference to the signal causing at some instances the loss of the signal completely. This multipath propagation arises in different ways depending upon the situation. For example, in HF skywave transmission, it arises because of reflections from two or more ionospheric layers. In mobile radio, it arises because of reflection and scattering from buildings, trees and other obstacles along the path.

Many solutions have been suggested to overcome the problem of fading. Those include additional system components (Hardware Solutions) such as space and frequency diversity, adaptive equalization; or by using advanced techniques of signaling with mixed coding and modulation such as the use of trellis coded modulation. However, the best solution will depend on the statistical model of the fading channel which will quantify the sensitivity of the different digital modulation techniques over fading channels [82].

1.2 Thesis Objectives

The main objective of this thesis is to find a suitable statistical model for some radio channels in the Southern Region of Saudi Arabia. Previous models used are not suitable

because they were not based on real data characterizing the channel. The new model will be based on real parameters found through channel measurements. This, in turn, should improve the performance of the system and will reduce the effect of fading once incorporated in the system design; here we will follow the same method done by Bultitude [18].

In the Southern Region of Saudi Arabia the problem of fading is severely affecting communication systems. Most of the paths have unusual geographic climatical features which lead to unstable communication characteristics encountered at certain times of the year. The terrain consists of a rocky canyon surface followed by a flattening out then a desert and finally a salt pan at the Red Sea coast.

The company that was involved in operating and maintaining these microwave links, faced daily complaints and problems from Saudi Telecom PTT concerning the outage due to microwave isolation. Thus, the company (AL BILAD B.C.I. Company) performed a study on the fading problem in the area. Their observations indicated severe fading during some particular periods of the year. The main objective of their study was to find the values of the fade margin and the availability time of the link. Thus, this study did not aim towards finding a suitable statistical model for the channel, which is the main objective of this thesis.

1.3 Literature Review

Continuous physical changes in the channel cause small changes in the individual path lengths, but these may, however, equate to large electrical phase changes for radio frequency. The variations between constructive and destructive interference resulting from the random phase changes comprise the effect called multipath fading.

In phasor terms, the observed received phasor is a vector sum of several phasors, with the phase of each varying individually and randomly over a full range. Fading that fits to this model; which has all the characteristics of a very narrow band stationary Gaussian noise; is called Rayleigh fading. It is characterized by Gaussian quadrature components with a non zero power spectral density, and with a Rayleigh distribution of the received envelope [12], [45], [65]. Another significant cause of fading can be the motion of the terminal in a static multipath environment. This shows up as a Doppler shift, and one can quantitatively identify the power spectrum with an intensity distribution of apparent Doppler shifts [20], [35], [52].

While the physical channel most likely consists of paths that have considerable persistence and changing delay, the

mathematical model that is used more often is one of fixed delays with varying gain and phase at each delay. The statistical model for fading channels assumes stationary statistics (or locally stationary), and the channel model is that of a linear time varying filter [81]. However, a linear time invariant filter model can be used as long as the variations occur slowly compared to the duration of the waveform. On the other hand, the mathematical model of the channel as complex Gaussian is less credible at large values of instantaneous envelope changes. Moreover, when there is a single dominant, non faded component in the received signal along with a fading process, the envelope statistics are Rician rather than Rayleigh. Correspondingly, the phase is no longer uniformly distributed and this type is called Rician fading [37], [67],[69],[72].

In sum, when the impulse response function is modeled as a zero mean complex valued Gaussian process, the envelope of it; at any instant, is Rayleigh distributed. In this case, the channel is characterized to be a *Rayleigh fading channel*. Whereas, when there are fixed scatterers or signal reflectors in the medium, in addition to randomly moving scatterers, then the impulse response function has an envelope of Rician distribution and the channel is called a *Rician fading channel* [1], [8], [17].

The frequency selective channel has a coherence bandwidth [69], which is small in comparison with the bandwidth of the transmitted signal. In this case, the signal is severely distorted by the channel. While if the coherence bandwidth of the channel is large in comparison to the bandwidth of the transmitted signal the channel is said to be frequency non-selective. Thus, the slowly varying channel has a large coherence time or, equivalently, a small Doppler spread. From the above consideration, the multipath channels can be characterized in terms of the scattering function which is a two-dimensional representation of the average received signal power as a function of relative time delay and Doppler frequency [4], [15], [27], [39] ,[48].

In our study, no constraints are placed upon the linearity of the channel, the channel scattering function, the Doppler spread, or the multipath spread. The channels may be overspread or underspread. They may be undispersive, dispersive only in time, in frequency, or doubly dispersive. Also, there are no constraints regarding the scattering function. When such assumptions about the channel are invoked, the complex envelope of the channel is known to approach a zero mean complex Gaussian process, thus, the envelope is Rayleigh and the phase is uniformly distributed. Other envelope statistics which serve as models of fading channels include Rician, Nakagami, the log-normal, Middleton

classes, Gaussian and non Gaussian mixtures, and Laplace distributions [13]. All of these models are described in the work of Bello and Nelin, Biyari and Lindsey, Nakagami, Turin, and Stein [11], [12], [13],[64], [83], [82].

Once the path profile of a radio link is designed, the next design step is path calculation, in which the specifications of the radio equipment needed to be installed and the channel parameters are assigned. Such parameters include :

1. the propagation and path loss in (dB).
2. the operating bandwidth and the peak deviation.
3. the receiver thermal noise and FM improvement.
4. the desired, unfaded, SNR of the channel.
5. the fade margin which ensures a certain noise level.

From these factors one can size the antenna to meet the channel noise objective. After that, the system is designed for specified signal levels. Microwave receiver automatic gain control (AGC) and frequency division multiplex (FDM) level regulation maintain these levels regardless of the SNR. Thus, in the system design, noise level in the derived voice channel is specified not to exceed a certain value for some percentage of the time, such as 0.01% [14], [17].

Theoretically, fading will not occur at the same time on each hop in the system, so the hop criterion can be relaxed considerably and still maintain the system noise limit. For the worst case, the designer (who often assigns the noise criterion as small as possible) depends on the model of the channel to get the accurate needed noise level which meets the availability time requirements [26], [28], [36], [84].

Two approaches may be taken to establish the *fade margin*. The first, was developed by the Bell Telephone Laboratories [14], and is shown in Figure (1). This Figure shows that the 6 GHz path fade margin can be derived from the path length for different availability times. For example a path with availability time of 99.99% and 79 Km (49.09 Mi) length has 40 dB fade margin. Another approach is to assume that the fading follows a Rayleigh distribution (see Table (1), and (2)) for different availabilities versus fade margin and conditions on noise limits [55], [57], [58].

Usually, to meet the fade margin limitations, there is a need to have a very complicated system or to improve the system design by applying one of the fading countermeasures techniques, such as, frequency or space diversity combiners, errorless frequency diversity protection switching (this combines the transmission with the switching stages to assure no error by giving each telephone circuit a special frequency

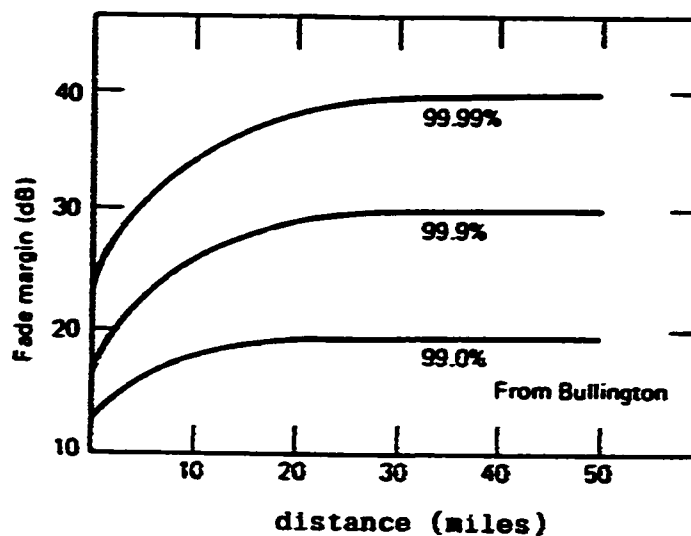


Figure 1. Fade margin vs. Distance.

* Propagation or Path Reliability	Required Fade Margin
90%	8 dB
99%	18 dB
99.9%	28 dB
99.99%	38 dB
99.999%	48 dB

*This is often called *time availability*.

Table 1. Fade margin and Reliability.

Short Haul (3 dB per Double Distance)	Long Haul (3 dB per Double Distance)
20-60 mi: 28 dBmC	250 mi: 28 dBmC
61-120 mi: 31 dBmC	1000 mi: 34 dBmC
121-240 mi: 34 dBmC	4000 mi: 40 dBmC

Table 2. Noise limits and Distance.

allocation [80], [81]) , double forward error correction (using TCM with concatenated codes) [4], adaptive frequency domain equalizer, and digital adaptive time domain equalizer [2].

1.4 Thesis Organization

In this section, we will state the steps that were carried out for gathering and analyzing the data needed to accomplish our objectives.

1.4.1 Test Path Parameters

The primary objective of this test is to determine the radio performance under multipath fading conditions. Two different paths were selected to be studied. The Nahran to NJ1 path is an example of analogue systems, and the Jizan to Atuwal path is an example of digital systems. Those links were chosen due to their past known history which indicates a great deal of fading activities.

The topology associated with these paths simulates a shallow bowl which is conductive under proper atmospheric conditions. In addition, the terrain traversed by these paths are highly reflective. The cumulative effects of both the

paths and the atmosphere create a large number of interesting events annually, which gives us the ability to collect a large amount of fading data in a short interval of time. From these tests, we can calculate the fade margin and the availability time of the channel.

1.4.2 Equipment and Experiments

The block diagram of the system that will be employed to collect the needed data from the radio link is given in Figure (4) and Figure (5). The transmitter and the receiver parts of Figure (4), are the actual (P.T.T) equipment. The baseband signals (which is the real in-service traffic) are to be transmitted by one of the stations, and then the off-air signals are to be received by the other station, which will down-convert it into baseband. Then, the receiver automatic gain control (AGC), will be passed to an analog to digital (A/D) converter device. The digital readings are then processed by a personal computer data acquisition system to store the data for further analysis. All data were sampled at a rate of 10 Hz or less, because, we are not interested of regenerating the signal (see [18]).

The recorded data are to be examined and modeled using some statistical software such as the Statgraphics system.

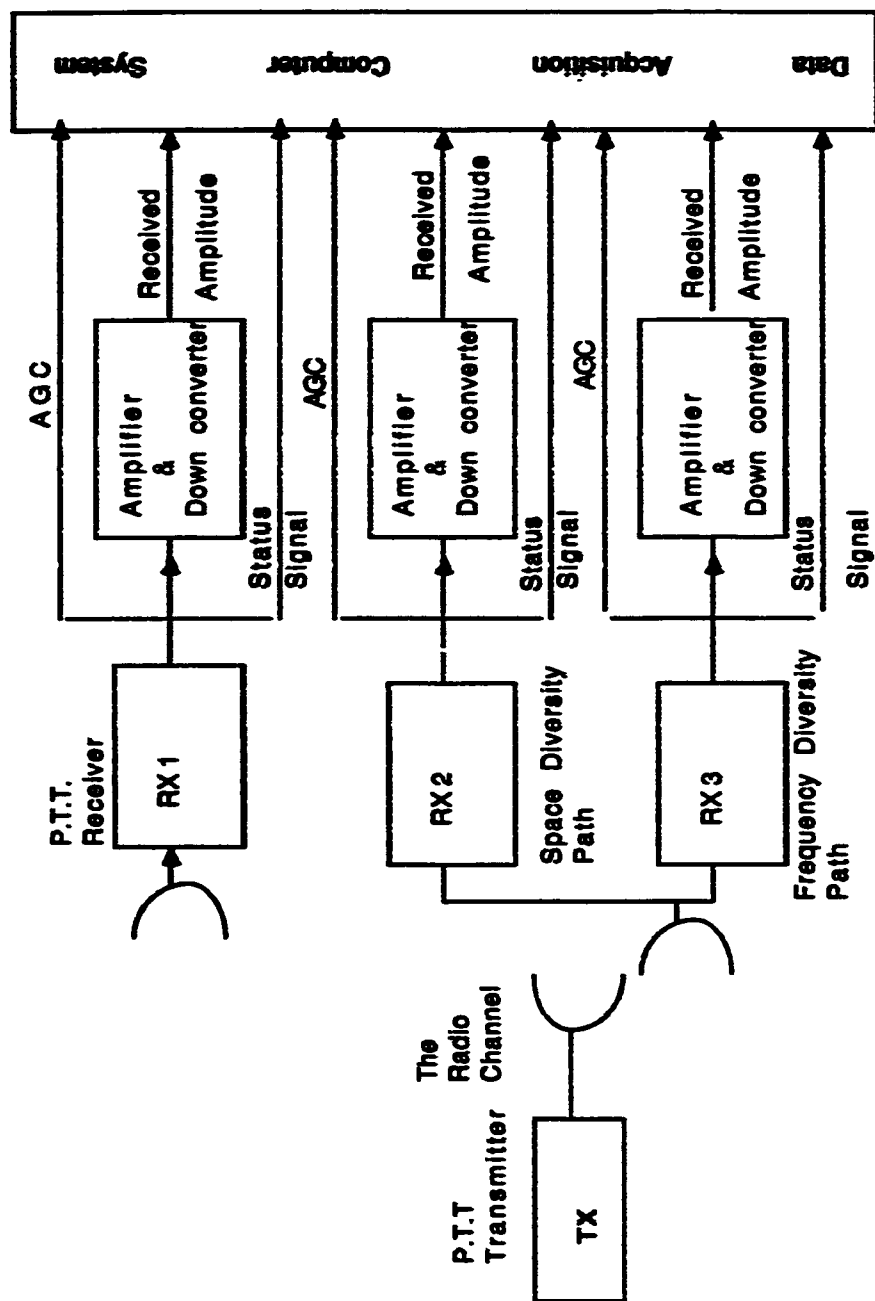


Figure 4 : The block diagram of the system used during the measurements.

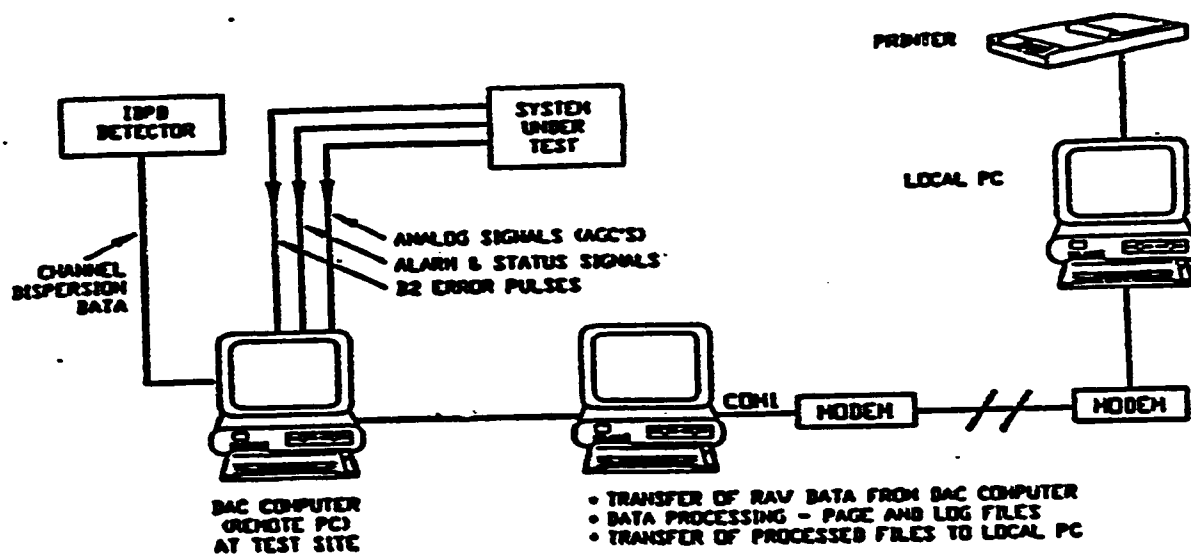


Figure 5. The data acquisition computer system used for recording the data.

Also, some comparison between the main path and the combined (diversity and main) antenna path will be conducted to see its effect on the system performance.

1.4.3 Data Analysis and Modeling

In order to characterize the measured channel for digital or analogue communication between two terminals, the temporal fading measurements done in the previous section will be used to:

1. Determine the type of the fading encountered.
2. Compute the cumulative distribution function (CDF) of the envelope of the received signal, by using a threshold detection algorithm to determine when fading periods occurred. We shall use the Kolomogorv-Smirnov analysis procedure to fit the computed CDF to any of the possible models [18], [29].
3. Compute the time-correlation function using time series analysis of the sampled signal data.
4. Estimate the availability time of each link according to real operating conditions and compare it with those found using the obtained models.

1.5 Summary

From what we mentioned above regarding unusual geographical and climatic features about the region, we conjecture that the model of the channel is that of a Rayleigh fading which is the worst case. Another possibility is having a mixture of Gaussian and Non-Gaussian statistics. In general, the obtained model would give the most accurate and suitable channel model to be used in redesigning the radio links of the Southern Region, to improve the availability of these links and help in solving existing problems.

CHAPTER TWO

REVIEW OF MODELS OF FADING CHANNELS

2.1 Introduction

Since the 1970's, microwave radio has been gaining an importance role as a transmission medium for digital communications. In a digital microwave system, line of sight (LOS) propagation is the most appropriate choice of transmission. A LOS link behaves as a wide band, low noise channel. LOS links are limited in distance by the curvature of the earth, obstacles along the path, free space loss,...etc. However, the progress of the technology toward

higher rates of transmission has necessitated the use of higher system spectrum efficiency. A system of such high spectrum efficiency is more exposed to channel distortion due to multipath fading [1], [3], [24], [52]. To a large extent, this distortion appears as asymmetric in the amplitude response and with variations in the group delay characteristics of the filter in the transmission path.

Much of the physical phenomena, many of the meteorological correlates associated with the multipath propagation, and the statistical modeling of LOS channels are, by now, rather well known [6], [50], [62]. The ultimate objective of these studies is the derivation of an accurate model that could estimate the loss due to fading. This chapter, is a summary of the different classification of these channels, their mathematical models, the performance of different models, and the fading countermeasures.

2.2 Channel Classification

The propagation mechanisms that cause fading include refraction, reflection and diffraction associated with both the atmosphere, and terrain along the path [2], [41], [69]. Atmospheric effects are usually caused by solar or meteorological influences. These influences happen with

different durations and varies from one millisecond to several hours in some cases. This gives rise to two types of channel variabilities, namely : *short term* and *long term fading*. The short term "*multipath fading*" assumes that the long term variability is sufficiently slow that the channel statistics can be regarded to be reasonably fixed over a certain time interval. This short term fading affects the received signal details, while the long term "*power fading*" affects the time availability of the channel [20], [44].

On the other hand, if the long term variability are so fast that the channel statistics change rapidly over a certain time interval, this type is called fast multipath fading. Moreover, the fading is further classified into *flat fading* "*frequency non-selective*", and *frequency selective fading*. The main difference between these two types is that, in the flat fading channels the attenuation affects equally all spectral components, while in the frequency selective channels the attenuation values vary with frequency across the bandwidth [43], [79].

Accordingly, fading channels can be classified into four different types namely :

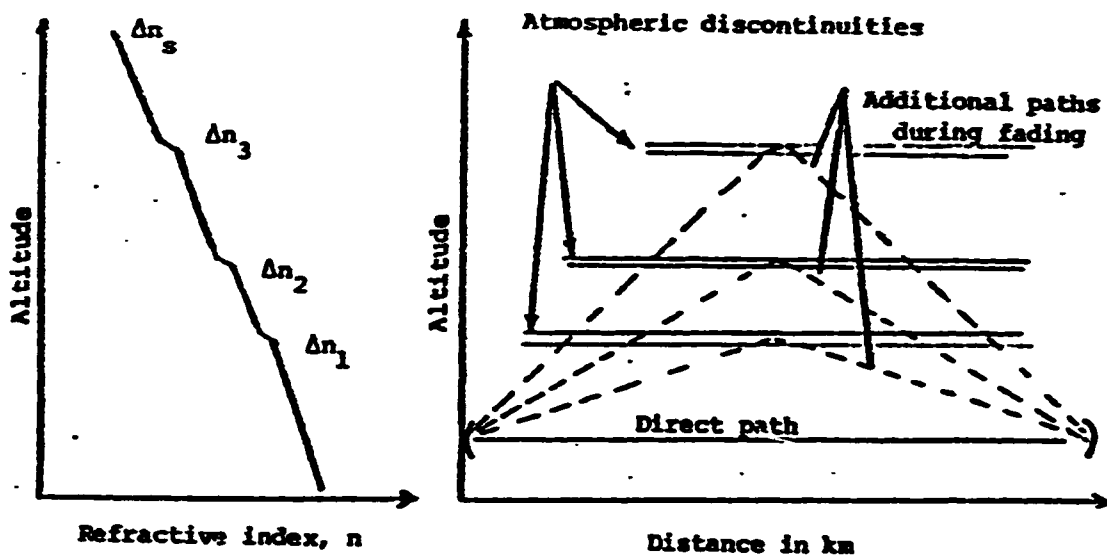
- * Frequency non-selective (flat) slowly-varying channels.
- * Frequency non-selective (flat) fast-varying channels.
- * Frequency selective (multipath) slowly-varying channels.

*** Frequency selective (multipath) fast-varying channels.**

Under normal conditions there should be only one propagation path between the two antennas on a LOS radio link. In practice, for some of the time, more than one propagation path may exist and interference between the signal received over these paths may give rise to significant fading. The additional paths are generally due to either reflections from the ground or from surface structures or from one or more tropospheric layers with steep vertical variations in the refractive index [28] (see Figure (6).)

The physical and statistical characteristics of fading on paths with weak surface reflections are different from those on paths with a strong stable surface reflection. Fading on both weakly reflective paths and on strong stable reflective paths will be considered in details throughout this section.

In LOS links, where deep multipath fading does not occur, small amplitude fluctuations are observed which are referred to as *scintillation*. The scintillation phenomenon occurs over all path lengths and at all frequencies. At the frequencies of interest, the amplitude of these rapid fluctuations is normally less than a few decibels peak-to-peak and they are not therefore considered to be of interest



NOTE: Altitude scale is exaggerated for clarity

Figure (6) : Atmospheric reflection due to refractive index discontinuities [35].

to the system performance [33], [59].

2.2.1 Paths with Weak Reflectors:

Fading on these paths can generally be divided into the insignificant rapid *scintillation* noted above, *slow non-selective* fading caused by single path propagation effects, and more rapid *frequency selective* fading caused by multipath propagation. The latter two types occur in the stratified atmospheric conditions associated with the formation of ducts, in which path trapped in elevated ducts may exhibit wide, slow level changes, above 30 dB in some instances, and thus ducts may be compared to a gigantic waveguide coupling the transmitting and the receiving antennas. In extreme cases of ducting, the path may have to be rerouted around the ducting area [47]. On overland paths in temperate climates, such conditions normally occur during *the night and early morning hours of summer days*. they can be even more prevalent in tropical climates for paths near large bodies of water. They may occur simultaneously (refer to CCIR/CCITT report No.563 and No.718).

Multipath fading is the most severe of the various clear-air mechanisms, and the one normally governing the amount of outage on both analogue and digital links.

Furthermore, in dual-polarized links, multipath fading can be the major factor in the reduction of cross-polarization isolation, thus fading increases the BER of the overall system [49], [60], [38], [54]. Various diversity techniques developed to reduce the effects of multipath fading on links of various geometries are discussed in Section 2.5.

The slow non-selective fading that also occurs during stratified atmospheric conditions is normally less severe than multipath fading. It has been attributed to antenna beam decoupling caused by large angle-of-arrival variations, to beam defocusing, or to a combination of these mechanisms [36]. The fading due to antenna decoupling can become significant on long paths if the antenna beamwidth is too narrow. Thus, a trade-off must be made between the large antenna gains required for long paths and the need to avoid beamwidths narrow enough to result in antenna decoupling. Frequently, combinations of these various fading mechanisms appear to occur [65], [64], [68]. For example, a slow relatively non-selective fade caused by one of the atmospheric mechanisms may combine with weak surface reflections to influence the character of deep selective fading.

Extreme atmospheric conditions may cause the receiving antenna be in a shade area. This happens due to extremely

positive or extremely negative vertical gradients of atmospheric refractive index. In which, extremely positive gradients bend the beam upward so that the actual beam travels a parabolic path and the resulting parabola has a minimum.

Very high negative gradients, conversely, bend the beam downward resulting in the beam having a parabolic shape with a maximum. At high altitude above the ground, the gradient is moderately negative and never exceeds the negative curvature of the earth. The ray that reaches high altitude can not come down again to reach the receiver. This also can happen in the flattened earth convention, if an extremely negative gradient affected the path. The rays remain bent downward. On the other hand, if the rays bent upward in the region where the refractive index has a positive slope. This phenomena is called the *total black-out fading* or *diffraction fading*, and it usually happens in tropical regions; mainly on coastal areas [2], [3], [4], [45].

2.2.2 Paths with Strong Reflectors

If the radio paths passes over a very reflective ground, fading is more dependent on reflections from the ground than on tropospheric multipath especially on short paths. High

ground reflections (i.e., whose signal levels are with about 10 dB of the normal direct signal level) could occur over such areas as sea, lake, flat and humid areas, wet ground and moist river valleys or moors where total reflection can occur in an atmospheric layer near the ground when mist or ground fog occurs [78], [71], [83]. The fade characteristics are then different from those described in the above section. This type of fading is called the surface multipath fading to differentiate it from the atmospheric multipath fading.

2.2.3 Paths with Rains and Storms

Attenuation can also be experienced on LOS radio links as a result of absorption and scattering by rain, snow, dust or sand. Some attenuation due to absorption by Oxygen and water vapour is always present and should be included in the calculation of total propagation loss at frequencies above 10 GHz. Also, on long paths it is desirable to take into account known statistics of water vapour concentration and temperature in the vicinity of the path. Although the rain attenuation can be ignored at frequencies below about 5 GHz, it must be included in the design calculations at higher frequencies (refer to CCITT report No.721). Many detailed measurements and model extrapolations have been made in recent years of short interval rainfall rates. These are

discussed in CCITT report No.563. Other methods have been developed to estimate the long-term statistics of rain attenuation, which is applicable in situations where the necessary detailed rainfall statistics are not readily available. Synthetic storm predictions of rain attenuation distributions suggest that the probability of occurrence of a given depth of fade increases more rapidly than the corresponding increase in path length [65], [81], [82]. Reliable experimental data relating to this factor are needed before definitive guidelines can be provided.

Attenuation due to absorption and scattering from sand and dust particles may occur in desert areas. However, significant propagation effects have not been reported. Information on specific attenuation is given in CCITT report No.721, but as yet there is little information on horizontal and vertical extent of such storms. However, worst-case calculations have been carried out assuming that such storms extend over the whole path [6], [8], [29]. In such calculations it has been found useful to relate the specific attenuation to visibility as a measure of the particle density. Sand and dust storms usually contain particles with sizes ranging from a fraction of a micron to few hundred microns in radius. Due to the heavy particles of sand storms, which is never less than .04 mm in radius, the air two meters above the earth's surface will be clear of sand. Hence, one

may expect that radio link will not be affected by sand storms, especially when antennas are mounted high enough [30], [32], [53], [58], [68] .

Dust storms comprising much smaller particles (less than .01 mm in radius) may be found at heights between 100-200 meters. Hence, dust storms may affect propagation at frequencies higher than 10 GHz where scattering and/or absorption might result [25], [37].

2.2.4 Propagation Losses

The propagation loss on a terrestrial (LOS) path relative to the free-space loss is the sum of all different contributions as follows :

- * attenuation due to atmospheric gases;
- * diffraction fading due to obstruction of the path;
- * fading due to multipath, defocusing and scintillation;
- * attenuation due to variation of the angle-of-arrival;
- * attenuation due to precipitation and rain;
- * attenuation due to sand and dust storms.

Each of these contributions has its own characteristics as a function of frequency, path length, and geographical location.

2.2.4.1 Free Space Losses

Under normal conditions, energy radiated from a transmitter undergoes scattering of energy as it travels through space following the inverse-square law principle. The free space loss (L) between two antennas is given as [34] :

$$L = 20 \text{ Log } (4 \pi f d) \quad (1)$$

where :

d = the distance between the two antennas in Km.

f = the operating frequency in GHz.

2.2.4.2 Atmospheric Gases Losses

Some attenuation due to absorption by atmospheric gases such as Oxygen, Nitrogen, water vapour is always present. The attenuation on a path of length d Km is given by [30] :

$$A = \sigma . d \quad (2)$$

where σ is the specific attenuation of the path in dB/Km, and this factor can be estimated from statistical data of a given path; see CCITT report No.719, and No.563.

2.2.4.3 Diffraction Losses

The fade depth (diffraction loss) will depend on the type of the terrain and the vegetation. For a given path ray clearance, the diffraction loss will vary from a minimum value for a single knife edge obstruction to a maximum for smooth spherical earth. Methods of calculating diffraction loss for these two cases, and also , for paths with irregular terrain are discussed in [15], [18], [22]. These upper and lower limits for the diffraction loss are shown in Figure (7). The diffraction loss over average terrain can be approximated for losses greater than 15 dB by the formula [34] :

$$A_d = -20 (h / F) + 10 \quad (3)$$

where F is the radius of the first fresnel zone¹ and h is the height of the most significant path blockage above the path trajectory². A curve based on equation (3) is also shown on Figure (7).

¹ The fresnel zone is a series concentric ellipsoid surrounding the path.

² h is negative if the top of the obstruction of interest is above line-of-sight.

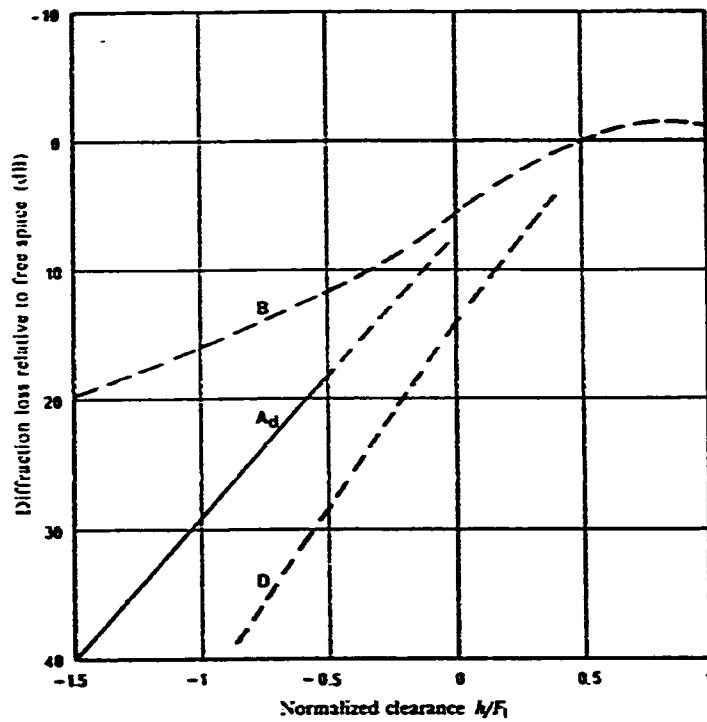
Equation (3) is based on measurements over average terrain in the united states [19]. Data obtained in the USSR over average terrain show that the diffraction loss may be approximated by equation (3) for 50 % of radio links. A method for calculating the diffraction loss, based on the curvature of the obstruction and statistics of the refractive index gradient has been also developed [35]. In the following paragraphs, the fade depth statistics for different paths (with weak and strong surface reflections) will be considered for various percentages of times [42], [61], [63], [73].

PART I. Paths with Weak Reflectors

A. Fade Depth Statistics for small Percentages of Time

For large fade depths, the average worst-month fading time fraction can be approximated by the asymptotic equation [45]:

$$P(W) = K \cdot Q \cdot W/W_0 \cdot (f)^B \cdot (d)^C \quad (4)$$



B: the theoretical knife-edge loss curve,
 D: the theoretical smooth spherical Earth loss curve,
 A_d : an empirical diffraction loss derived in the United States for
 intermediate terrain,
 h : the amount by which the radio path clears the Earth's surface and
 F_1 : the radius of the first Fresnel zone

Figure (7) : Diffraction loss for obstructed LOS microwave radio paths [35].

- d :** path length (Km)
f : the operating frequency (GHz)
K : a factor for climatic conditions
Q : a factor for terrain conditions
W : the actual received power (W)
Wo: the received power in non-fading conditions (W)¹.

From the results of statistical tests on data from 47 links in the United Kingdom and France, equation (4) can be considered valid for fade depths greater than 15 dB or the value exceeded for 0.1 % of the worst month, whichever is the greater. The range of validity in path length is 10-15 Km and in frequency 2-27 GHz.

It is not yet possible to give a general set of rules for the parameters K, Q, B and C in equation (4). In the absence of more general rules, the values proposed for these parameters by various administrations (Table (1)) can be employed with equation (4) to determine the probability of exceeding a given fade level in an average worst month.

Equation (4) is a semi-empirical formula based, in part, on the observation that for sufficiently large fade depths, the measured cumulative distributions of fade depth can be

¹ $W / W_o = 10^{-(a/10)}$, where a is the fade depth in (dB).

TABLE 1 - Empirical values of parameters for equation 4

Proposed for	Japan (1)	N.W. Europe	United Kingdom	United States	USSR	Northern Europe (1)
Reference	(Morita, 1970)		(Dobie, 1979)	(Barnett, 1972; Vignati, 1975)	(Nedemko, 1980)	(Laine, 1979; Blomquist et al., 1980; Danielson, 1983; Tancm, 1985)
B	1.2	1.0	0.85	1.0	1.5	1.0
C	3.5	3.5	3.5	3.0	2.0	3.0
K, Q for maritime temperate, mediterranean, coastal or high-humidity-anti-temperature climate regions				$\frac{4.1 \times 10^{-1}}{S_1^{1.2}}$	2×10^{-1}	
K, Q for maritime sub-tropical climate regions				$\frac{3.1 \times 10^{-1}}{S_1^{1.2}}$		
K, Q for continental temperate climates or mid-latitude inland climatic regions with average rolling terrain	10^{-1}	1.4×10^{-1}	$\frac{8.1 \times 10^{-1}}{S_1^{1.2}} \cdot 10$ $\frac{4.0 \times 10^{-1}}{S_1^{1.2}}$	$\frac{2.1 \times 10^{-1}}{S_1^{1.2}}$	4.1×10^{-1}	$\frac{2.3 \times 10^{-1}}{S_1^{1.2}}$
K, Q for temperate climates, coastal regions with fairly flat terrain	$\frac{9.9 \times 10^{-1}}{\sqrt{h_1 + h_2}}$			$\frac{10^{-1}}{S_1^{1.2}}$	2.3×10^{-1} to 4.9×10^{-1}	$\frac{6.5 \times 10^{-1}}{S_1^{1.2}}$
K, Q for high dry mountainous climatic regions	3.9×10^{-10}					10^{-1}
K, Q for temperate climates, inland regions with fairly flat terrain					7.6×10^{-1} to 2×10^{-1}	$\frac{3.3 \times 10^{-1}}{S_1^{1.2}}$
Accuracy of equation (4) with coefficients indicated		$\bar{\sigma} = -2.9$ dB $\sigma = 6.6$ dB 47 links in UK/France, 73-95 km 2-37 GHz	$\bar{\sigma} = 1.3$ dB $\sigma = 5.0$ dB 28 links, 73-75 km, 2-37 GHz		$\bar{\sigma} = -0.04$ dB $\sigma = 2.0$ dB 26 links, 36-75 km, 3.7-8 GHz	

(1) The Japanese data apply for the warm season.

(2) The coefficients are based on data from Finland and Sweden for non-mountainous regions, and data from Norway for mountainous regions.

Note: - h_1 and h_2 are antenna heights in meters.

S_1 is the terrain roughness measured in meters by the standard deviation of terrain elevations at 1 km intervals (6 m $\leq S_1 \leq 42$ m). The height of the radio sites has to be excluded.

S_1 is defined as the r.m.s. value of the slopes (measured between points separated by 1 km along the path, but excluding the first and the last complete km interval).

(1 $\leq S_1 \leq 80$).

It is possible that some of these parameters may be distorted by the inclination of data from paths which experience surface reflection problems and/or diffraction fading.

$\bar{\sigma}$ is the mean value of the errors (predicted minus measured fade depths) (dB).

σ is the standard deviation of the errors (dB).

distribution [70]. The theoretical basis of this result is described in [17], and [34].

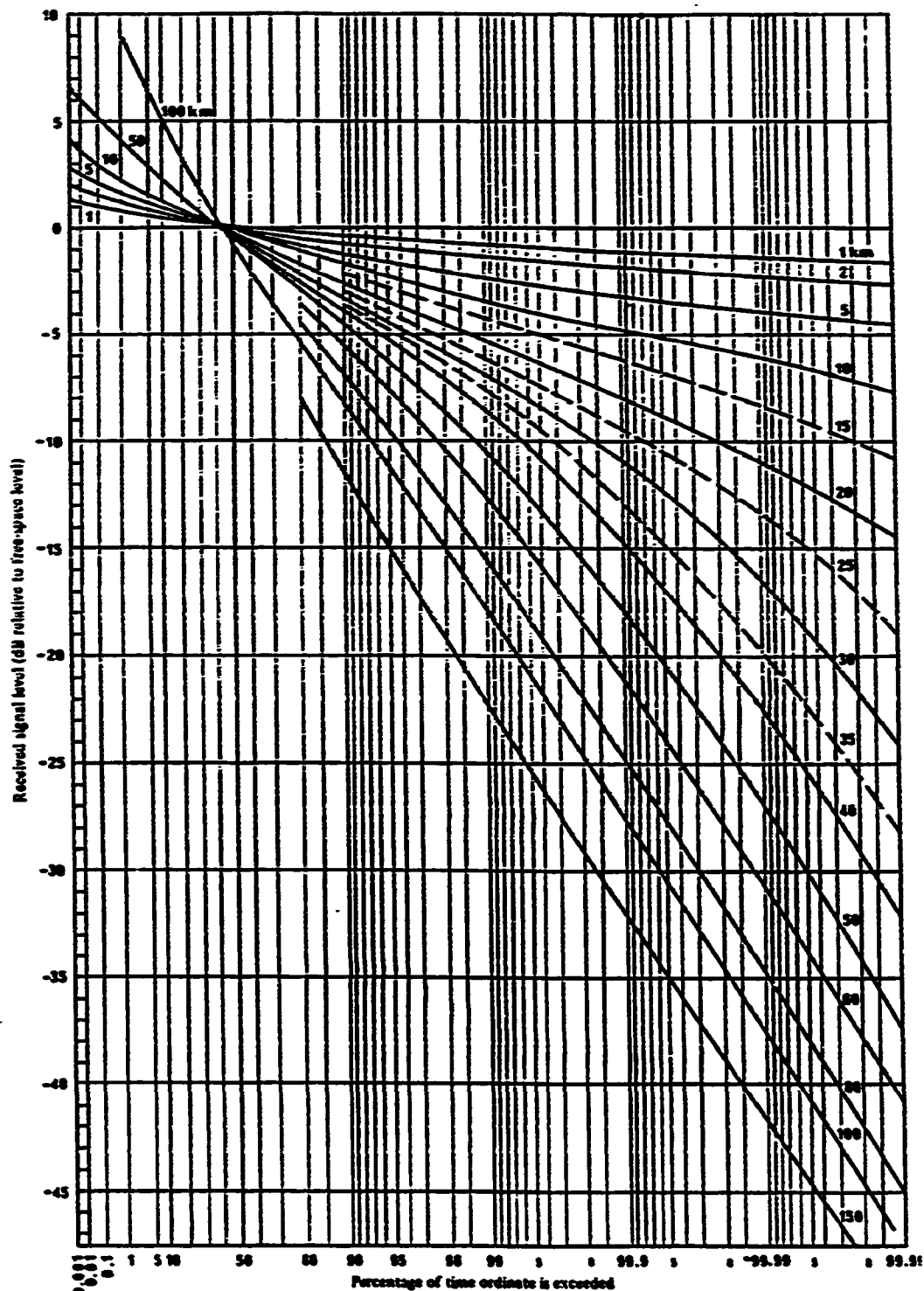
B. Fade Depth Statistics for Various Percentages of Time

The results of fitting a Nakagami-Rice distribution to data measured over average rolling terrain in north-west Europe are given in Figure (8) for frequency of 4 GHz.

The curves in Figure (8) are based on the observation that the measured cumulative distributions of fade depth can be approximated by the well-known Nakagami-Rice distribution (which is the sum of a constant vector plus a Rayleigh-distributed vector with equi-probable phase) and two additional assumptions:

- * The sum of the power in the deterministic vector P_d and the average power in the random vector P_r is constant for a given distance [13], and [16].
- * The deterministic vector undergoes an exponential decrease with distance as [46] :

$$P_d = e^{-d/\alpha} \quad (5)$$



34

Figure (8) : Worst month atmospheric multipath fading for an average rolling terrain $f = 4$ GHz-temperate climate [45].

where α is the reference length that must be derived experimentally for a given climate and frequency [7]. A value of $\alpha = 265$ Km, based on measurements on a 50 Km path at 4 GHz in north-west Europe was found to give the results shown in Figure (8), from which one also can get other information about the worst month fading at the same regions at distances up to 100 Km with different values of α .

This method was developed for 4 GHz, but can be used for other frequencies if the path length d is replaced by an equivalent value d_{eq} given by :

$$d_{eq} = d \cdot (f/4)^{0.25} \quad (6)$$

This method predicts fade depths in an average worst month for any percentage of the time. The method is most accurate for average rolling terrain and it is the least accurate in climates corresponding to the first, second, and fourth rows of Table (1).

C. Statistics of Number and Duration of Fades

The duration and the number of fades over a certain period of time affect transmission quality. These quantities also influence the choice of the countermeasure required to

Measurements of the number and the duration of fades have been carried out by several administrations. The results generally agree in the following points :

* If the ratio between the power under consideration and the power under free-space conditions is designated by (W/W_0) , and if only fades deeper than approximately 15 dB are considered, the number of fades/hour, N , is given by the following expression [46] :

$$N = C_1 (W/W_0)^\alpha f^\beta \quad (7)$$

where we note that N tends to increase with path length.

* For a given fading depth, the fade duration is distributed as Log-normal whose average (mean) value is :

$$M = C_2 (W/W_0)^\sigma f^\delta \quad (8)$$

The constants of proportionality C_1 and C_2 depend on the period under consideration, path length, climate, .. etc.; α , β , σ , δ , C_1 and C_2 have been calculated by several experimental workers [55],[67],[73].

Measurements in the USSR and Republic of China have shown, however, that M decreases with path length (without

obstacle) and with relative path clearance. In each case the sum of the exponents α , and σ is equal to 1, as the product $(N * M)$ represents the total fade duration which, for deep fades, is proportional to the received power (see equation (4).)

D. statistics of the Rate of Change in Signal Level

The rate of change of signal level can be measured in one of two ways; either as a change in signal level in a specified small time interval, or time interval associated with a specified small change in level. In general, few experimental data available have shown that this rate increases with frequency and fade depth (as the behavior of M in equation (8)) and increases with path length. Measurements carried out in France over one year on a 53 Km path at 13 GHz have shown that the rate of change in level had Log-normal distributions with the same standard deviation for average attenuation of 20 dB and 30 dB. The measurements were carried out over a 10 dB interval.

PART II. Path with Strong Reflector

A. Fade Depth Statistics

If the radio path passes over very reflective ground, fading is more dependent on reflections from the ground than on tropospheric multipath. There are few data available from which to develop prediction methods for paths with strong surface reflections.

One method has been proposed by Morita [59] for calculating the probability of "equivalent Rayleigh fading" from a reflective ground, on the basis of fading in non-reflective conditions, taking the equivalent reflection as a parameter. For some paths, however, Rayleigh distribution is not necessarily a good model if there are stable reflections [31].

B. The Statistics of Number and Duration of Fades

Over sufficiently flat paths, the number of fades rises with the increased in path clearance [9], [11]. On costal paths, the number of fades is substantially higher than over land paths. For Example, the number of fades measured on oversea paths was found to be 5-10 times higher than on overland paths with flat region in the vicinity of the ground-

reflection point [72], [75].

Measurements on a 22 Km oversea path off the west coast of France showed a decrease in the median value of fade durations as well as in the standard deviation, with an increase in frequency from 2-15 GHz . Furthermore, fading rates of 5 dB/s at 2 GHz were measured and values above 100 dB/s were attained at 15 GHz in 10 dB intervals.

2.2.4.4 The Rain Losses

The following simple technique may be used for estimating the long-term statistics of rain attenuation. The average annual probability P , of exceeding a given attenuation level may be derived from the worst month probability $P_r(W)$ by using the following equation [45] :

$$P = 0.3 \cdot P_r(W)^{1.15} \quad (9)$$

The prediction given in (9) was derived from an analysis of joint rainfall and propagation measurements obtained mainly in Europe with some additional data from Japan and the United States of America [27]. The relationship between the average annual statistics and those for the worst month, shows the precise nature of the climatic dependance of the

coefficient in the power law relationship is not clear at the present time because of the lack of long-term data in rainfall and link attenuation. The estimate given by equation (9) is, thus; an average based on the currently available experimental data.

2.3 The Mathematical Models

Any model of the fading phenomena should take into consideration the effects of the atmospheric conditions. In general, there are two approaches of modeling: the atmospheric models and the channel models. The atmospheric models describe the physical propagation on the radio path, while the channel models try to fit the propagation response mathematically over a finite bandwidth. Some of the earliest research into the multipath phenomena was done at AT&T Laboratories, where researches showed that microwave fading could be explained in terms of multipath transmission [34],[47].

Kaylor reported a statistical analysis of extensive swept frequency measurements made during fading [3], and [12]. He confirmed that fading can be explained in terms of relative small number of interfering rays with small magnitude and long delay rays. He, also, showed that this

explanation is responsible for the most severe fading events [26]. A number of models were proposed and each attacks the problem from different points of view. Examples of such models include polynomial models and ray models. Czekaj and Greenstein have shown that the former can be used to accurately model multipath fading response over 40-60 MHz bandwidth using only first and second order complex polynomials respectively. Many investigators have studied the properties of ray models, especially the three rays model and proposed channel models based on the three rays model[75]. Rummel proposed a simplified three rays model which has since become one of the most widely cited studies of its kind [76], [77].

Frequency selective fading is the main cause of impairment in microwave digital communication along LOS. It causes a severe intersymbol interference (ISI) and results in serious defects on the rate of transmission. Today, most countries are moving toward replacing analog systems by digital systems, but fading is one of the major obstacles facing these countries. The ultimate objective of the study of multipath fading is to find an accurate method to estimate the transmission quality of a link with specified characteristics such as frequency, hop length, height of antenna, and so on [23].

In general, there are three main categories of fading channels models. These are :

I. Non-Diversity Single Polarization Models

- a) *Three-Ray Model.*
- b) *Two-Ray Model.*
- c) *Polynomial Model.*

II. Diversity Models.

III. Dual-Polarization Models.

The basic components of any channel model are the following:-

- * The transfer function over a finite frequency interval as needed by the system; in which, we specify the channel parameters.
- * The joint probability distribution function of the parameter of the fading channel which is drawn from the transfer function.
- * A scale factor which represents the probability of fading on the path [64].

An important point to be clarified, is that these models are applicable under two assumptions. The first is that the time variation of the channel response is much slower than the dynamic response of the radio equipments to be used. The second is that the performance of the link at any time is

uniquely related to the current state of the channel, that is, there is no delirium in the system behavior [55]. The dynamics of the channel can be measured by a simple method which is used for both analogue and digital systems. In which, the dynamics of the channel is defined as the rate of change of the receiver signal power at a single frequency expressed in dB/sec.

2.4 Effects of Fading

The study of propagation effects on LOS paths began with the introduction of frequency modulation (FM) system in the early 1950s. Although much work was done to develop propagation models for predicting the performance of the FM systems, the introduction of digital radios in the 1970s; fueled an interest in more detailed models, because digital radio systems are more sensitive to channel distortion than analogue (FM) systems. The effects of fading on both communication systems will be described in the following sections.

2.4.1 On Analogue Systems

An FM signal contains most of its energy at the carrier frequency and carries its information redundantly encoded in

its sidebands. Hence, it is adversely affected by the loss of power at the carrier frequency, but relatively unaffected by loss of signal in only one of the sidebands. For this reason, radio channel modeling for FM systems focuses on single-frequency fading statistics. In analogue FM-FDM systems, multipath transmission contributes to an increase in the thermal noise (due to power fading) and in the intermodulation noise (due to frequency selectivity). Measurements on a 6 GHz path in Germany showed significant increases in intermodulation noise as well as considerable variations in the baseband levels for low percentage of the times. This was due to multipath propagation caused by reflection from atmospheric layers [65].

Theoretical and experimental studies carried out in Japan by Nomura in 1967 have shown that ground reflections can give a distribution of total noise more unfavorable than that for thermal noise alone, even on propagation paths having relatively weak reflections.

The cumulative distribution of the duration of noise level increases can be represented by a log-normal law [40]. In microwave analogue radio-relay system, the thermal noise variations due to multipath fading are accumulated at the circuit end. The relationship between the thermal noise power distribution on the single link and that on the multi-relay

links of arbitrary length was studied by Morita [60], [61]. This is one of the best references for analogue system designers.

2.4.2 On Digital Systems

Under many propagation conditions, the loss or gain of signal due to the atmosphere is uniform across the radio channel bandwidth. An example is the loss due to extreme rain rate. In these cases, the approaches developed for the FM system are applicable to digital radios. However, unlike FM signal, a spectrally efficient digital radio signal does not have redundant information in its sidebands. Consequently, the selective loss of some of its frequency components can affect the detectability of the received signal. Thus, the modeling of frequency selective effects is crucial for evaluating the performance of digital radios.

For the purpose of using fixed frequency measurements to calculate the quality of digital systems, the notation of *net fade margin* has been introduced. It is defined as the single frequency fade depth that is exceeded for the same percentage of time as a specified error ratio. It will depend mainly on the bit rate and the type of modulation. Measurements have been carried out in France on 4-phase digital links at a 6

GHz and an 11.7 GHz with a capacity of 40 and 200 Mbit/s, respectively. For the higher bit rate, the net margin increased by 0.5 dB for a 7 dB increase in transmitting power. From this study, the parameters of a two-ray model were determined. The median value of time delay of the indirect ray was about 0.4 ns; which was used to calculate the quality of 4-PSK and 8-PSK for various bit rates as in Figure (9). It also has been observed that for a given link, the value of the net margin is practically equal to the value of the attenuation on the carrier frequency for which the error ratio is exceeded during 50 % of the time [14].

In digital systems, BER vs. SNR are usually used to give an indication of the system performance. According to CCIR/CCITT recommendations, an outage event can be said to occur in a digital radio receiver if its BER exceeds a specified value (typically 10^{-3}) for not more than 10 consecutive seconds.

However, when the BER lasts more than 10 consecutive seconds, the system is said to be unavailable [10]. The severe amplitude and delay distortion caused by selective fading degrades the system reliability beyond that expected from the flat fading (thermal noise) [76]. The degradation due to selective fading is caused by signals propagating along several paths (each with a different electrical length

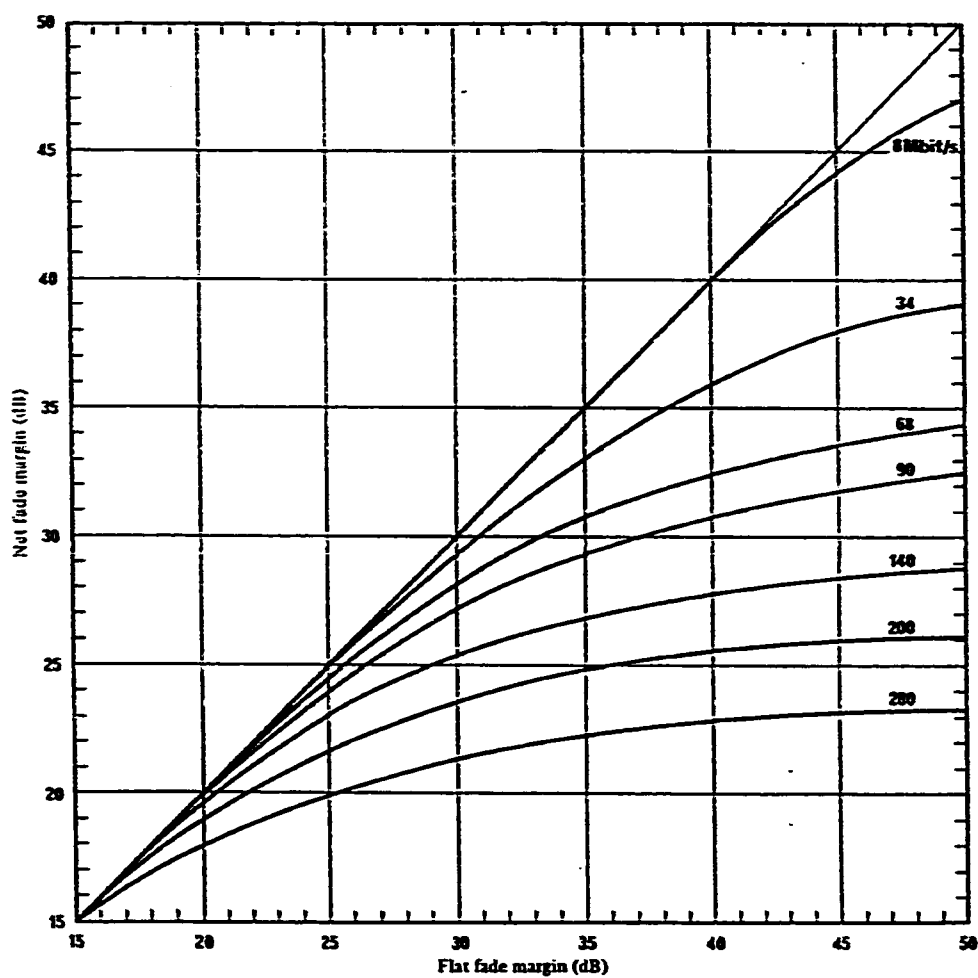


Figure (9): Calculations of fade margin as a function of flat fade margin for 8-PSK system with $BER=10^{-3}$ over 40-60Km paths from 11-13 Ghz without diversity or equalization [35].

and delay) reach the receiver. Thus the different components interfere with each other and affect the received signal randomly [3], [4], [5], [9].

There are several proposed criteria for evaluating the performance of the communication system undergoing selective fading channels.

A/B curves, Signature curves, and Signal-to-Distortion are examples of these criteria. However, the most widely used criterion are the A/B curves, and Signature curves. The aim of the A/B criterion is to obtain critical curves from which one can measure to which level the concerned communication system can be stressed. See [24] for more details on these criteria.

2.5 Fading Countermeasures

Several techniques are available to countermeasures the severe distortion caused by fading channels, and to improve the system performance to cope up with the needs of high-level modulation schemes. However, the most widely used techniques fall into the following state-of-the-art categories:

- * Space and/or frequency diversity w/without combiners.
- * Adaptive frequency and/or time equalizer.
- * Protection switching with forward control and error correction.

The choice of one or more of the countermeasures depends on the channel carrying the information and the applications for which the system is built. In the following section, a brief idea about these solutions will be given. This is to help us in the suggestion of the best solution for the systems under study.

2.5.1 Diversity Techniques

These techniques suggest the transmission of the information over more than one independent channel or path. This will enhance the system availability and performance of the system, since the probability of having the signal in all paths unavailable is much smaller than in the case of one path. Hence, the probability of symbol error will decrease. Diversity refers to simultaneous reception of a radio signal over several paths; this is can be done via space, frequency, angle, time or by using the cross-polarization transmission.

The two diversity paths in space diversity are derived at the receiver end from two separate receivers with a combined output. Each receiver is connected to its own antenna, separated vertically on the same tower. The separation distance should be at least 70 wavelengths and preferably 100 wavelengths. Frequency diversity is more complex and more costly than space diversity. It has advantages as well as disadvantages. Frequency diversity requires two transmitters at the near end of the link. The transmitters are modulated simultaneously by the same signal but transmit on different frequencies. Frequency separation must be at least 2 % , but 5 % is preferable [34]. The more the two frequencies are separated apart, the less chance there is that fades will occur simultaneously on each path. Frequency diversity is more expensive, but there is greater assurance of path reliability. It provides full and simple equipment redundancy and has the great operational advantage of two complete end-to-end electrical paths. In this case, failure of one transmitter or one receiver will not interrupt service, and a transmitter and/or a receiver can be taken out of service for maintenance. The primary disadvantages of frequency diversity is that it doubles the amount of needed frequency spectrum .

On the other hand, in the time diversity the information signal is repeated after a time greater than the coherence

time of the channel. This type increases the bandwidth since it lowers the effective rate of transmission [4], [6], [57]. These techniques were examined under fading channels by many investigator but the improvement induced was inadequate for digital radio [66]. Therefore, these technique are usually equipped with other techniques such as adaptive equalizers.

2.5.2 Channel Equalization

One of the mitigation techniques used in the transmission over radio link to overcome the problem of ISI caused by frequency selective fading is adaptive equalization. The two major sources of system degradation in digital transmission are the channel attenuation and the ISI. The aim of equalization is to reverse the distortion caused by the channel. Frequency-domain equalizers, for example, introduce correction to restore the equality in the spectral density of the signal.

The performance of these equalizers is acceptable in the case of few different levels of modulation. However, in the case of more efficient bandwidth systems this is not enough for reliable transmission. ISI is a time domain effect, so the time domain equalizers are the most efficient solution of ISI. They basically consist of delay elements with tap gains.

The different types of connections result of different time equalizers such as transversal, fractionally spaced, and decision feedback equalizers. Ideally, an infinite number of taps are needed to remove ISI completely. However, in the case of multipath fading, only few symbols are affected by the path. Hence, relatively short equalizers can be used. for digital application, a 5 to 7 tap equalizers is a typical choice [67], [80].

The process of equalization may result in noise enhancement, which suggests the use of a recursive filter (a feedback arrangement). This is called a decision feedback equalizer (DFE), in which; the received signal is processed by a feedforward equalizer then the decision made on the equalized signal is feedback through another transversal filter. This means that the ISI from the past symbol has been canceled totally. The major breakthrough in adaptive equalization techniques, beginning with the work of Lucky in 1965 coupled with the development of Trellis-coded modulation which was proposed by Ungerboeck 1976, has led to the best solution over all others to overcome most of problems of selective fading. The next section will describe the subject of error control coding and its impact with the other countermeasures in overcoming the problem of fading.

2.5.3 Coding and Error Correction

In analogue links, the degradation takes the form of a decrease in SNR. Thus, there is a trade-off between bandwidth and power to achieve a good SNR in the baseband. In digital links, we measure degradation of the information in terms of the bit error rate (BER). A fundamental difference between analogue and digital signals is that we can improve the BER of a digital signal by the use of error correction techniques. No such technique is available for analogue signals since once the information is contaminated by noise, it is extremely difficult to remove the noise. However in digital system, we can add extra redundant bits to our data stream, which can tell us when an error occurs and can also point to the particular bit or bits that have been corrupted. The system that can detect and correct errors uses forward error correction and control unit (FEC).

It is possible, in theory, to generate codes that can detect or correct every error in a given data stream. In practice, there is a trade-off between the number of redundant bits added to the information data bits and the rate at which the data is sent over the link. The efficiency of a coding scheme is a measure of the number of data bits that must be added to detect or correct a given number of

error. The goal is to design codes which are capable of correcting as many as possible errors with minimum redundancy.

The major problem with the error control coding is the bandwidth expansion. However, if coding and modulation are combined into one stage, no need for extra bandwidth and the system operates better than the uncoded system. Thus, this technique combines convolutional coding with modulation into a single stage which is called trellis-coded modulation (TCM). In an important class of TCM known as Ungerboeck codes, multilevel (amplitude and/or phase) modulation is combined with the convolutional coding, which gives coding gains of 3-6 dB and at the same time at bandwidth efficiencies equal to or greater than 2 bit/s/Hz.

2.6 Summary

In conclusion, the designer of any communication system has at this point several solutions to overcome the fading problem. For a particular solution, the recommended procedure is to analyze it under the appropriate statistical model, and present the results in comparison to other solutions. This analysis can be carried out by computer simulation methods, which proven to be superior and therefore presented as simple method of testing real channels. Thus, the designer will have identified a tangible scheme, and its appropriateness is questioned in the light of the designer's knowledge of the channel model.

CHAPTER THREE

MEASUREMENTS & EXPERIMENTAL WORK

3.1 Introduction

In this chapter, we will describe the measurements and the experimental work, that were conducted to accomplish our objectives to characterize and model some radio links in the Southern area of Saudi Arabia.

There were two major tests. The first test, was done to collect and record samples of the amplitude of the received signal. The second test was concerned with calculating the

availability time of the link. Both tests were conducted on two selected paths; namely : Nahran to MJ1 path and Jizan to Atuwai path. The details of each test is described and some of the observed results and comments are summarized in this chapter.

3.2 Test One

3.2.1 Introduction

We recall that the main objective of this thesis is to find a suitable statistical model for some radio links in the Southern Region of Saudi Arabia. Previous models which are being used in operating these links are not appropriate because they were not based on real parameters found through channel measurements. The new models which we are trying to find will be based on real data collected from these channels during usual operation. Incorporating these models in redesigning these systems, will improve the performance of the system and will reduce the effects of fading on these systems. Most of the paths in the Southern region have unusual geographical and climatical features which lead to the unstable communication characteristics encountered at certain times of the year.

The first step of the study was to visit the region to discuss the problem with the PTT technical staff. During the first visit, we put our schedule with the coordination of the operating and maintaining company of the radio links, that will be followed during the study. To select the suitable links for study, we examined the past history of all paths in the area with the help of the regional engineer of Detasad company and other PTT engineers. The selection was based on the following factors:

- * Type of the geographical features of the path.
- * The type of the communication system.
- * Paths with great deal of fading activity.

We found that the terrain consists, in general, of a rocky canyon surface followed by a flattening out desert land and finally a salt pan at the Red Sea Coast. Other significant abnormalities are the steep sided canyon bordering both side of the path.

We spent two months monitoring various links in the area via the digital control computer systems of the (PTT) to locate the links that meet our objective. Also, we examined all previous studies done on the area. The latest was conducted by AL- BILAD B.C.I company, which had been involved in operating and maintaining these links. The company was

faced with daily complaints and problems from the (PTT) concerning the outage due to microwave isolation. Their study indicated severe fading problem. Also they calculated the fade margin and the availability time of the link. After that, we divided the links of this region into two categories according to the type of the communication system (analogue/digital).

The second step was to arrange a visit to all locations to see the real situation and to select two links among others. The following links were visited :

*** Analogue Links include :**

1. ABHA MICROWAVE CENTER.
2. NAHRAN LINK.
3. NJ1 LINK.
4. NJ2 LINK.

*** Digital links include :**

1. JIZAN MICROWAVE CENTER.
2. AL SOODA LINK.
3. MADAIYA LINK.
4. ATUWAL LINK.

The Nahran to NJ1 link and Jizan to Atuwat links were selected to be studied. In the following sections, we will describe both communication paths and will characterize these paths according to their geographical features as was

described in section (2.2).

3.2.2 Nahran to NJ1 Link

The Nahran to NJ1 radio path consists of an analogue upper 6 GHz radio system with six channels using space and frequency diversity. The RF spectrum consists of a vertically polarized 2+1 message channel, together with a non-utilized 2+1 video system on the opposite polarity. The path itself consists of a 79 Km dropping in altitude from 2642 to 159 meters at NJ1. The terrain consists of a rocky canyon surface for the first 40 Km, flattening out to typical Saudi desert for about 20 Km, and finally a salt pan at the Red Sea coast. Always, there is a significant difference in the temperature over the path which ranges from 5-21° C at Nahran to 20-50° C at NJ1. Other significant abnormalities are the steep sided canyon bordering both side of the path which bisects the coast directly at Darb 60 Km away from Nahran.

It is to be noted that, the weather at Nahran is always cloudy and there is some formation of ducts, while it is temperate at the midway, and tropical at Darb. From all of the above conditions, we can see the reason why the existing models fails to cope with the needs of having a stable communication system. All parameters of this model were taken

from the general model of the Saudi desert, which is not suitable for this specific link. This link does not fall into any of the categories described in Section (2.2). It is a new mixed category, in which we find a path with strong surface reflection, then weak reflection, and there is ducting, rain, sand, dust, and a very stratified atmospheric conditions.

3.2.3 Jizan to Atuwat Link

The Jizan to Atuwat radio path consists of a digital upper 8 GHz link. The path goes from Jizan to Madaiya repeater at a 24.22 Km, then completes its way to Atuwat at a distance of 37.3 Km. The path starts with a leveled sandy land which goes parallel to the coast of the Red Sea. Then the path traverses wheat fields, between Madaiya and Atuwat, which are irrigated during the summer season. Thus, the topology associated with this path simulates a shallow bowl which is conductive under the proper conditions to extensive atmospheric stratification, leading to duct formation. In addition, the terrain traversed by this path (being wheat fields) is highly reflective. The last portion of the path is a typical Saudi desert. The path layout summary is given in Appendix B.

Space and frequency diversity radio system are available

at Jizan, and Madaiya sites; but at Atuwal there is only frequency diversity system. From all of the above conditions, we can see again that the existing models fails to cope with the needs of having a stable communication system. All parameters of this model were taken from the general model of the Saudi desert, which is not suitable for this specific link. This link falls in the category of highly reflective tropical region described in section (2.2).

3.2.4 Experimental Procedures

The block diagrams of the testing system that were employed for the propagation experiments are shown in Figure (4) and (5). The transmitter and the receiver parts of the system were the PTT, which were actually in service. The description of these systems will be given subsequently. The transmitted signals are those of real traffic on each link, which is a continuous wave. The off-air signals were received via both the regular and the diversity antennas at the other side of the link. Then, these signals were amplified and down converted into signals in the baseband via the PTT system.

After that, we recorded the amplitude of the baseband signal via a data acquisition computer system. This data acquisition system consists of a 33 MHz , 80386 personal

computer, added to it a Math-co-processor chip, and a 120 Mb Hard Disk for storage purposes.

Also, a commercially available data processing board (DT-2801/A) from Data Translation Inc. was used to convert the analogue signal into a digital one and then store the data in the Hard Disk. The operating and controlling software was developed and designed to meet the needs of having a very low sampling frequency. The written program is given in Appendix A. All data were sampled at a rate of 10 Hz. We also recorded the receiver Automatic Gain Control (AGC) output, which also represents the power gain or loss of the received signal.

3.3 Results and Comments

In this section, we will give a brief description of the test on each path individually. In which, we will also describe the communication equipments at the transmitter and the receiver, type of modulation, coding scheme, and the points at which we collect the data from the system. After that, we will give a general idea about the performance of each link, during the period of the test. Some comments about the weather during days of testing will also be given to help

in analyzing the data.

3.3.1 Analysis of Nahran Path

The Nahran to NJ1 radio path consists of an FM-FDM upper 6 GHz link; six channels: space and frequency diversity radio system. The RF spectrum consists of a vertically polarized 2+1 message channel, together with a non utilized 2+1 video system on the horizontal polarity. The points at which data were collected during the test are : the receiver AGC of the main antenna (RX1), the receiver AGC of the (space-diversity) antenna (RX2), and the receiver AGC of the spare (frequency-diversity) channel (RX3). Note that both (RX1) and (RX2) have the same frequency allocation; but they differ in the height of the receiving antennas, specifically (RX2) is 20 meters higher than (RX1). However, (RX3) has the same height as (RX1) but with different frequency allocation. The outage condition happens, when (RX1), (RX2), and (RX3) are all fading. For this path, the fading condition happens if the receiver AGC exceeds the fade margin of this link which is 38 dB. The test was started on the 15th of December, 1992 and lasted for a period of four days during which we recorded 400,000 samples from each point. Figure (10) shows some drawing samples of these measured data. The same test was done by AL- BILAD B.C.I company, from 11/5/1989 to 17/4/1990;

Time: 9:15.05 - 9:16.05

Date: 10 December 1993

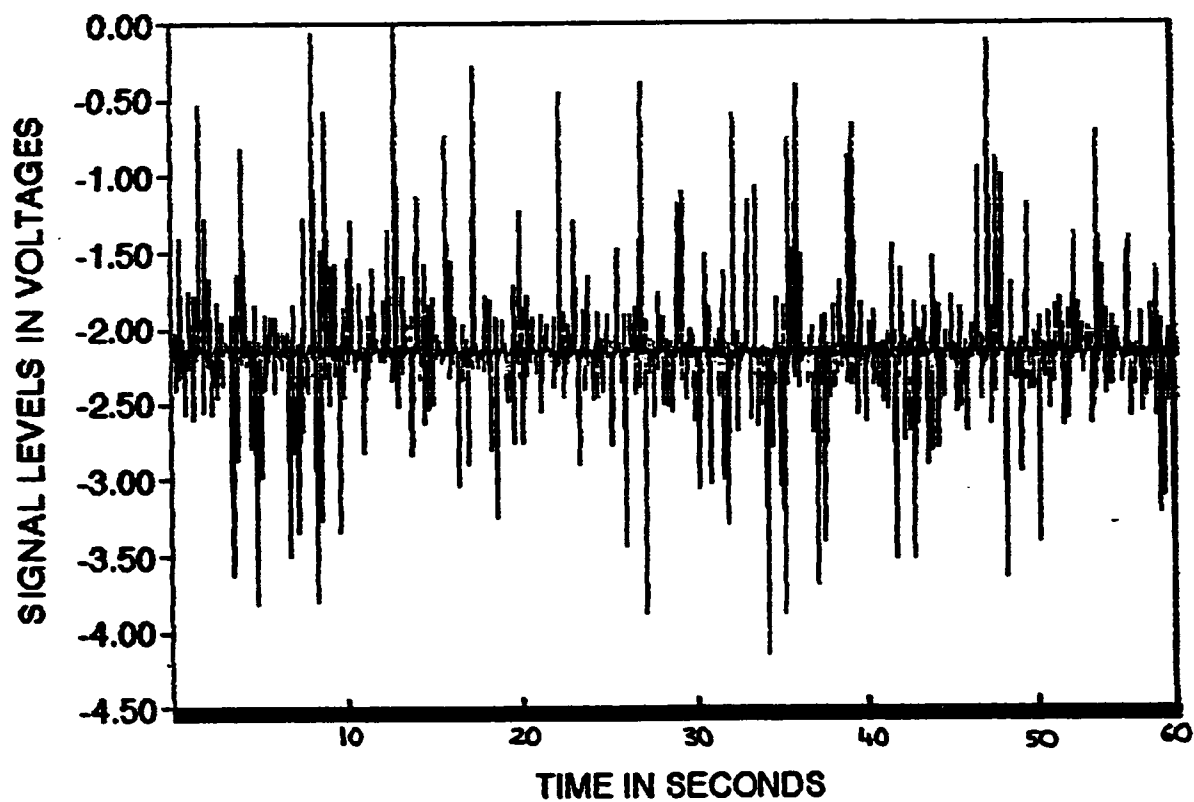


Figure (10): Sample drawing of the receiver AGC recorded during this test.

by using a channel recording device and recording the data on graph paper rather than a computer system as we did. During this test, they collected a large volume of data; which we will utilize to increase the database file, and thus the degree of accuracy of our model. This was done by converting their data into digital one, then adding it to ours. Their data covers a complete period of one year, so it gives an accurate measure of the performance of the channel during all seasons. From these tests we noticed the following points :

1- Extended analysis of the received carrier levels (AGC) indicates that the primary fading type encountered on this path is mainly due to the interference between the main beam and the others delayed beams. These beams are arriving to the antenna with different phases and with different delays due to the path obstacles and elevated layers of atmosphere.

2- The observations indicate that there are two different cases of fading, coupled with the weather conditions encountered in these path at certain times of the day. The first effect occurs early afternoon; as noticed from the recorded data. The explanation of the mechanisms involved in this case is, that usually during calm hot days layering is formed by the convection and upward drift of warm moist air from the cost to the canyon face. As the air rises the

humidity gradient steepens forming elevated sheets and cloud layers. This particular fading type appears to be selective in nature. The fading becomes more serious during the summer days due to the thickness of the formed clouds which generates a waveguide, that carries the beam away in the sky and the communication tower will be in the shadow. Total outage happens and lasts for various periods of time (from 1 minute to some hours).

3- The second case occurs usually in the early morning hours between (2-8 AM) and also during the hot still weather. The fading type appears similar to the one in the first case, but less significant from the interfering fading case. The mechanism of this case appears to be a direct result of the temperature inversion process , which is related to heat retention of the elevated rock formation. Thus, on clear still evenings, air trapped in the box canyon escarpment retains heat from rock formation generated during the day and becomes lighter compared to that of the desert floor during the early morning hours. This effect again produces sheets layering; and moreover, ducting.

4- The worst case of fading happens during the summer days as seen above, and the case gets more critical as sand storms

blow and dust particles hang in the air all across the coastal path; while up on the mountains the reflections due to the rocky surfaces increase the number of delayed signals and clouds, ducts add more barrier blocking the signals.

5- Insignificant rapid scintillation (15-25 dB) was noted to occur during more than 55 % of the time, and the analogue system was less affected by this process than digital system. This type of fading is slow non-selective caused by signal path propagation effect.

3.3.2 Analysis of Jizan Path

The HA-8S digital microwave radio is designed for operation in the 7.75 to 8.25 GHz frequency band. It is ideal for short-haul, point-to-point transmission of digitized voice, data, video, and facsimile. There are many options for the transmission rate, but the one which is used in this link is 34 Mb/s. The basic microwave link consists of two radio terminals. Each radio terminal consists of an RF unit and a digital Modem. Figure (11) illustrates the HA-8S microwave system; for the specification of the system see Appendix B.

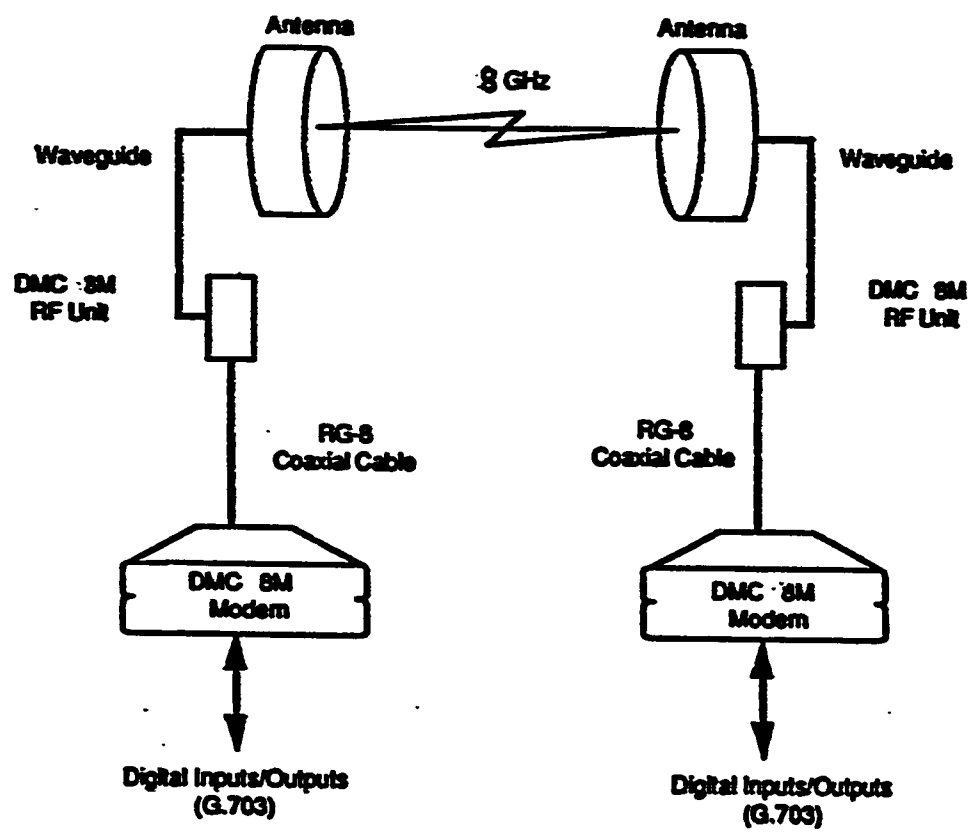


Figure (11): Block diagram of The HA-8S microwave system.

The type of modulation is the Minimum Shift Keying (MSK) and the coding scheme is the High Density Binary-3 (HDB3). At Jizan and Madaiya sites, there are two radio terminals with space and frequency diversity. But for Atuwai there is only a frequency diversity system. This test lasted three days, during which we collected 300,000 sample from each point. Figure (12) shows a drawing sample of the measured data during this test. From these tests we noticed the following points :

1- The fading type encountered on this path is due to the interference between the main beam and the others delayed beams. Insignificant rapid scintillation (10-45 dB) noted to occur during more than 69 % of the time; the system is affected by this process which always causes data failure ($BER > 10^{-3}$) and affect all data link in the path; but this process lasts for less than 5 consecutive seconds.

2- Two different cases of fading, coupled with the weather conditions encountered in these path at certain times of the day. The first effect occurs between (2-4 PM). The explanation of the mechanisms is that usually during calm hot days, the warm moist air forms ducts with different humidity gradient steepens forming elevated sheets. This particular fading type appears to be selective. Total outage happens and

Time: 23:25.15 - 23:26.15

Date: 4 January 1993

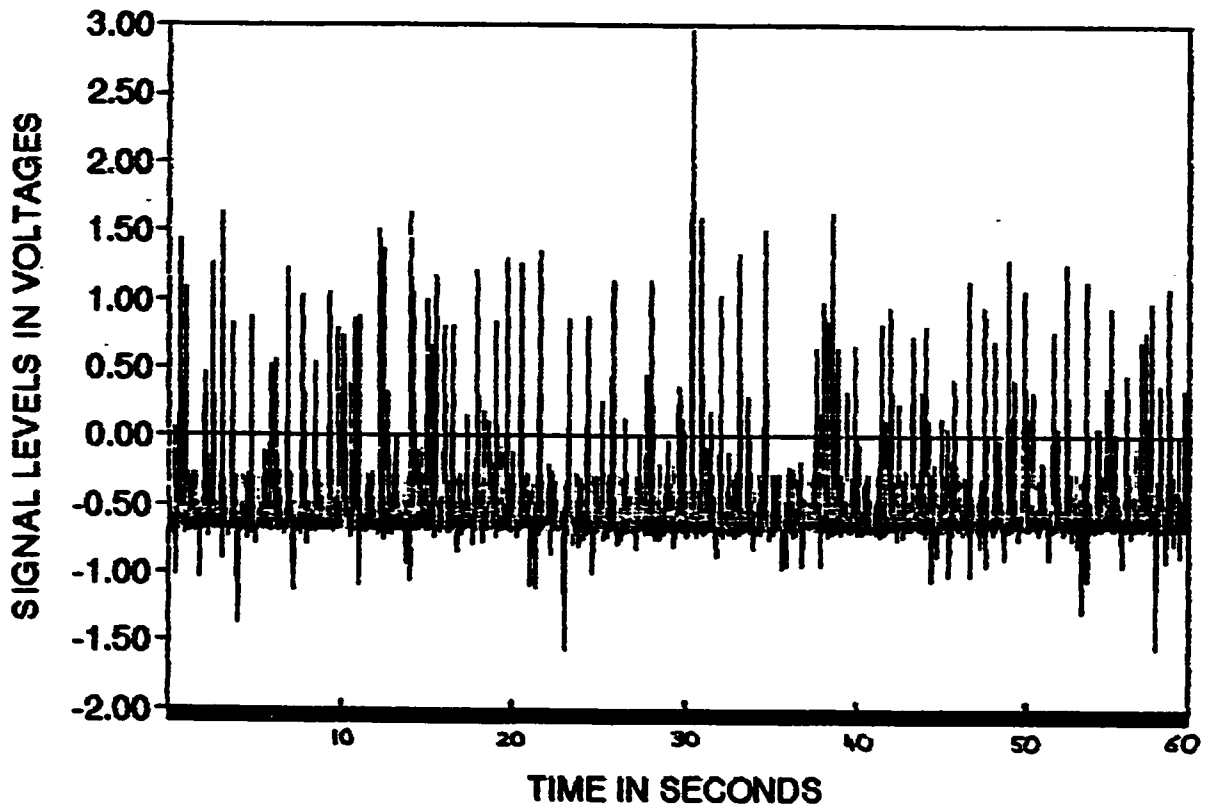


Figure (12): Drawing sample of the measured data from the RX-1 antenna of Jizan link.

lasts for various periods of time (from 0.1 second to 1.5 hours).

3- The second case occurs usually in the night and early morning hours between (2-6 AM) and also during the hot still weather. The fading type appears to be frequency selective, but more significant form the first case. The mechanism of this case appears to be a direct result of the tropical climates and due to the path which goes near large bodies of water. Also, the path traverses wheat fields, between Madaiya and Atuwai, which are irrigated during the summer season. Thus, the topology associated with this path simulates a shallow bowl which is conductive under the proper conditions to extensive atmospheric stratification, which leads to duct formation.

3.4 Test Two

3.4.1 Link Available Time

In this part, we will describe the equipment and the experimental procedures that were used to calculate the outage time and the availability time of the two links under studying. For the analogue system, this calculation is easy and can be made using the same experiments done in test one;

since the outage condition happens simply if the AGC exceeds the fade margin of the link. On the other hand, the case is not simple for digital links, since the critical measure in this is the (BER). Moreover, there are different types of outages according to CCITT recommendations. Thus, we need more special sophisticated equipment to calculate the availability time of digital links.

3.4.2 Available Time of Nahran to NJ1

For this path, we used the same database file which was recorded during test one, and also the data recorded during the company test. First, we shall calculate the availability of this link from our database file only and then from both sets of data. This should be more reliable since it covers a period of more than 13 months. Thus, we can compare the results and draw some conclusions about the season of deep fading. During our tests, the results of the three radio channels are shown in Table (2). The table gives the availability time of each radio channel alone, but as we said before; the outage condition occurs when all paths are faded at the same time. It was found that all three paths were fading at the same time for (0.0346 %) of the time in our test. Thus, the availability time of this link is (99.9654 %) which is not good taking in consideration that the test was

TABLE (2)

AGC	20 - 30 dB	30 - 38 dB	38-... dB ¹	Available.
RX-1	56 %	43.167 %	0.8330 %	99.1670 %
RX-2	63 %	36.350 %	0.6500 %	99.3500 %
RX-3	95.3653 %	4.6000 %	0.0346 %	99.9654 %

Table (2): Time percentage of different AGC levels during our testing period.

TABLE (3)

AGC	10 - 30 dB	30 - 38 dB	38-... dB	Available
RX-1	52 %	46.949 %	1.051 %	98.9490 %
RX-2	67.3 %	31.76 %	0.94 %	99.0600 %
RX-3	97.35 %	2.3 %	0.35 %	99.6500 % ²

Table (3): time percentage of different AGC levels during both testing periods.

¹ Note these percentage times are the outage times of each individual radio channel, the least time is considered to be the net link unavailable time of the path.

² the spare channel RX-3 always carries the pilot tone only when any radio link RX-1 or RX-2 is capable of carrying the traffic; otherwise, it carries the traffic.

done during the spring time.

The accurate calculation of the availability of a link should be based on the largest available database. So, by using our measurements with those done by the company, we should be able to get a good estimate of the real link available time. Table (3) summarize the results.

From Table (3), the least unavailable time was (0.35 %) thus, the availability time of this link is (99.65 %). Later in chapter four, we will calculate the time availability based on the founded statistical model of the link which will be the critical value for the system design and compare it to this value.

3.4.3 Available Time of Jizan to Atuwai

For this path, as we have already mentioned in the introduction that digital links are more difficult to study, because of different definitions and types of outage and available times on digital links. According to CCIR/CCITT recommendations, the outage events occurs when (BER) exceeds a specified value (typically, 10^{-3}) for not more than ten consecutive seconds; and outage time is the accumulated seconds for all outages events in a given time period, say, a month. If the events lasts for more than ten consecutive

seconds, the link is said to be unavailable. The distinction between outage time and the unavailable time, arises from the fact that digital switching lose framing when high bit error ratios persist beyond ten consecutive seconds. One should considers that data failure occurs when $BER > 10^{-4}$, while the link is totally blocked when $BER > 10^{-3}$. Thus, in between these critical values the link can still carries voice applications but not data applications. So more accurate definitions are needed for digital links, such as the errored seconds, the error free seconds, the severely errored seconds, and the degraded minutes. The errored seconds are defined as the number of one second intervals containing at least one bit error during the available time. However, the error free seconds are defined as the number of one second intervals containing no bit errors during the available time, while, the severely errored seconds are the number of one second intervals having a BER worse than 10^{-3} during the available time. Moreover, the degraded minutes are the number of "packaged minutes" having a bit error ratio worse than 10^{-4} ; while the packaged minute is a grouping of 60 seconds which does not include severely errored seconds or periods of unavailability.

Two different experimental approaches will be followed in calculating the availability time of this link, while a third one will be given in chapter four, which is based on

the statistical model of the link. The first approach is based on the readings of the receiver AGC level which was measured from RX1 and RX2 in test one, and the corresponding values of BER1 and SWN1+1 points. Then, according to the system description manual we used the following critical measures to evaluate the path performance:

- * Accepted receiver levels for data and voice is (15-45 dBm), which is equivalent to BER between (10^{-10} - 10^{-6}).

- * Accepted receiver levels for voice but not data is (45-85 dBm), which is equivalent to BER between (10^{-6} - 10^{-3}).

- * The link is unavailable if the receiver level greater than 85 dBm or $BER < 10^{-3}$.

- * The designed net path performance for this link is to have an availability of 99.99957 % of the operating time. The results according to the previous limitation is reported in Table (4). From Table (4), both radio channels do not meet the net path performance criterion. Moreover, the net available time of (RX1) is 99.991 % ; while it is 99.87 % for (RX2). Thus, both radio channel are totally non suitable as a data carrier links; furthermore, (RX2) is more affected by fading than (RX1). This gives an indication that (RX2) path has more atmospheric problems (large duct layers) than the (RX1) path. Also note that (RX1) and (RX2) are allocated two different frequency bands which may causes different performance levels.

TABLE (4)

BER	10^{-10} - 10^{-6}	10^{-6} - 10^{-3}	$>10^{-3}$	Outage ¹	Avail. ²
RX1	68.34 %	31.651 %	.00897%	.0055%	99.99653%
RX2	54.90 %	44.97 %	0.1300%	0.060%	99.93000%

Table (4): Time percentage of different BER values during testing period.

To have more accurate results and to follow the CCIR/CCITT recommendations in calculating the link available time, we did another test using special sophisticated equipment. We borrowed this equipment from Teltra company which constructed this link. The device is a product of HEWLETT PACKARD (Hp) called Digital Transmission Analyzer (Hp 37721A). The Hp 37721A is a multi-rate bit error measuring instrument. It can generate and receive a range of data patterns, and provide analysis of received errors to meet the

¹ Note that the accurate value of link availability is the net available time (L_a). Where $L_a = 100 - \text{outage time} - \text{unavailable time} - \text{degraded minutes}$.

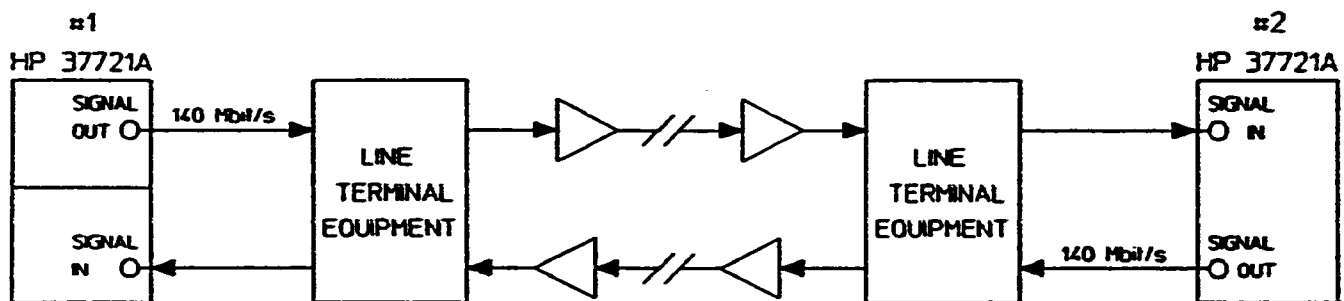
² available time = 100 - unavailable time.

CCIR/CCITT requirements of G.821. Accurate error measurements can still be made in the presence of half-rate cable loss up to 12 dB, and at protected monitor points. The device has an operator interface display and panel keys to control and monitor the measurements as shown in Figure (13).

This device is capable of performing the following tests and applications:

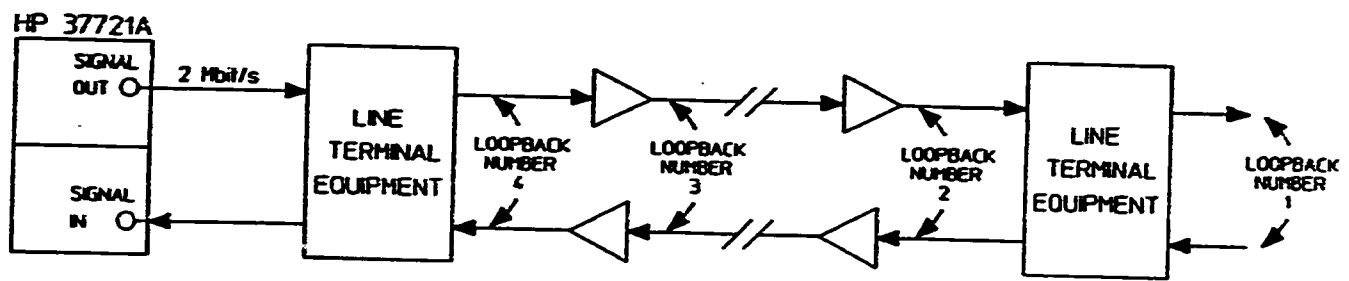
1. **End-to-End Testing** : Any transmission system (radio link) must be specified for an overall error performance, and net availability time. During installation or commissioning it is necessary to check that the link meets this error performance requirements. This test is made on an end-to-end basis, testing the Go and Return paths separately but simultaneously. The measurements are often performed unattended and the results logged to a printer and timed by a real time clock facility. Two Hp 37721A's are needed for this test, one at each end of the link; Figure (14) shows the block diagram of this test.

2. **Loopback Testing** : Loopback testing is used for fault location to a particular piece of line terminal equipment or a repeater. The loopback is normally made at the outermost point of the link for the first test and then moved nearer to the test instrument until the faulty area is located. Figure (15) shows the block diagram of this test.



140 Mb/s End-to-End Test

Figure (14): The End-to-End testing setup.



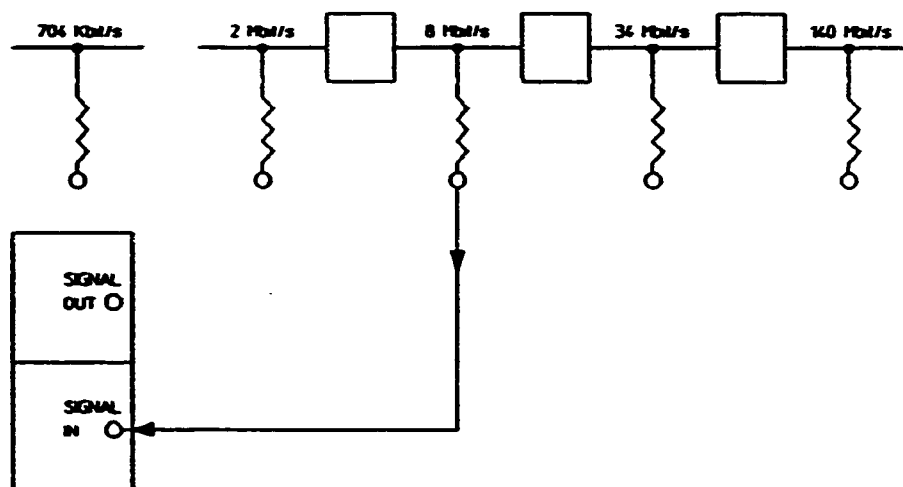
2 Mb/s Loopback Test

Figure (15): The Loopback testing setup.

3. System Monitoring : This test helps us to meet CCITT G.821 availability objectives; by testing the performance of a link without disturbing traffic. Figure (16) shows the block diagram of this test. This setup procedure is based on 34 Mb/s, with HDB3 coded line traffic interfaced at the line equipment monitor point. Alarms and occurrence of code error seconds are logged in real time on the internal printer. Errors count (EC), error ratio (ER), error seconds (ES), error free seconds (EFS), unavailable seconds (UNS), and degrade minutes (DM) results are logged on the printer at 24 Hour intervals and at the end of the test period. When live traffic is being monitored, maximum bit errors will be measured. This will result in a set of analysis results which are used in calculating the available time of the link. In-service testing enables identification of the following :

- * Deterioration in circuit performance before the service seriously affected.
- * Detection of problems which only occurs at certain times of the day, or when certain line traffic conditions exist.

This device is capable of doing more special sophisticated tests such as frequency measurement, frequency offset tolerance, and some statistical analysis with graphics outputs of all stored results. The second test that was conducted to calculate the outage time and the available time of this link includes all of the above described tests.



System Monitoring

Figure (16): The block diagram of System Monitoring test.

This test took place on the period from 10th of November 1992 to 30th of December 1992. Table (5) summarize the results¹.

TABLE (5)

Test Path ²	ES	UNS	EFS	DM	link avail. time
Madiya to Jizan	482	720	2 X10 ⁶	0	99.999399 %
Madiya to Atwal	985	1230	2 X10 ⁶	0	99.998893 %

Table (5): Results of system monitoring of Jizan to Atwal link using the Hp device.

The results of this test are accurate more than the first test, because the device which is used here is designed to perform this test on high rates digital links. As we can see that the results; in general, agrees with the results of the first test and does not meet the design requirement of this link. Moreover, one should not forget that the time of both tests were in spring season, which is not the worst fading season.

¹ For the meaning of the abbreviations see the definitions in the section (3.3.2).

² The unit of measurements of this test are in seconds.

3.5 Summary

This chapter builds the backbone and the basic infrastructure of the experimental work needed to evaluate the performance of the radio links under study. All needed data are collected and the prime investigation shows the urgent need to find the accurate statistical model which fits the needs of this specific region. The obtained model will give solutions to the existing problems and will give the real parameters of this region, which can be used in any future digital communication system design.

CHAPTER FOUR

DATA ANALYSIS AND INTERPRETATION

4.1 Introduction

In order to characterize the microwave channels under study, some statistical analysis of the collected data from the field measurements are needed. This chapter, will summarize the analysis procedures that were conducted, and will describe the statistical methods used in fitting the measured data to the known statistical distributions. Both approximated probability distribution function (PDF), and cumulative distribution function (CDF) of each path will be found.

Also, a study of the channels stationarity will be provided by analyzing the time-correlation functions of each link. One more important channel characteristic, which can be found from the field measurements is the frequency spectrum of the fading, and the coherence fading bandwidth. Some interpretations will also be drawn from the found models, which should help in calculating the available and the outage time of each link.

4.2 Nahran to NJ1 Link

4.2.1 Data Analysis

On this link, the receiver AGC of the three radio channels (RX1), (RX2), and (RX3) were monitored. In general, the fades occurred in bursts of 0.1 to 17 seconds duration, separated by periods during which the received signal remained almost constant. Measurements showed big differences between the main path (RX1) and the space diversity path (RX2), where the latter was having better levels during fading periods. Thus, the higher antenna path (RX2) is receiving stronger signal level, and this may be due to the ducting phenomena in which, the heavy layers of clouds guide the signal higher in altitude, while the lower antenna is in the shade area of the signal.

On the other hand, the frequency diversity path (RX3) (placed on the higher antenna) is the best path and has the best available time. Note that (RX3) is a standby channel for (RX1) and (RX2). Moreover, the received signal level were statistically non-stationary in general.

The mean signal level, for all channels, falls in the range of 15 - 35 dB. Also, the mean time of fading events falls in the range 0.1 - .15 seconds. The typical dynamical range for fading was found to be 35 dB.

4.2.2 Model Fitting

Probability distribution functions (PDF's), and cumulative distribution functions (CDF's) of each channel were computed. In the computation of these functions, interest was in the determination of the envelope (amplitude) statistics during the fading intervals only. For this reason, data collected during the periods between fading bursts were filtered out and omitted from the analysis. This was done by writing a program, that will remove the mean variations, then using a threshold detection algorithm to determine when fading periods occurred and recorded them into a new file.

A drawn samples of the new data found from the collected

fades periods is shown in Figure (17). The new data was used to compute both the (PDF) and (CDF) of each channel. The fitted PDF's of each channel on this path (RX-1, RX-2, and RX-3), and the CDF's of these models are shown in Figures (18), (19), (20), and (21), respectively. These functions were found using the Kolmogorov-Smirnov analysis procedure [29], which is programmed to be used in Statgraphics software. This procedure gives the significant level and the error limits of each fitting which gives an indication to how good is the found model. For example, in the case of (RX-1), the fitted model determined that there is 99 % probability that the true distribution lies within the 2.9 % error region.

Table (6) summarizes the results found from fitting the measured data to the known statistical models. The fade depth statistics for various percentage of time can be easily found from the fitted models as shown in Figures (22), and (23) for each channel on the path. Some critical values of fade depth probability of occurrence are given in the Table (7). From which, we can now calculate the estimated available time of this path according to the statistical models. Thus, the best available time of this path is 99.9977 % which is still less than the objective available time of this link (99.99957 %) specified by the designer.

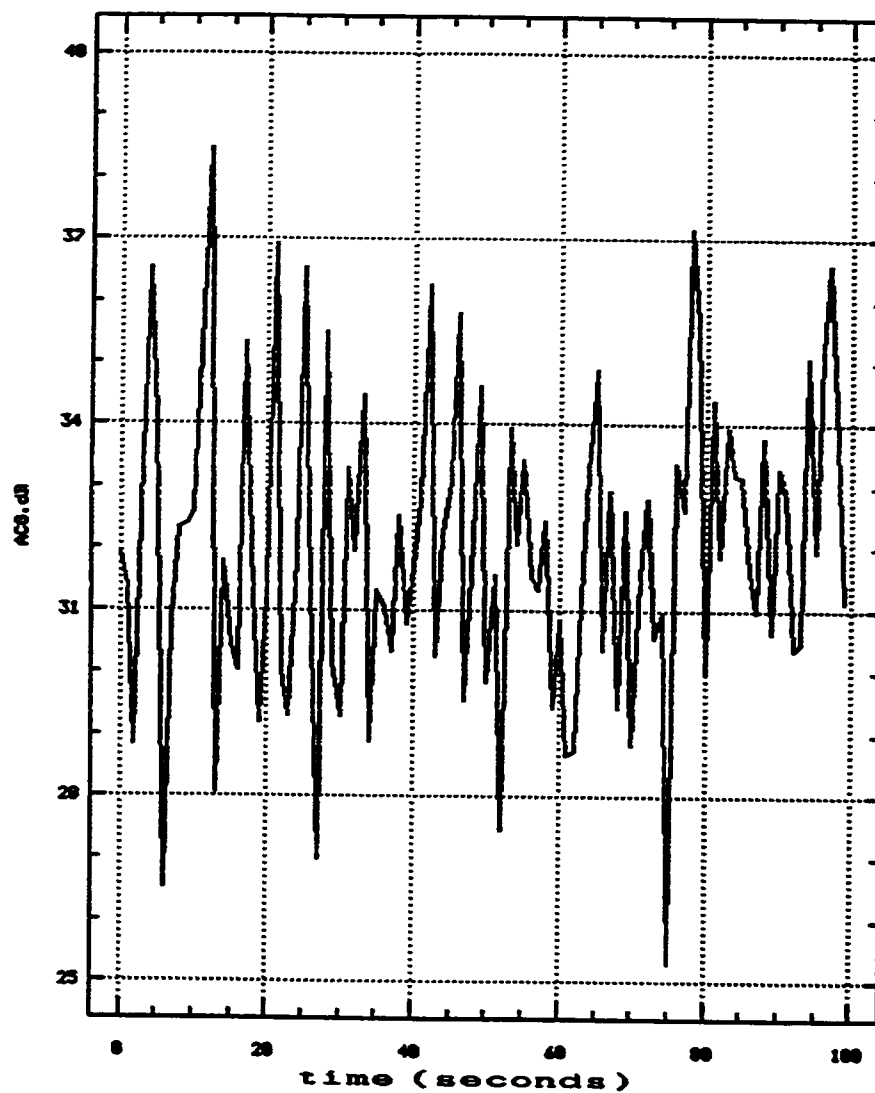


Figure (17): Sample of the new data after filtering out the data of non-fading periods.

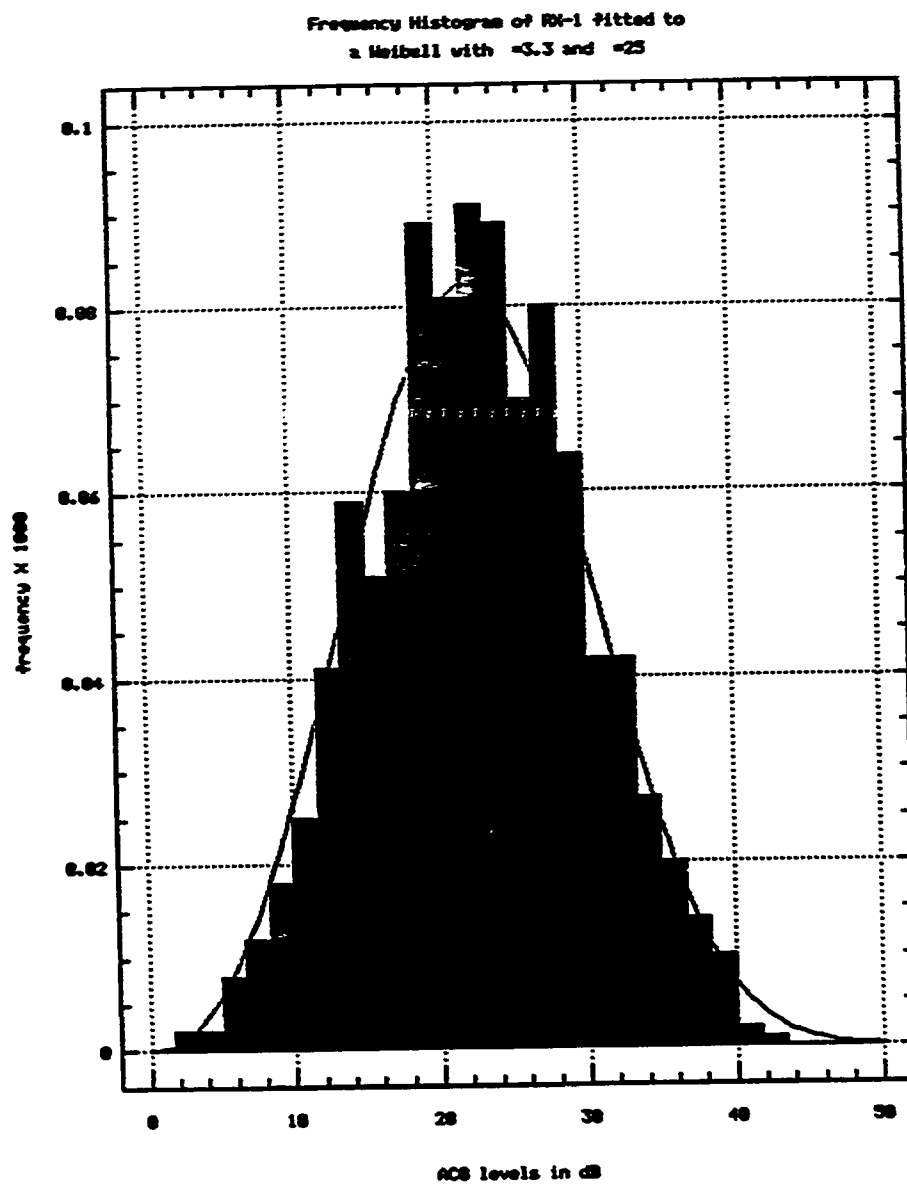


Figure (18): The PDF's of channel RX-1 with the best fitted distribution.

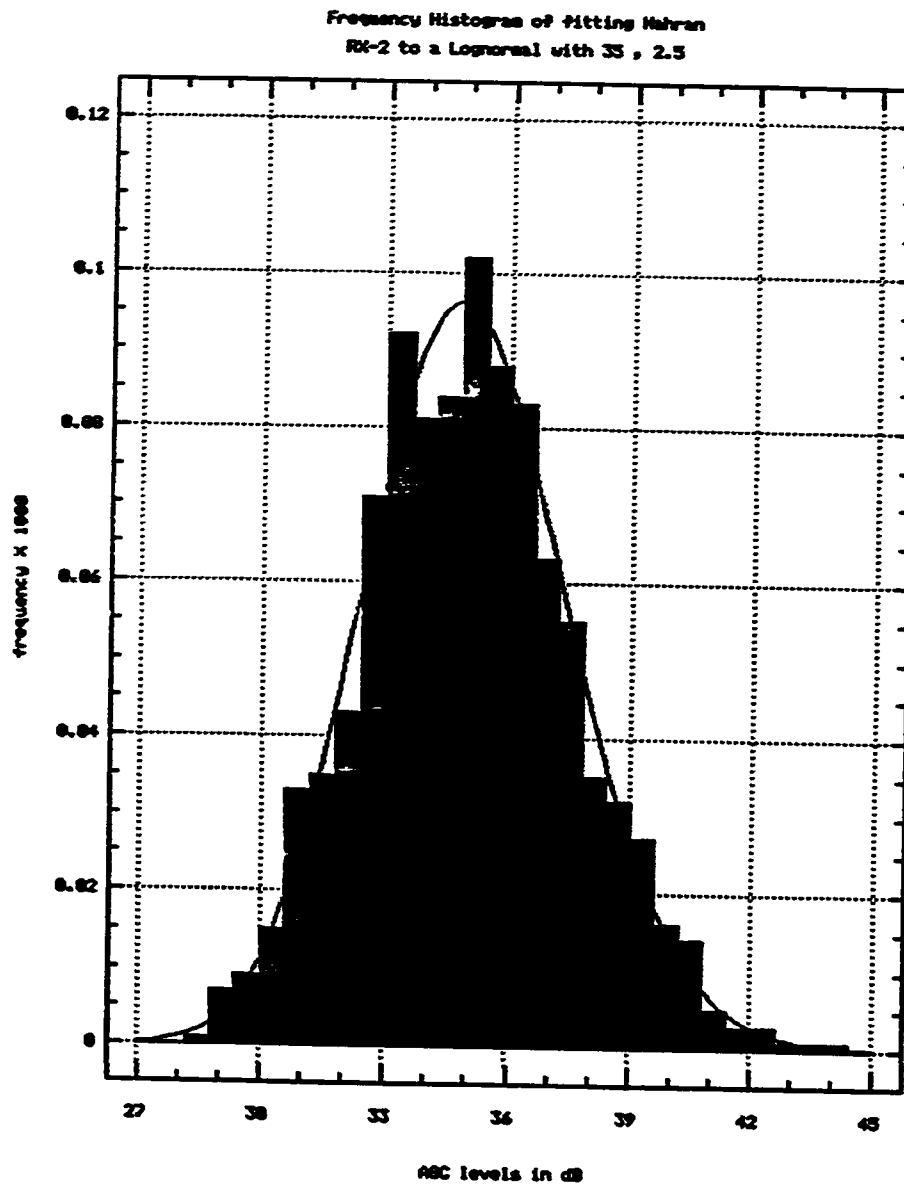


Figure (19): The PDF's of channel RX-2 with its best fitted distribution.

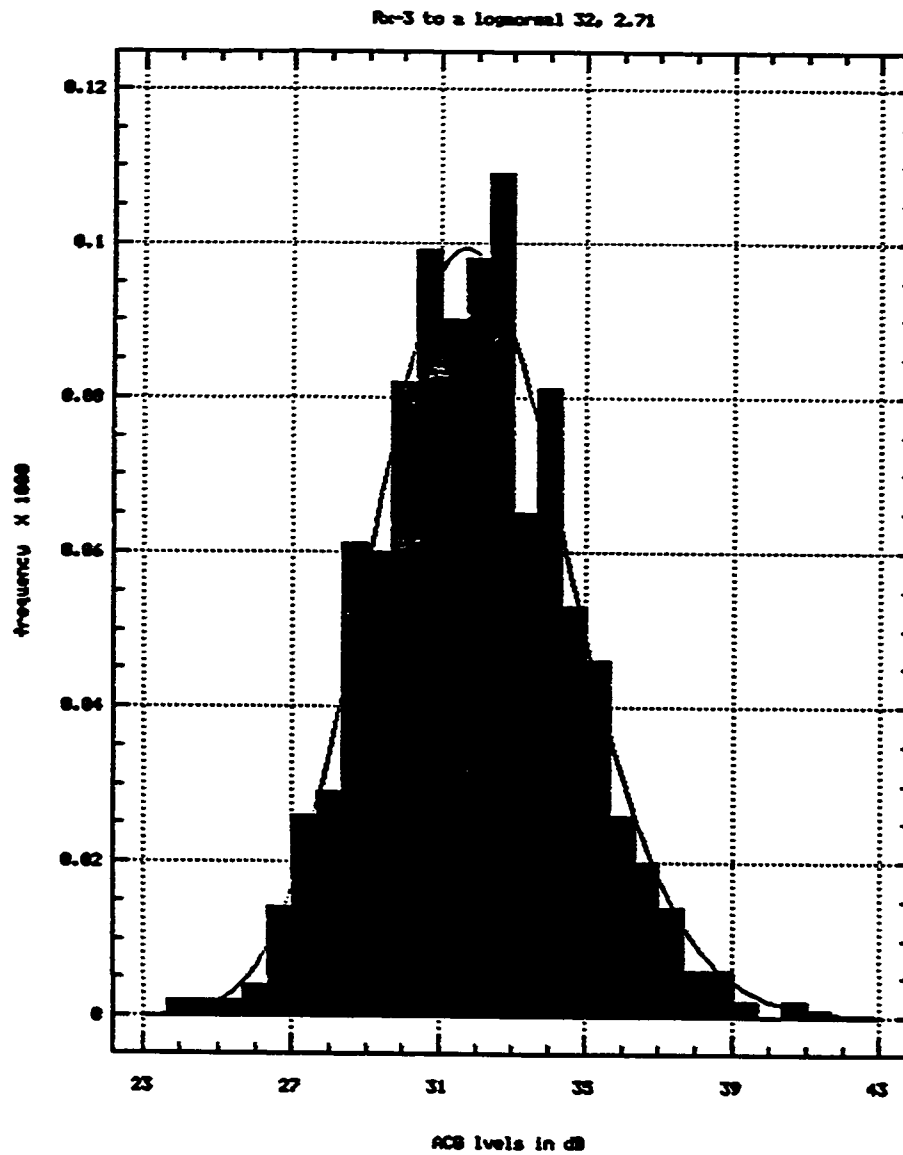


Figure (20): The PDF's of channel RX-3 with its best fitted distribution.

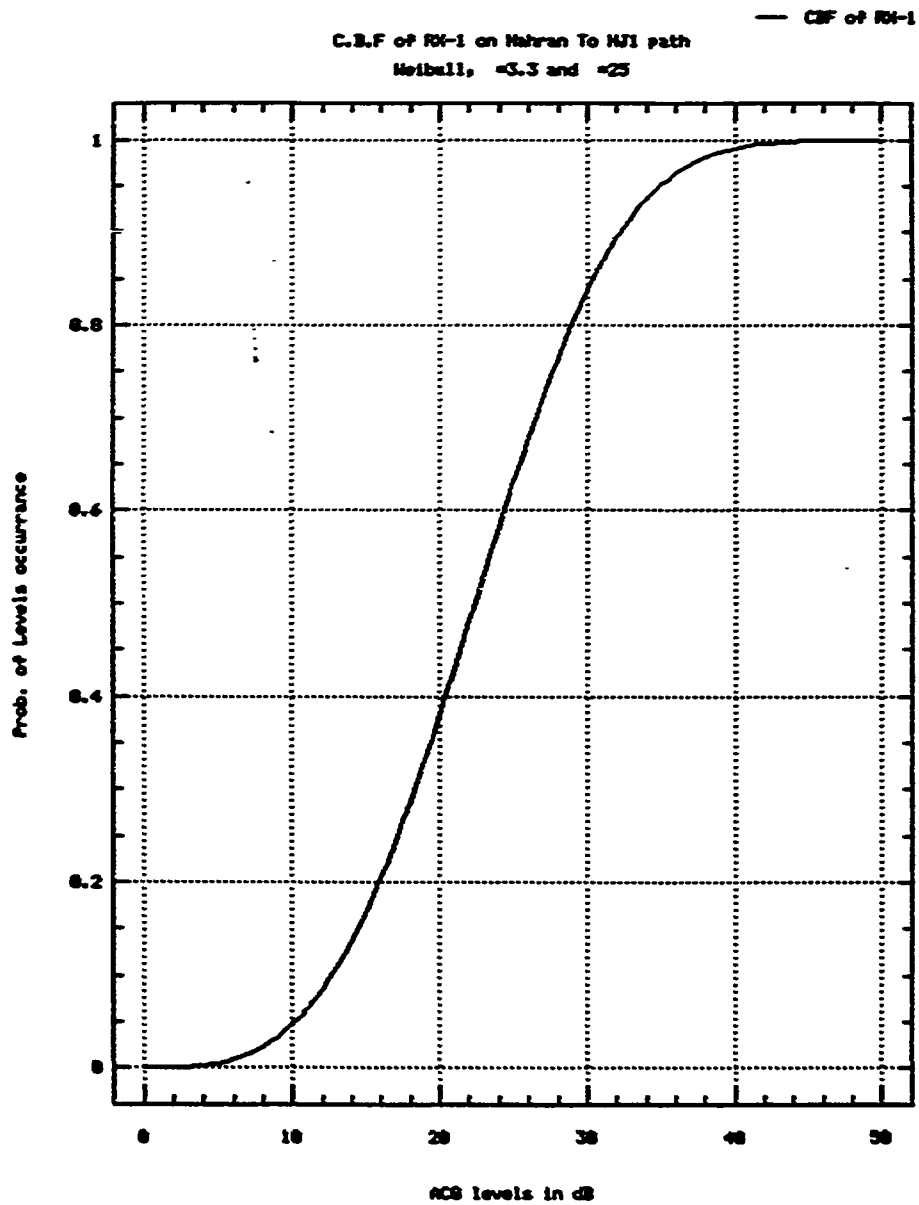


Figure (21-A) : The CDF of channel Rx-1.

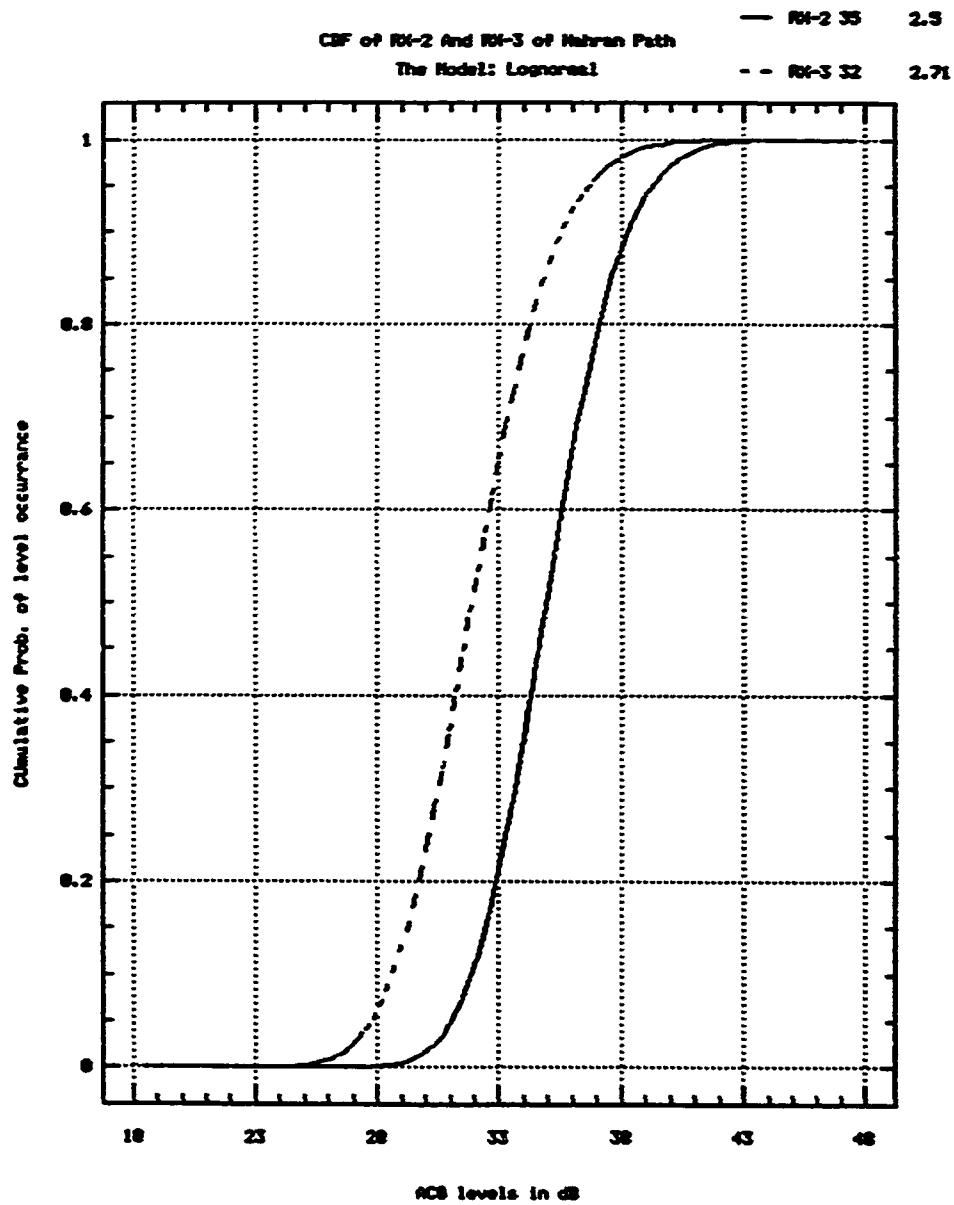


Figure (21-B) : The CDF's of channels Rx-2 and RX-3.

TABLE (6)

Nahran To NJ1	Fitted model and Its Parameters	Significant Level	Error Limits
RX-1	Weibull With $\alpha = 3.3$ $\beta = 25$	99 %	2.9 %
RX-2	Log-Normal With Mean (μ) = 35 dB Variance(σ^2) = 2.5	98 %	2.3 %
RX-3	Log-Normal With Mean (μ) = 32 dB Variance(σ^2) = 2.7	98 %	1.1 %

Table (6): The statistical models of Nahran path.

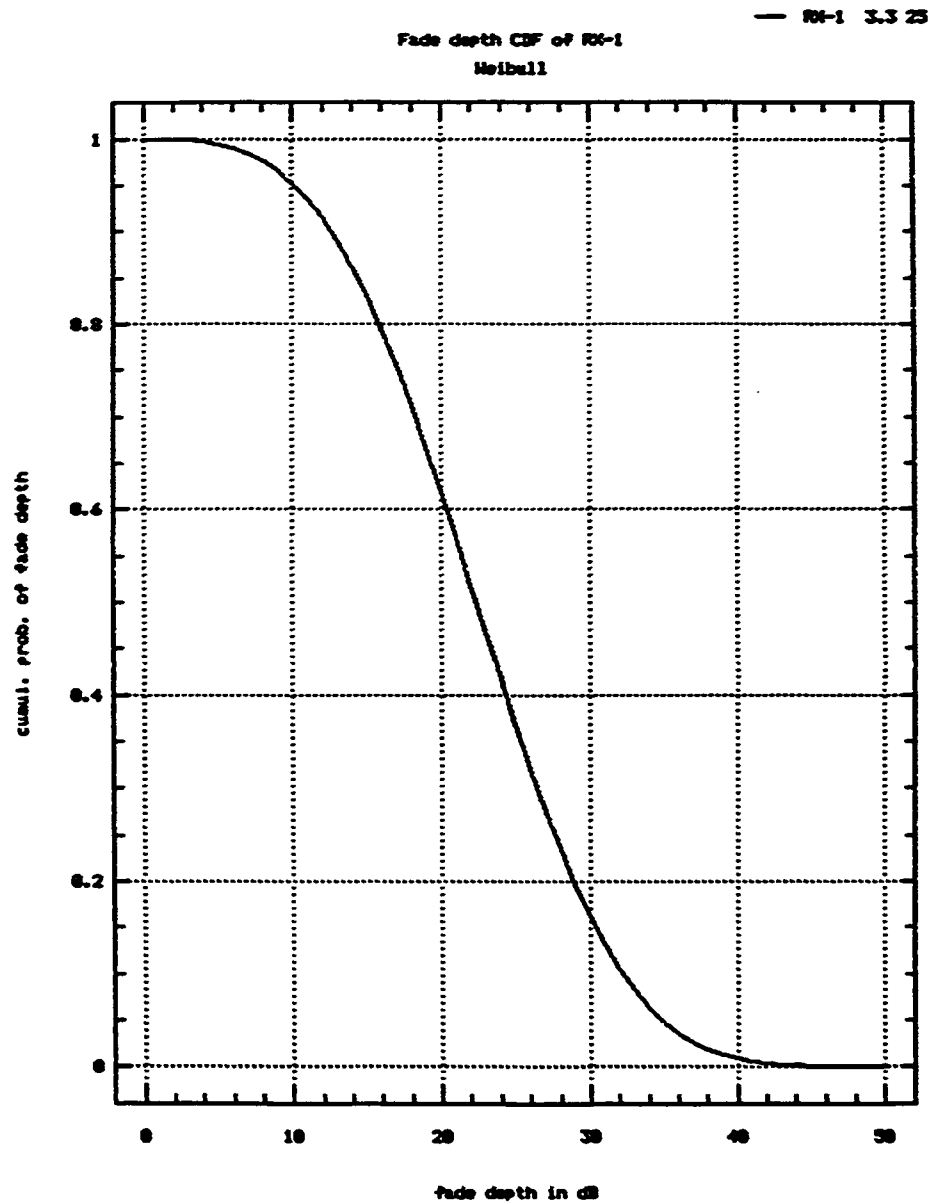


Figure (22): The fade depth statistics for RX-1.

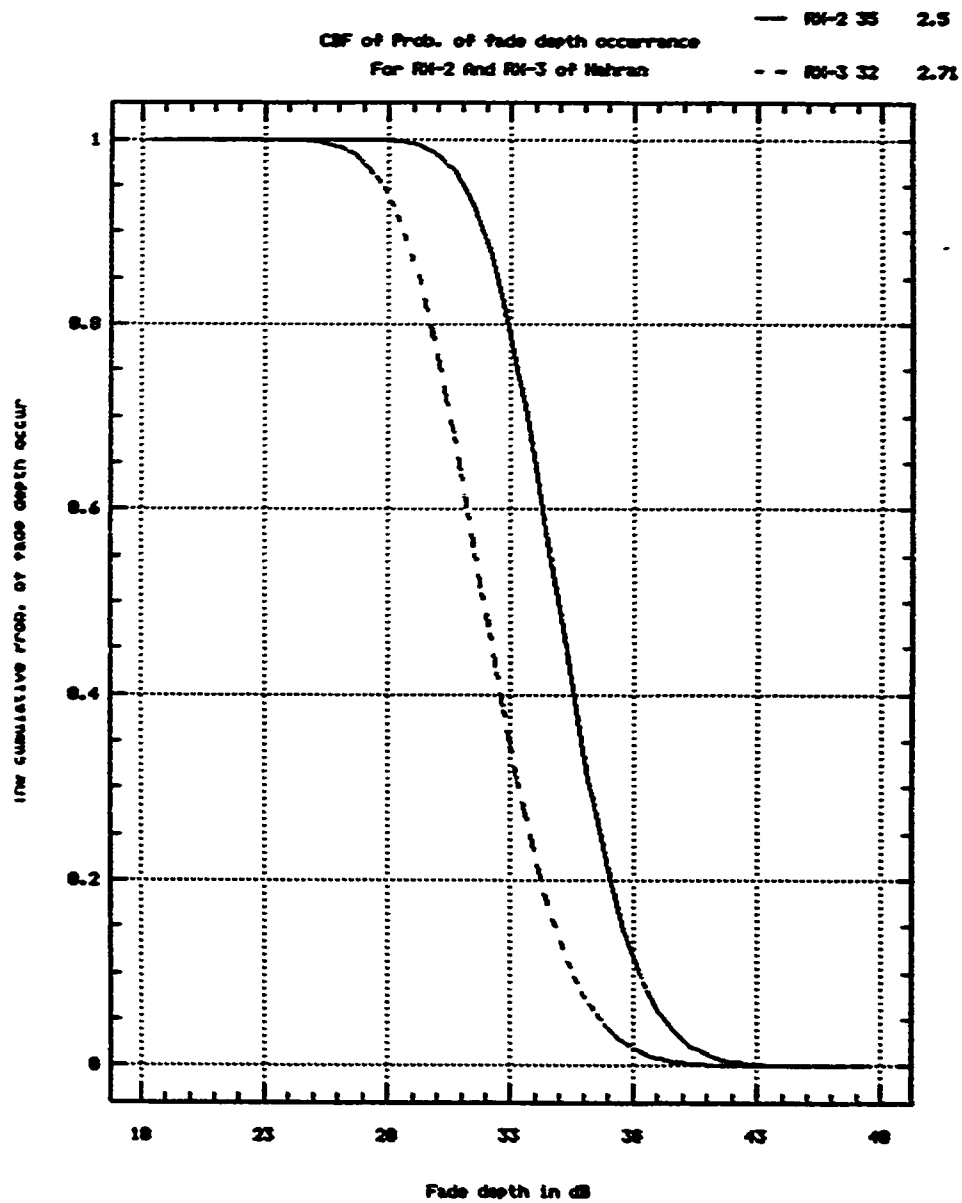


Figure (23): The fade depth statistics for RX-2 & RX-3.

TABLE (7)

AGC A	0 < A < 30	30 < A < 35	35 < A < 38	A > 38
RX-1	85 %	10.7 %	4.2208 %	0.0792 %
RX-2	2 %	49.4 %	48.5814%	0.0186 %
RX-3	23.5 %	22.63 %	53.8677%	0.0023 %

Table (7): Time percentage of AGC levels.

The extent to which the measured channel can be considered to be statistically stationary was determined through the analysis of the time-autocorrelation functions of the received signals (TAF). These functions were estimated using the time series analysis procedure which is available in the Statgraphics program. In general, a random process can be considered to be statistically stationary if its statistical properties are invariant to translation of the index parameters (time or frequency)for the process. In particular, it is classified as a wide-sense stationary process if it has finite variance, and its autocorrelation function is independent of its index parameter.

The time period over which a radio channel can be

considered to be wide-sense stationary, is therefore the range through which the reference time in the (TAF) can be shifted without any significant changes occurring in the (TAF) or its estimate. Thus, to test the channel stationarity one should plot the time-correlation function with different time references on the same set of axis, then if the different time lags give approximately the same shape then the channel is stationary.

Figure (24) shows the correlation function of AGC recorded levels on Nahran path; plotted with different time references (- 2, 0, + 2) seconds. It can be seen that there is little differences in the correlation function shape within the fading interval for time reference shifts up to (+/- 2 seconds). Note that the correlation function in this case is symmetrical with respect to the different references. Thus, this channel is stationary in the wide-sense for periods of times up to at most 4 seconds. On the other hand, the whole system is considered to be non-stationary in the strict-sense. One more channel characteristic that can be derived from the measured data is the frequency spectrum. Such spectra result from the Fourier transforms of the correlation function. Figure (25) is the spectrum for Nahran path. The range over which the spectrum value does not equal approximately to zero is called the fading bandwidth [17].

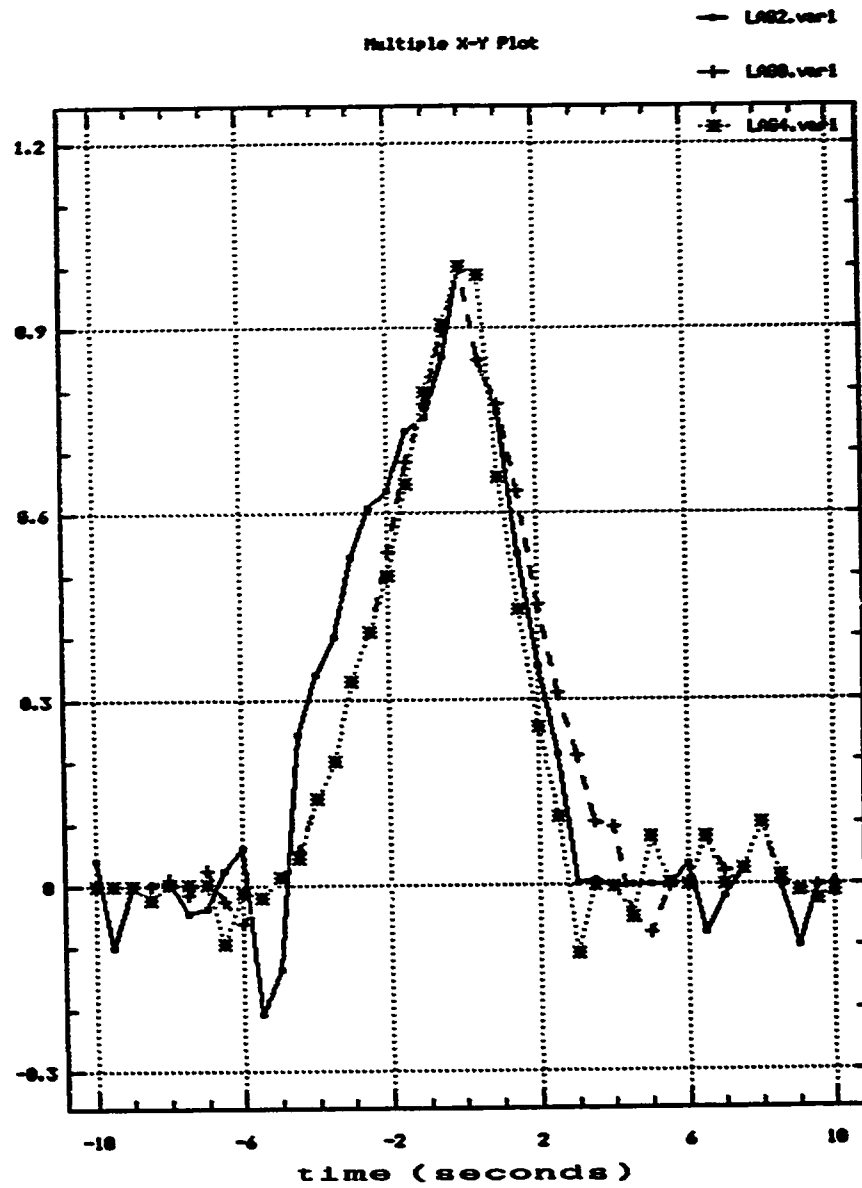


Figure (24): The time correlation function of Nahran.

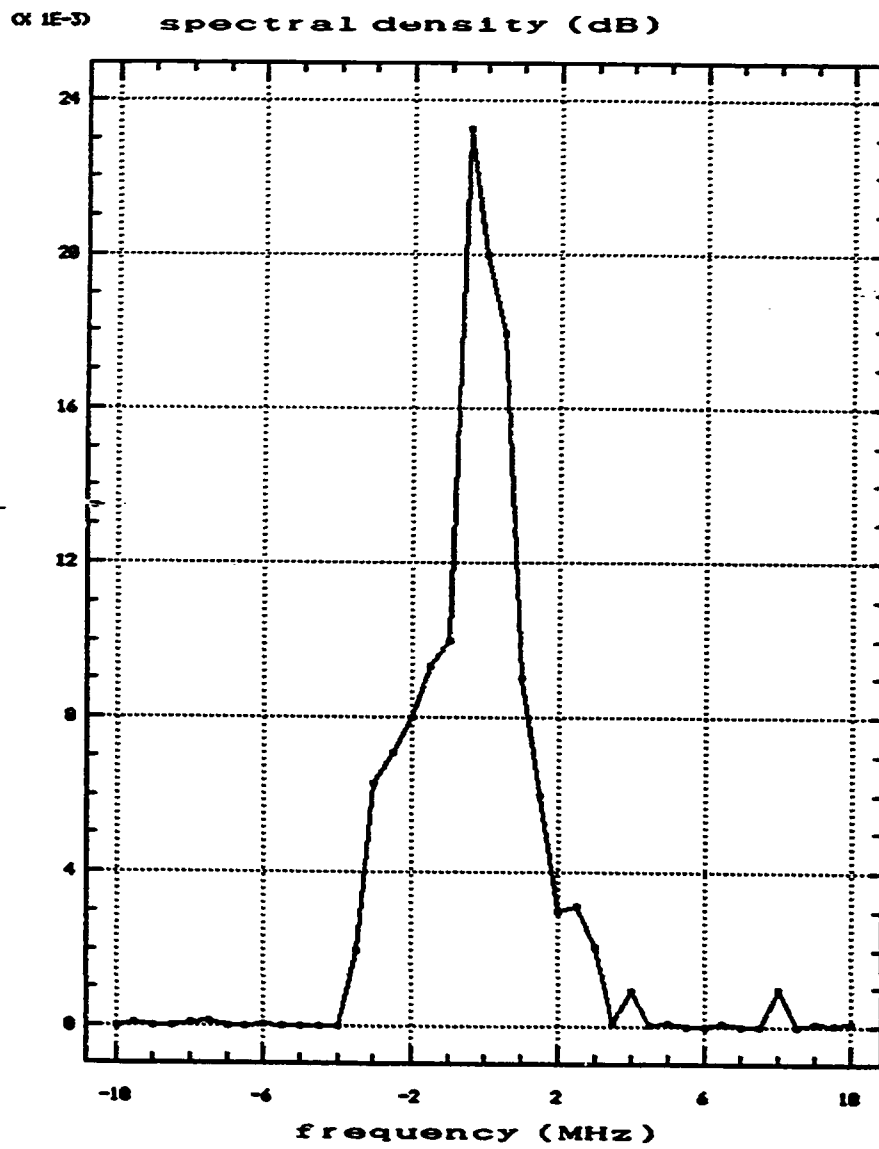


Figure (25): The spectrum for Nahran path.

Thus, the fading bandwidth of the best channel (RX-3) on this path is 7 MHz.

4.2.3 Data Interpretation

Finding different models for the channels in this path, gives us an indication that the spatial field pattern is not uniform. Thus, different altitudes have different field strength and totally different models due to the turbulence associated with the cloud and duct formation on this path. Also, we found that the environment is statistically non-stationary in the strict-sense, except for small periods of time (about 2 sec.).

And since high symbol rates communication systems, transmit large amount of data during this time, the type of fading here is referred to as a quasi-wide-sense stationary fading [11], [12]. So, the statistical methods which are applicable to wide-sense stationary random processes can be applied for error rate calculations of this system. The fading on this path is slow, having a bandwidth of 7 MHz.

4.3 Jizan to Atuwat Link

4.3.1 Data Analysis

The receiver AGC of the two radio channels (RX1), and (RX2) were monitored. The fades occurred in bursts of 0.2 to 22 seconds duration. The measurements showed good similarities between the main path (RX1) and the space and frequency diversity path (RX2), where the former was having better levels during fading periods. Thus, the lower antenna path (RX1) is receiving stronger signal level due to the ducting layers. Moreover, the received signal level were statistically non-stationary during the afternoon period. The mean signal level falls in the range of 15 - 44 dB. Also, the mean time of fading events falls in the range 0.1 - .25 seconds. The typical dynamic range for fading was found to be 42 dB. Thus, the type of fading in this link is a slow frequency selective fading.

4.3.2 Model Fitting

Probability distribution functions (PDF's), and cumulative distribution functions (CDF's) of each channel were computed as in section 4.2.2. The fitted PDF's of each channel on this path (RX-1, and RX-2), and the fitted CDF of

these models are shown in Figures (26), (27), and (28), respectively. Table (8) summarizes the results of fitting the measured data.

The fade depth statistics for various percentage of time was found from the fitted models as shown in Figure (29). Some critical values of fade depth probability of occurrence are given in the Table (9). From which, we can now calculate the estimated available time. Thus, the best available time of this path is 99.9977 % which is still less than the objective available time of 99.99957 % specified by the designer. Figure (30) shows the correlation function of AGC recorded levels on RX-1; plotted with different time references (- 3, 0, + 3) seconds. It can be seen that there is little differences in the correlation function shape within the fading interval for time reference shifts up to (-/+ 3 seconds). Note the correlation function in this case is symmetrical with respect to the different time references. Thus, this channel is stationary in the wide-sense for periods of times up to at most 6 seconds. On the other hand, the whole system is considered to be non-stationary in the strict-sense. Figure (31) is the fading spectrum for RX-1. Thus, the fading bandwidth of the best channel (RX-1) on this path is 9 MHz.

TABLE (8)

Jizan To Atuwal	Fitted model and Its Parameters	Significant Level	Error Limits
RX-1	Rayleigh With Mean =29 Variance= 214	98.5 %	2.2 %
RX-2	Rayleigh With Mean =30 Variance= 386	99 %	1.6 %

Table (8): The statistical models of Jizan path.

TABLE (9)

AGC A	0< A< 45	45< A< 65	65<A <85	A > 85
RX-1	86.59 %	12.4 %	0.988 %	0.021 %
RX-2	82.65 %	14.764 %	2.3937 %	0.1923 %

Table (9): Time percentage of AGC levels on Jizan path.

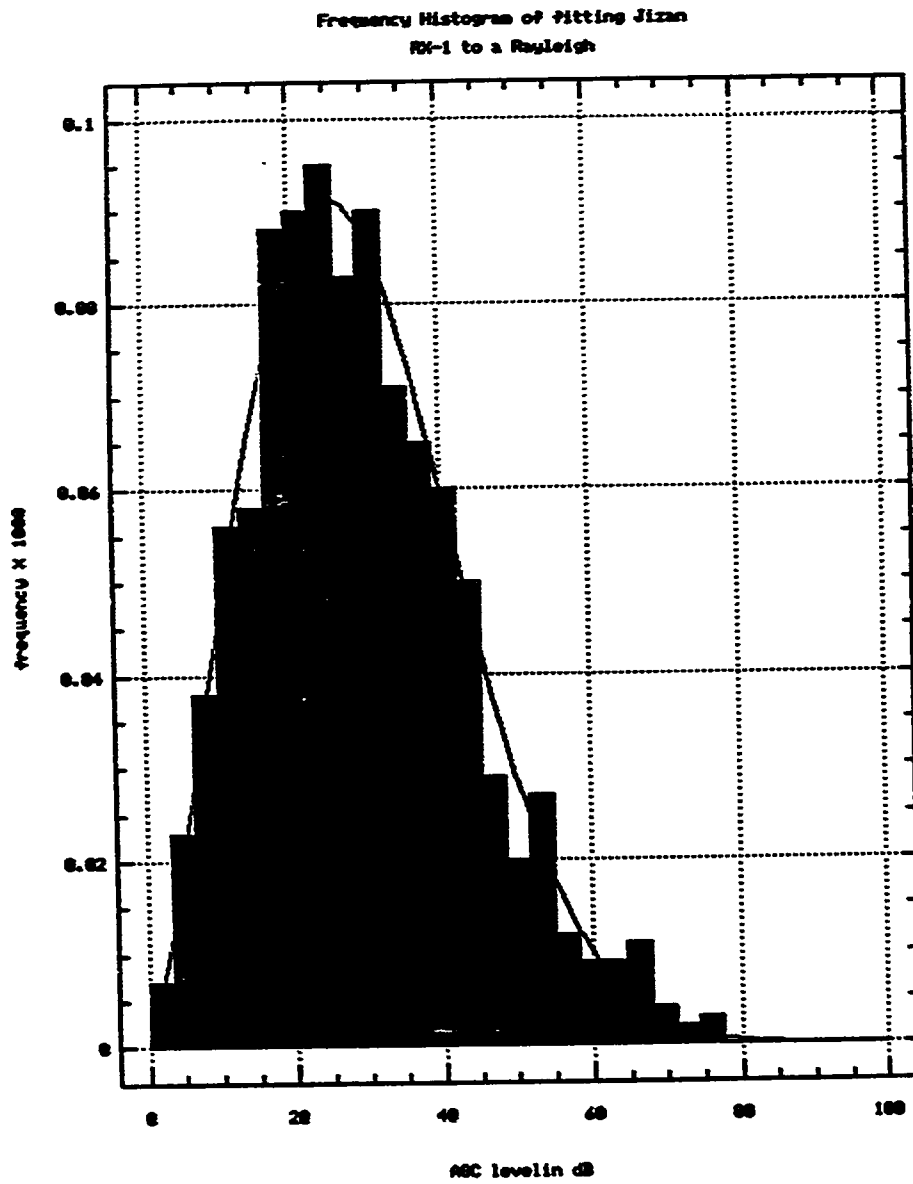
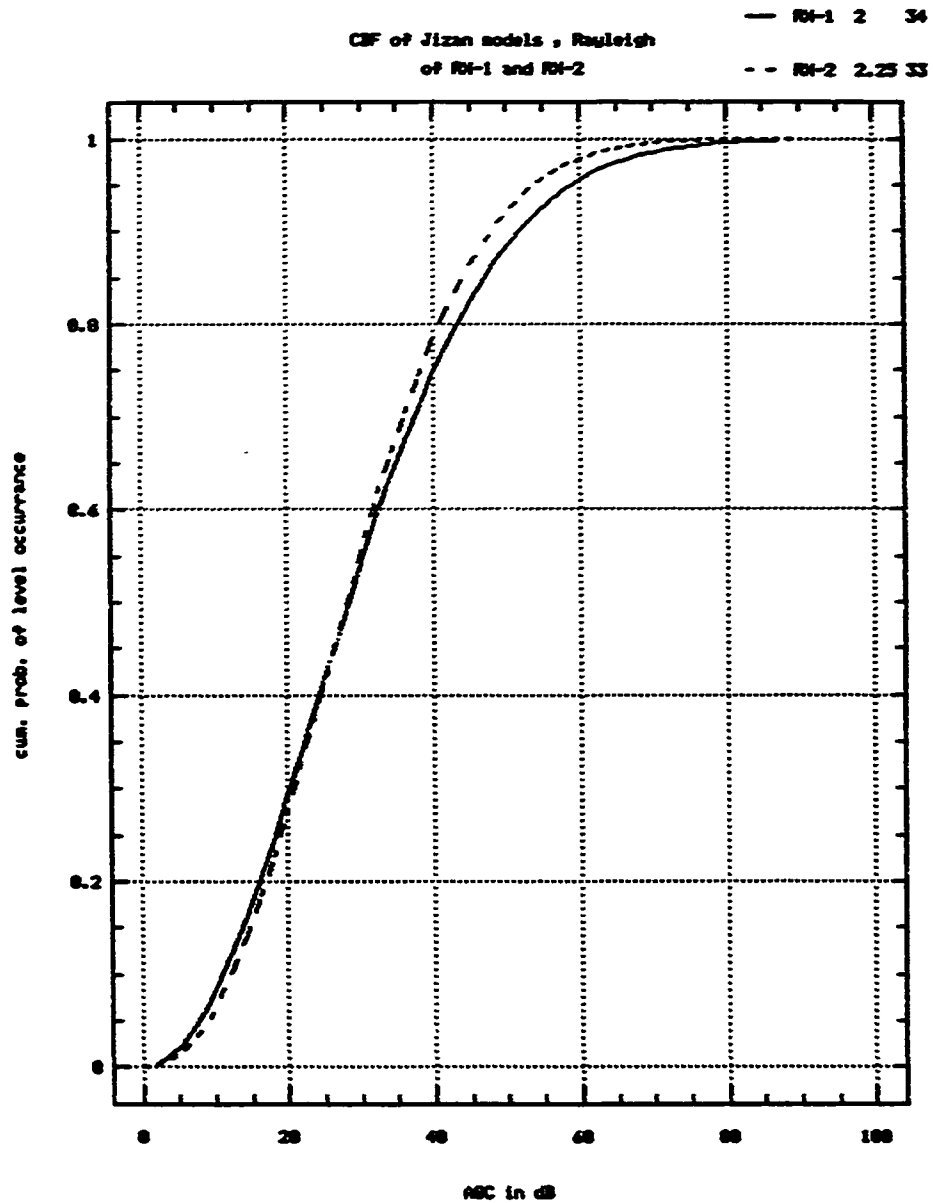


Figure (26): The PDF's of channel RX-1 with its best fitted distribution.



Figure (27): The PDF's of channel RX-2 with
its best fitted distribution.



Figuer (28): The CDF's of channels Rx-1 and RX-2.

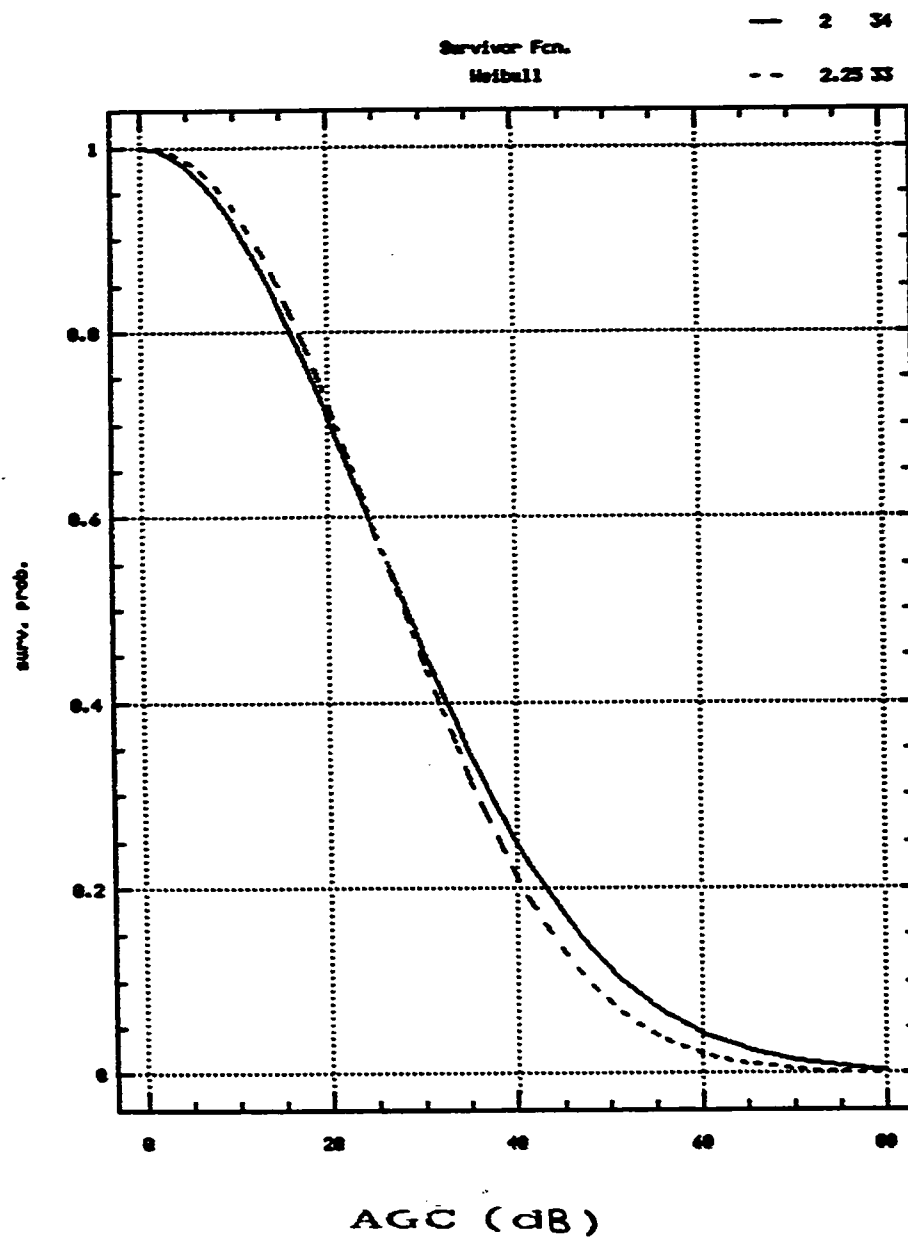


Figure (29): The fade depth statistics for RX-1 & RX-2.

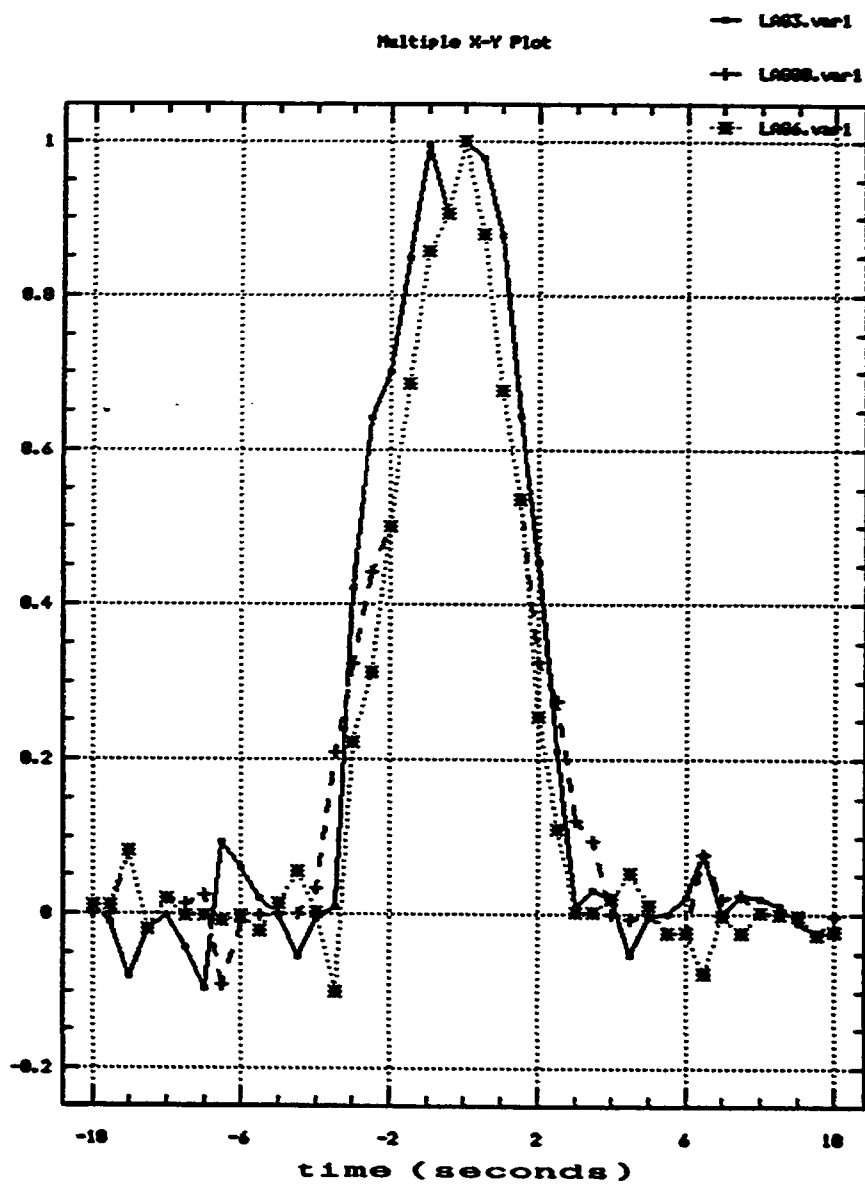


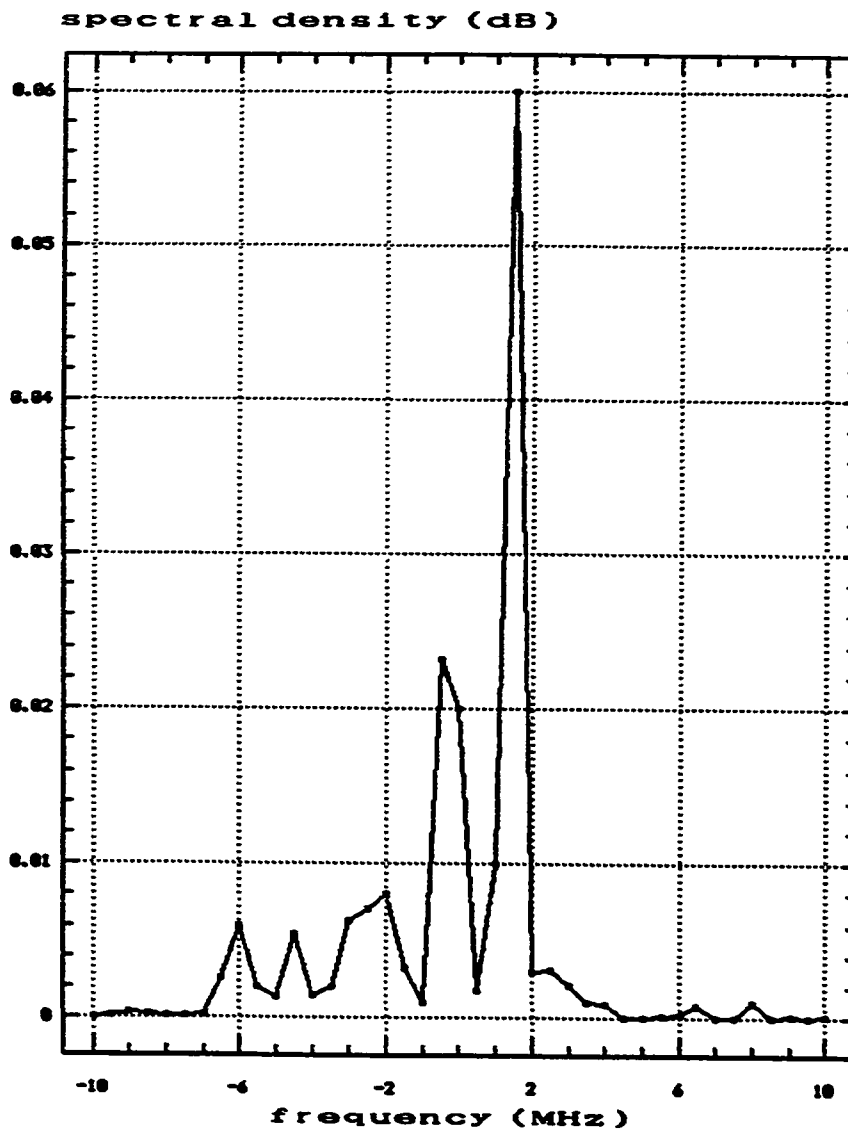
Figure (30): The time correlation function of Jizan.

4.3.3 Data Interpretation

The spatial field pattern of this path is quasi-uniform and is changing from a steady constant to a completely non-uniform during the early morning and afternoon. Different altitudes have different field strength due to the duct formation on this path. Also, we found that the environments is statistically non-stationary in the strict-sense, except for small periods of time (about 6 seconds). This type of fading is referred to as a quasi-wide-sense stationary fading [11], [12]. So, as we found for Nahran path, all statistical methods are applicable for error rate calculations of the system. this path is a quasi-static.

4.4 Summary

This chapter summarize the statistical analysis procedures, which were used in modeling the two links under study. Furthermore some analytical methods were used to find some important parameters of these link such as the TAF's, the fading spectrum, and the coherence fading bandwidth. At the end some comments were given based on the results of these analysis.



Figuer (31): The spectrum for Jizan path.

CHAPTER FIVE

CONCLUSIONS AND SUGGESTIONS FOR FURTHER WORK

In this chapter, we shall present a brief summary of our findings regarding the two microwave links we studied. This is followed by some possible conclusions drawn from the results of this study then some extension analytical works and experimental plans are suggested for future studies.

5.1 Summary & Conclusions

The following summary and conclusions were reached from our study to two different radio links in the Southern Region of Saudi Arabia. It was noticed that the Nahran to NJ1 (analogue) link does not fall into any of the known channel

categories. It is a new mixed model, in which, the path has both weak and strong surface reflection, ducting, rain, sand, dust, and a very stratified atmospheric conditions.

On the other hand, the Jizan to Atuwai (digital) link simulates a shallow bowl which leads to duct formation, and the terrain traversed by this path is highly reflective. This link falls into the category of highly reflective tropical region. Our results show that the existing system model fails to cope with the needs of having stable communications on these links.

For the first link, it was noticed that the fading type encountered is different from one radio channel to the other due to different frequency allocation and antenna height. Two different fading occasions (coupled with the weather conditions) occur at early afternoon and early morning hours, in which we noticed that the channel of the higher antenna and frequency RX3 is performing better than the other two.

The fading type is found to be slow and frequency-selective, but during some times we noticed that RX1 and RX2 are suffering from frequency non-selective (flat) fading during the hot still weather. This fading is caused by single path propagation effects, but it is less significant form the multipath fading case.

It was found that the actual available time is 99.65 % while it should reach 99.9977 % based on the new statistical model of the link. One noted that the real available time is much less than the model's one and this can happen due to other causes of such as old equipment failures and human errors. Furthermore, the best available time is less than the objective available time specified by the designer which is 99.99957 % . Thus, one should remember that to achieve this target time availability system design should be adjusted, or reconfigured, and other fading countermeasures should be incorporated.

This channel is stationary in the wide-sense for periods of times up to at most 4 seconds. On the other hand, the whole system is considered to be non-stationary in the strict-sense. The coherence fading bandwidth of this path is 7 MHz. Since the fading bandwidth is narrower than that of the system, this path is referred to as quasi-static.

The effect of such slow fading on the performance of analogue systems is not bad as to that on digital systems. Thus, analogue systems can cope with the multipath fading exist on this path unless it is a power fading or a total system outage. On the other hand, the effect of this fading on digital systems is dependant upon the duration of signal transmission, and the continuity of the fading.

The fading type on the second path is due to the interference between the main beam and other delayed beams caused by duct layers and humid dust storms. Also, there are two different types of fading; the first effect occurs between 2-4 PM while the second case occurs usually in the night and early morning hours between 2-8 AM. The fading type is slow and frequency-selective.

Also, we noticed no big difference between the performance of Madiya to Jizan path and Madiya to Atuwat path, where the first has both frequency and space diversity at both sides and the second has only frequency diversity toward Atuwat. This point, gives more indication that the design of this path and the model used is not suitable and the more realistic model which we found should help the designer to modify the system to overcome the existing problems.

This channel is stationary in the wide-sense for periods of times up to at most 6 seconds. The whole system is considered to be non-stationary in the strict-sense.

After all of these tests, it was found that this path is suitable for carrying voice but not data. Moreover, the company which designed this path thinks that the problem is due to a miss-balance in the design, since no space diversity

was installed between Madiya and Atuwai. However, from the result of this study, we see that it is almost impossible to achieve the designed time availability of 99.99957 % without advanced fading countermeasures like coding and channel equalizers.

The Nahran to NJ1 system is an analogue (FM-FDM), it contains most of its energy at the carrier frequency and its information is redundantly encoded in its sidebands. Hence, it is adversely affected by loss of power at the carrier frequency, but relatively unaffected by loss of the signal in only one of the sidebands. For this reason, in FM systems modeling we focus on single-frequency fading statistics. However, unlike FM signals, a digital radio signal does not have redundant information in its sidebands and adds more difficulty when a selective loss damages some of its frequency components.

One important point we should stress on here is that the path is very sensitive to climatical effects and we would face lots of problems if we were having digital system unless we know the real parameters of the statistical model.

5.2 Future Work

Future work should include two different approaches. Those are the experimental and the analytical approaches. In the experimental part, one should conduct more advanced tests to find the following points :

1- The scattering function which will include both the time delay and frequency shift due to fading. Moreover, one can identify or locate the sources of fading and how much each one is contributing loss of the transmitted signals. In general, this is can be done by using the new models and doing some computer simulation tests in which one would fix all parameter and assume that only one factor is contributing the fading and find how much does this factor affect the system and so on. Also this is can be done by using impulse transmission techniques, which permit direct amplitude and delay measurements to resolve received signal components. To have some guidance on the steps of these test one should refer to [17], [18], and see CCIR report 338-5.

2- The envelope and phase statistics of digital system by using advance equipments such as the HP 37721A which is capable of monitoring in service links, and we need to have a quadrature double-balanced mixer circuit to split the In-

phase and quadrature components.

On the other hand, the analytical part should include the calculation of the following points :

1- The predicted performance of different digital system with different type of coding and modulation under the new model of this region.

2- The different parameters of the microwave system such as the frequency plan, hop-to-hop length, type of diversity, type of coding, type of modulation and signalling.

Appendix A

Sample Program

This program was written to control the A/D translating board using basic language. This program assumes that there is a DT2801-A or any other type of the DT280's family with expander installed at the factory base address of &H2EC. The on-board pacer clock is set to a period of 30000 base 90 period ticks. This corresponds to a frequency of 10 Hz for 100 standard speed boards and 20 Hz for the high-speed DT2801-A or DT2818. The user is asked if the board is a DT2801, if it is a DT2805, etc., until the user answers yes or until all of the board types are used up. If all the board types are used up, the program halts. Once the user answers yes for a particular board type, values are assigned to various board parameters. If the board includes SE/DI options, the user is asked whether the board is being run SE or DI.

If the board includes unipolar/bipolar options, the user is asked whether the board is being run unipolar or bipolar. At this point the program can determine all of the parameters of the A/D converter. After the program determines all the parameters of the A/D converter, the user is asked for the gain, start channel, end channel and number of conversion values to be used for the A/D operation. The "SET A/D PARAMETERS" command is then issued, using the gain, start channel, end channel and number of conversion value parameters determined from user input. The user is asked to decide whether or not the EXTERNAL TRIGGER and EXTERNAL CLOCK are to be used. Then the "READ A/D" command is issued. The

data values are read from the Data Out Register as they become available. The A/D data values are converted to voltage and printed.

```

350     CLS : PRINT
400     PRINT "  contiuous READ A/D controlling program "
420     PRINT : PRINT
430 ''
440 OPEN  "nahran" AS #1 LEN=16
442 field #1,4 as ch1$,4 as ch2$,4 as ch3$,4 as ch4$
450     DEFINT A-Z
460     BASE.ADDRESS      = &H2EC
470     COMMAND.REGISTER  = BASE.ADDRESS + 1
480     STATUS.REGISTER   = BASE.ADDRESS + 1
490     DATA.REGISTER    = BASE.ADDRESS
500     COMMAND.WAIT      = &H4
510     WRITE.WAIT        = &H2
520     READ.WAIT         = &H5
530 ''
540     CSTOP             = &HF
550     CCLEAR            = &H1
560     CERROR            = &H2
570     CCLOCK            = &H3
580     CSAD              = &HD
590     CRAD              = &HE
600     EXT.CLOCK         = &H40
610     EXT.TRIG          = &H80
620     PERIOD#           = 30000!
630     MENU$             = "EP00.BAS"
640     MIN.CONV           = 3
650     MAX.CONV          = 1000
660 ''
670 '' Dimension arrays to hold high and low bytes of A/D
    Data.
680 ''
690     DIM ADL(MAX.CONV), ADH(MAX.CONV)
700 ''
710 '' A/D parameter constants.
720 ''
730     PGH(0) = 1 : PGH(1) = 2 : PGH(2) = 4 : PGH(3) = 8
740     PGL(0) = 1 : PGL(1) = 10 : PGL(2) = 100 : PGL(3) = 500
750     PGX(0) = 1 : PGX(1) = 1 : PGX(2) = 1 : PGX(3) = 1
760 ''
770     SE.CHANNELS = 16 : DI.CHANNELS = 8

```

```

780    DT2818.CHANNELS = 1      : EXP.CHANNELS = 64
790 ''
800    FACTOR.10# = 1024      : FACTOR.12# = 4096
810    FACTOR.16# = 32768!
820 ''
830    UNI.RANGE = 10          : UNI.OFFSET = 0
840    BIP.RANGE = 20          : BIP.OFFSET = 10
850    BIP16.RANGE = 10       : BIP16.OFFSET = 0
860    UNI8.RANGE = 5          : UNI8.OFFSET = 0
870 ''
880 '' Check for legal Status Register.
890 ''
900    STATUS = INP(STATUS.REGISTER)
910    IF NOT((STATUS AND &H70) = 0) THEN GOTO 4210
920 ''
930 '' Stop and clear the DT2801.
940 ''
950    OUT COMMAND.REGISTER, CSTOP
960    TEMP = INP(DATA.REGISTER)
970    WAIT STATUS.REGISTER, COMMAND.WAIT
980    OUT COMMAND.REGISTER, CCLEAR
990 ''
1000 '' Set internal clock rate to 10 Hz (20 Hz DT2801-A,
      DT2818)
1010 ''
1020 '' Write SET CLOCK PERIOD command.
1030 ''
1040    WAIT STATUS.REGISTER, COMMAND.WAIT
1050    OUT COMMAND.REGISTER, CCLOCK
1060 ''
1070 '' Write high and low bytes of PERIOD#.
1080 ''
1090    PERIODH = INT(PERIOD#/256)
1100    PERIODL = PERIOD# - PERIODH * 256
1110    WAIT STATUS.REGISTER, WRITE.WAIT, WRITE.WAIT
1120    OUT DATA.REGISTER, PERIODL
1130    WAIT STATUS.REGISTER, WRITE.WAIT, WRITE.WAIT
1140    OUT DATA.REGISTER, PERIODH
1150 ''
1160 '' INPUT "          Is the board a DT2801 (Y/N)";Y$
1170    IF Y$ = "N" OR Y$ = "n" THEN GOTO 1250
1180    IF NOT (Y$ = "Y" OR Y$ = "y") THEN GOSUB 3920
1190    IF NOT (Y$ = "Y" OR Y$ = "y") THEN GOTO 1150
1200 ''
1210    FACTOR# = FACTOR.12#
1220    GAIN(0) = PGH(0) : GAIN(1) = PGH(1)

```

```

1230  GAIN(2) = PGH(2) : GAIN(3) = PGH(3)
1240  GOSUB 3540 : GOSUB 3730 : GOTO 1920
1250  ''
1260  '' INPUT "          Is the board a DT2805 (Y/N)";Y$
1270  IF Y$ = "N" OR Y$ = "n" THEN GOTO 1350
1280  IF NOT (Y$ = "Y" OR Y$ = "y") THEN GOSUB 3920
1290  IF NOT (Y$ = "Y" OR Y$ = "y") THEN GOTO 1250
1300  ''
1310  FACTOR# = FACTOR.12#
1320  GAIN(0) = PGL(0) : GAIN(1) = PGL(1)
1330  GAIN(2) = PGL(2) : GAIN(3) = PGL(3)
1340  GOSUB 3540 : NUMBER.CHANNELS = DI.CHANNELS : GOTO
1920
1350  ''
1360  '' INPUT "          Is the board a DT2801-A (Y/N)";Y$
1362  Y$="Y"
1370  IF Y$ = "N" OR Y$ = "n" THEN GOTO 1450
1380  IF NOT (Y$ = "Y" OR Y$ = "y") THEN GOSUB 3920
1390  IF NOT (Y$ = "Y" OR Y$ = "y") THEN GOTO 1350
1400  ''
1410  FACTOR# = FACTOR.12#
1420  GAIN(0) = PGH(0) : GAIN(1) = PGH(1)
1430  GAIN(2) = PGH(2) : GAIN(3) = PGH(3)
1440  GOSUB 3540 : GOSUB 3730 : GOTO 1920
1450  ''
1460  INPUT "          Is the board a DT2801/5716
      (Y/N)";Y$
1470  IF Y$ = "N" OR Y$ = "n" THEN GOTO 1560
1480  IF NOT (Y$ = "Y" OR Y$ = "y") THEN GOSUB 3920
1490  IF NOT (Y$ = "Y" OR Y$ = "y") THEN GOTO 1450
1500  ''
1510  FACTOR# = FACTOR.16#
1520  GAIN(0) = PGH(0)      : GAIN(1) = PGH(1)
1530  GAIN(2) = PGH(2)      : GAIN(3) = PGH(3)
1540  RANGE = BIP16.RANGE : OFFSET = BIP16.OFFSET
1550  NUMBER.CHANNELS = DI.CHANNELS : GOTO 1920
1560  ''
1570  INPUT "          Is the board a DT2805/5716
      (Y/N)";Y$
1580  IF Y$ = "N" OR Y$ = "n" THEN GOTO 1670
1590  IF NOT (Y$ = "Y" OR Y$ = "y") THEN GOSUB 3920
1600  IF NOT (Y$ = "Y" OR Y$ = "y") THEN GOTO 1560
1610  ''
1620  FACTOR# = FACTOR.16#
1630  GAIN(0) = PGL(0)      : GAIN(1) = PGL(1)
1640  GAIN(2) = PGL(2)      : GAIN(3) = PGL(3)

```

```

1650  RANGE = BIP16.RANGE : OFFSET = BIP16.OFFSET
1660  NUMBER.CHANNELS = DI.CHANNELS : GOTO 1920
1670  ''
1680  INPUT "          Is the board a DT2818 (Y/N)";Y$
1690  IF Y$ = "N" OR Y$ = "n" THEN GOTO 1770
1700  IF NOT (Y$ = "Y" OR Y$ = "y") THEN GOSUB 3920
1710  IF NOT (Y$ = "Y" OR Y$ = "y") THEN GOTO 1670
1720  ''
1730  FACTOR# = FACTOR.12#
1740  GAIN(0) = PGX(0) : GAIN(1) = PGX(1)
1750  GAIN(2) = PGX(2) : GAIN(3) = PGX(3)
1760  GOSUB 3540 : NUMBER.CHANNELS = DT2818.CHANNELS :
      GOTO 1920
1770  ''
1780  INPUT "          Is the board a DT2808 (Y/N)";Y$
1790  IF Y$ = "N" OR Y$ = "n" THEN GOTO 1880
1800  IF NOT (Y$ = "Y" OR Y$ = "y") THEN GOSUB 3920
1810  IF NOT (Y$ = "Y" OR Y$ = "y") THEN GOTO 1770
1820  ''
1830  FACTOR# = FACTOR.10#
1840  GAIN(0) = PGX(0) : GAIN(1) = PGX(1)
1850  GAIN(2) = PGX(2) : GAIN(3) = PGX(3)
1860  RANGE = UNI8.RANGE : OFFSET = UNI8.OFFSET
1870  NUMBER.CHANNELS = SE.CHANNELS : GOTO 1920
1880  ''
1890  '' Board type not found.
1900  ''
1910  GOTO 4290
1920  ''
1930  '' Get A/D gain.
1940  ''
1950  PRINT
1960  '' PRINT "          Set gain, start channel, end
      channel and number of"
1970  '' PRINT "          conversions values to be used for
      A/D parameters."
1980  '' PRINT : PRINT "          ";
1990  PRINT "Legal values for gain are ";GAIN(0);",
      ";GAIN(1);
2000  PRINT ", ";GAIN(2);", and ";GAIN(3);"."
2010
2020  ''
2030  FOR GAIN.CODE = 0 TO 3 : IF GAIN(GAIN.CODE) = Y
      THEN GOTO 2080
2040  NEXT GAIN.CODE
2050  ''

```



```

2060     PRINT : PRINT "           Please use legal gain
           value."
2070     GOTO 1980
2080 ''
2090 '' Get A/D channel.
2100 ''
2110     PRINT : PRINT : PRINT "           ";
2120     PRINT "Legal values for A/D channels are 0 through ";
2130     PRINT (NUMBER.CHANNELS - 1);"."
2140     START.CHANNEL=0
2150     END.CHANNEL=4
2160 ''
2170     IF START.CHANNEL < 0 THEN GOTO 2220
2180     IF START.CHANNEL > (NUMBER.CHANNELS - 1) THEN GOTO
2220
2190     IF END.CHANNEL < 0 THEN GOTO 2220
2200     IF END.CHANNEL > (NUMBER.CHANNELS - 1) THEN GOTO 2220
2210     GOTO 2250
2220 ''
2230     PRINT : PRINT "           Please use legal channel
           values."
2240     GOTO 2080
2250 ''
2260 '' Get number of conversions to do.
2270 ''
2280     PRINT : PRINT : PRINT "           ";
2290     PRINT "Legal values for number of conversions are
           ";MIN.CONV;
2300     PRINT " through ";MAX.CONV;"."
2310     NUM.CONV=4
2320 ''
2330     IF (NUM.CONV >= MIN.CONV AND NUM.CONV <= MAX.CONV)
THEN GOTO 2370
2340 ''
2350     PRINT : PRINT "           Please use legal number of
conversions value."
2360     GOTO 2250
2370 ''
2380 '' Do a SET A/D PARAMETERS command to set up the A/D
converter.
2390 '' Write SET A/D PARAMETERS command.
2400 ''
2410     WAIT STATUS.REGISTER, COMMAND.WAIT
2420     OUT COMMAND.REGISTER, CSAD
2430 ''
2440 '' Write A/D gain byte.

```

```

2450 ''
2460     WAIT STATUS.REGISTER,  WRITE.WAIT, WRITE.WAIT
2470     OUT  DATA.REGISTER,    GAIN.CODE
2480 ''
2490 '' Write A/D start channel byte.
2500 ''
2510     WAIT STATUS.REGISTER,  WRITE.WAIT, WRITE.WAIT
2520     OUT  DATA.REGISTER,    START.CHANNEL
2530 ''
2540 '' Write A/D end channel byte.
2550 ''
2560     WAIT STATUS.REGISTER,  WRITE.WAIT, WRITE.WAIT
2570     OUT  DATA.REGISTER,    END.CHANNEL
2580 ''
2590 '' Write high and low bytes of NCONVERSIONS#.
2600 ''
2610     NUMBERH = INT(NUM.CONV/256)
2620     NUMBERL = NUM.CONV - NUMBERH * 256
2630     WAIT STATUS.REGISTER,  WRITE.WAIT, WRITE.WAIT
2640     OUT  DATA.REGISTER,    NUMBERL
2650     WAIT STATUS.REGISTER,  WRITE.WAIT, WRITE.WAIT
2660     OUT  DATA.REGISTER,    NUMBERH
2670 ''
2680     PRINT
2690     2710     COMMAND = 0
2720     IF Y$ = "Y" OR Y$ = "y" THEN COMMAND = EXT.CLOCK
2730     IF Y$ = "Y" OR Y$ = "y" THEN GOTO 2770
2740     IF Y$ = "N" OR Y$ = "n" THEN GOTO 2770
2750 ''
2760     GOSUB 3920 : GOTO 2670
2770 ''
2780     PRINT
2790
2800 ''
2810     IF Y$ = "Y" OR Y$ = "y" THEN GOTO 2850
2820     IF Y$ = "N" OR Y$ = "n" THEN GOTO 3000
2830 ''
2840     GOSUB 3920 : GOTO 2770
2850 ''
2860 '' Write READ A/D WITH TRIG command.
2870 ''
2880     WAIT STATUS.REGISTER,  COMMAND.WAIT
2890     OUT  COMMAND.REGISTER, CRAD + EXT.TRIG + COMMAND
2900 ''
2910 '' Wait for external trigger.
2920 ''

```

```

2930     PRINT : PRINT "           Apply EXTERNAL TRIGGER,
        then wait."
2940 ''
2950     FOR LOOP = 1 TO NUM.CONV           : WAIT
        STATUS.REGISTER, READ.WAIT
2960     ADL(LOOP) = INP(DATA.REGISTER) : WAIT
        STATUS.REGISTER, READ.WAIT
2970     ADH(LOOP) = INP(DATA.REGISTER) : NEXT LOOP
2980 ''
2990     GOTO 3110
3000 ''
3010 '' Write READ A/D command.
3020 ''
3030     PRINT : PRINT "           Starting conversions." :
PRINT
3040 ''
3050     WAIT STATUS.REGISTER, COMMAND.WAIT
3060     OUT COMMAND.REGISTER, CRAD + COMMAND
3070 ''
3080     FOR LOOP = 1 TO NUM.CONV           : WAIT
        STATUS.REGISTER, READ.WAIT
3090     ADL(LOOP) = INP(DATA.REGISTER) : WAIT
        STATUS.REGISTER, READ.WAIT
3100     ADH(LOOP) = INP(DATA.REGISTER) : NEXT LOOP
3110 ''
3120 '' Check for ERROR.
3130 ''
3140     WAIT STATUS.REGISTER, COMMAND.WAIT : STATUS =
        INP(STATUS.REGISTER)
3150     IF (STATUS AND &H80) THEN GOTO 3970
3160 ''
3170 '' Calculate and print the A/D readings in volts.
3180 ''
3190     NCHAN = END.CHANNEL - START.CHANNEL + 1
3200     IF NCHAN <= 0 THEN NCHAN = NCHAN + NUMBER.CHANNELS
3210     PRINT
3220 ''
3230     FOR LOOP = 1 TO NUM.CONV
3240     DATA.VALUE# = ADH(LOOP) * 256 + ADL(LOOP)
3250     IF DATA.VALUE# > 32767 THEN DATA.VALUE# =
        DATA.VALUE# - 65536!
3260     VOLTS#(LOOP) = ((RANGE * DATA.VALUE#/FACTOR#) -
        OFFSET)/GAIN(GAIN.CODE)
3270     CHANNEL = START.CHANNEL + ((LOOP - 1) MOD NCHAN)
3280     IF CHANNEL >= NUMBER.CHANNELS THEN CHANNEL =
        CHANNEL - NUMBER.CHANNELS

```

```

3290 ''
3300 '' PRINT#1, USING "###.#####";VOLTS#;
3310 PRINT, USING "###.#####";VOLTS#(LOOP);
3320 IF LOOP=1 THEN ZX#=VOLTS# : IF LOOP=2 THEN
      ZY#=VOLTS#/ZX#
3330 ''
3340 IF CHANNEL = END.CHANNEL THEN PRINT#1,
3350 IF CHANNEL = END.CHANNEL THEN PRINT#1,
3360 NEXT LOOP : ' PRINT#1,ZY#
3370 PRINT#1, :PRINT#1,
3380 R#=(LOF(1)/16)+1
3390 LSET CH1$=MKS$(VOLTS#(1)):LSET
      CH2$=MKS$(VOLTS#(2)):LSET CH3$=MKS$(VOLTS#(3)):LSET
      CH4$=MKS$(VOLTS#(4))
3400 PUT #1,R#
3410 GOTO 1920
3420 '' Ask if more conversions are desired.
3430 ''
3440 PRINT : PRINT
3450 INPUT " Do you want to do more conversions
      (Y/N)";Y$
3460 ''
3470 IF Y$ = "N" OR Y$ = "n" THEN GOTO 3510
3480 IF Y$ = "Y" OR Y$ = "y" THEN GOTO 1920
3490 ''
3500 GOSUB 3920 : GOTO 3410
3510 ''
3520 PRINT : PRINT : PRINT " READ A/D Operation
      Complete"
3530 GOTO 4290
3540 ''
3550 '' Get board range.
3560 ''
3570 PRINT
3580 PRINT " Is the A/D bipolar ('B') or
      unipolar ('U')";
3590 Y$="b"
3600 IF Y$ = "B" OR Y$ = "b" THEN GOTO 3650
3610 IF Y$ = "U" OR Y$ = "u" THEN GOTO 3690
3620 ''
3630 PRINT : PRINT " Please respond with 'B' or
      'U' only."
3640 GOTO 3540
3650 ''
3660 '' Bipolar range and offset.
3670 ''

```

```

3680     RANGE = BIP.RANGE : OFFSET = BIP.OFFSET : RETURN
3690 ''
3700 '' Unipolar range and offset.
3710 ''
3720     RANGE = UNI.RANGE : OFFSET = UNI.OFFSET : RETURN
3730 ''
3740 '' Get channel configuration.
3750 ''
3760     PRINT "           Is the A/D Single-Ended ('S')";
3770     PRINT " or Differential ('D')";
3780
3790     IF Y$ = "S" OR Y$ = "s" THEN GOTO 3840
3800     IF Y$ = "D" OR Y$ = "d" THEN GOTO 3880
3810 ''
3820     PRINT : PRINT "           Please respond with 'S' or
           'D' only."
3830     GOTO 3730
3840 ''
3850 '' Single-Ended number of channels.
3860 ''
3870     NUMBER.CHANNELS = SE.CHANNELS : RETURN
3880 ''
3890 '' Differential number of channels.
3900 ''
3910     NUMBER.CHANNELS = DI.CHANNELS : RETURN
3920 ''
3930 '' Respond to query with 'Y' or 'N'.
3940 ''
3950     PRINT : PRINT "           Please respond with 'Y' or
           'N' only."
3960     RETURN
3970 ''
3980 '' Fatal board error.
3990 ''
4000     PRINT
4010     PRINT "FATAL BOARD ERROR"
4020     PRINT "STATUS REGISTER VALUE IS ";HEX$(STATUS);"
           HEXIDECIMAL"
4030     PRINT : BEEP : BEEP : GOSUB 4080
4040     PRINT "ERROR REGISTER VALUES ARE:"
4050     PRINT "     BYTE 1 - ";HEX$(ERROR1);"
           HEXIDECIMAL"
4060     PRINT "     BYTE 2 - ";HEX$(ERROR2);"
           HEXIDECIMAL"
4070     PRINT : GOTO 4290
4080 ''

```

```

4090 '' Read the Error Register.
4100 ''
4110 OUT—COMMAND.REGISTER, CSTOP : TEMP =
      INP(DATA.REGISTER)
4120 ''
4130 WAIT STATUS.REGISTER, COMMAND.WAIT
4140 OUT COMMAND.REGISTER, CERROR
4150 ''
4160 WAIT STATUS.REGISTER, READ.WAIT
4170 ERROR1 = INP(DATA.REGISTER)
4180 WAIT STATUS.REGISTER, READ.WAIT
4190 ERROR2 = INP(DATA.REGISTER)
4200 RETURN
4210 ''
4220 '' Illegal Status Register.
4230 ''
4240 PRINT
4250 PRINT "FATAL ERROR - ILLEGAL STATUS REGISTER VALUE"
4260 PRINT "STATUS REGISTER VALUE IS ";HEX$(STATUS);"
      HEXIDECIMAL"
4270 BEEP : BEEP
4280 ''
4290 PRINT : PRINT
4300 ''
4310 INPUT "      Run program again (Y/N)";Y$
4320 IF Y$ = "Y" OR Y$ = "y" THEN RUN
4330 IF Y$ = "N" OR Y$ = "n" THEN GOTO 4370
4340 ''
4350 PRINT : PRINT "      Please respond with 'Y' or
      'N'."
4360 GOTO 4300
4370 ''
4380 INPUT "      Return to MENU (Y/N)";Y$
4390 IF Y$ = "Y" OR Y$ = "y" THEN RUN MENU$
4400 IF Y$ = "N" OR Y$ = "n" THEN GOTO 4440
4410 CLOSE#1
4420 PRINT : PRINT "      Please respond with 'Y' or
      'N'."
4430 GOTO 4370
4440 END

```

Appendix B¹

Jizan Radio System description

The DMC 8M Digital Microwave Radio is designed for operation in the 7.75 to 8.25 GHz frequency band. It is ideal for short-haul, point-to-point transmission of digitized voice, data, video, and facsimile.

The DMC 8M system includes a built-in multiplexer located on the Personality CardTM. The Personality Card determines the electrical interface of the system, performs all DMC 8M multiplex functions, and establishes the system digital input/output rate. Table 2-A lists the transmission rate options that distinguish each Personality Card.

Table 2-A
DMC 8M Transmission Rate Options

CCITT G.703

1 x 2.048 Mbit/s (1 x CEPT-1)
2 x 2.048 Mbit/s (2 x CEPT-1)
4 x 2.048 Mbit/s (4 x CEPT-1)
16 x 2.048 Mbit/s (16 x CEPT-1)
1 x 8.448 Mbit/s (1 x CEPT-2)
1 x 34.368 Mbit/s (1 x CEPT-3)

The basic microwave transmission link consists of two radio terminals. Each DMC 8M Radio terminal consists of an RF Unit and a digital Modem. The RF Unit can be mounted on a pole or installed indoors. The RF Unit is connected to the indoor Modem with RG-8 coaxial cable (Belden 9913 or equivalent). The coaxial cable carries all of the electrical signals between the Modem and the RF Unit, including power and alarms; no other cables are required. The Modem and RF Unit can be separated by up to 300 meters (1000 feet) of RG-8 coaxial cable. Each standard terminal is powered by -48 VDC input to the Modem. Figure 2-1 illustrates a typical DMC 13M microwave link.

¹ This appendix was gathered from various PTT system description and specifications.

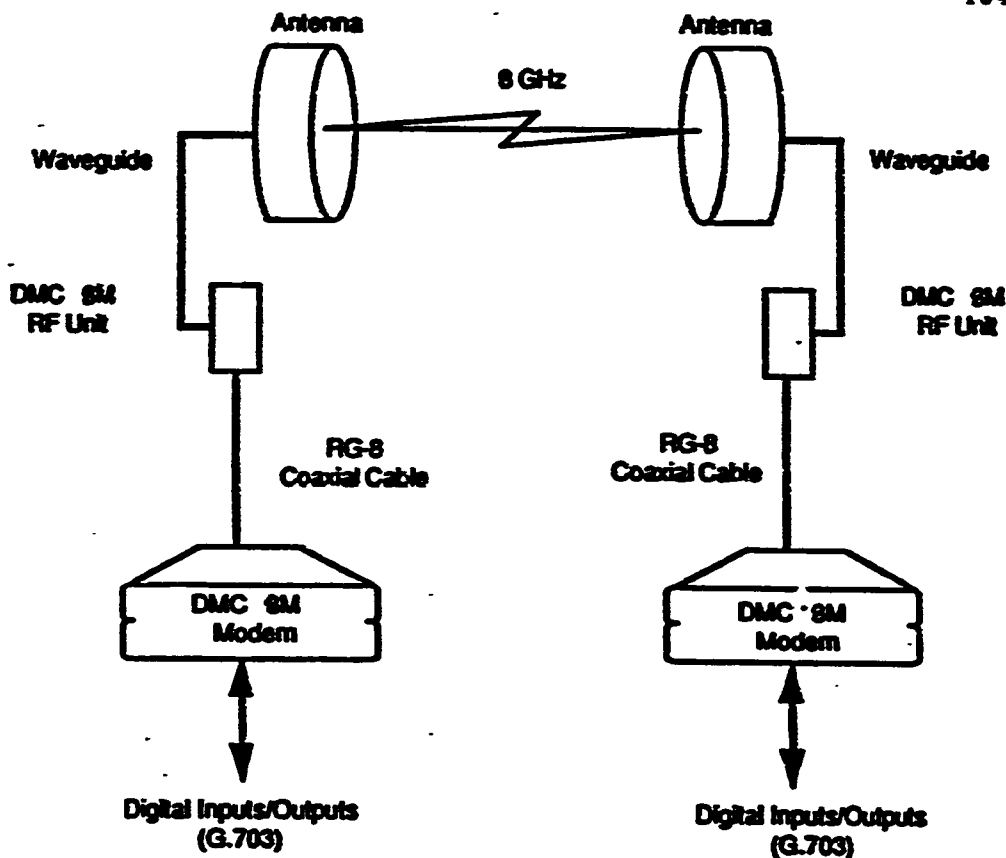


Figure 1: Typical DMC 8M Microwave System.

System Options

The DMC 8M Radio is available in a variety of configurations: CEPT rate multiplex variations, non-protected, protected (Monitored Hot-Standby), with a voice frequency orderwire and data port, and with various power input options. The standard non-protected DMC 8M terminal consists of a Modem with an integral multiplexer and a single RF Unit.

Multiplexer Options

The DMC 8M Personality Card options provide flexibility in determining the number of channels (digital signals) to be transported by the system. In a multi-link network, lower capacity systems can be used for light traffic and higher capacity systems can be used for higher density routes, all with similar system hardware. For detailed information on specific Personality Card configurations, refer to Section 5.0.

Monitored Hot-Standby Protection Options

A protected (Monitored Hot-Standby) DMC 8M system provides backup in the event of equipment failure. The protected terminal includes two complete systems, one in service and one on standby. Each protected terminal consists of two Modems (with integral multiplexers), a Protection Unit, and a single RF Unit with redundant RF Unit components in a single housing and protection switching circuitry. For detailed information on protection configurations, refer to Appendix 1.0.

Orderwire Options

An optional voice-frequency orderwire equipped with a digital data port provides a convenient overhead communications channel for maintenance and alarm transmission. Detailed information on the Orderwire Card option is discussed in Appendix 2.0.

System Power Output Options

The DMC 8M is available in a standard power or high-power output option. The high-power output option will increase system gain by 10 dB. The specifications at the end of this section outline both standard and high-power output performance for the DMC 13M.

Alternate Power Input Card

If the power input voltage differs from -48 VDC, the DMC 8M Modem can be equipped with an optional Alternate Power Input Card to facilitate external power inputs in the range of 12 to 32 VDC, either polarity. Included with the Alternate Power Input Card is an internal back-up battery for 30-60 minutes emergency power. Detailed information on the Alternate Power Input Card option is covered in Appendix 4.0.

Features

The features and benefits of the DMC 8M Digital Radio are described below:

- High-performance, point-to-point digital microwave radio operation, which ensures an effective communication system
- Personality Card that performs all multiplexing functions, eliminating external multiplex equipment
- Meets CCITT Recommendation G.703 for unbalanced 75-ohm digital interfaces and the CCIR Rec. 497-2 frequency plan
- High system gain for extremely reliable microwave radio operation during rainy weather
- Dynamic range in excess of 60 dB which provides superior protection against RF signal fades
- DMC Net™ (optional) network monitor and control interface feature for control of an entire system from a single master terminal

- Sophisticated built-in diagnostics, including individual channel loopback testing and BER monitoring, eliminating the need for expensive test equipment
- Local display of the remote terminal status and alarm indicators, simplifying system maintenance and fault isolation
- Low power consumption and input power voltage options with back-up battery
- Full-duplex operation in a single-polarized antenna configuration
- User-selectable scrambling codes
- Compact, modular, office-style design for easy installation that requires no special tools or expensive test equipment

DMC 8M Specifications

GENERAL

Operating Frequency	7.75 to 8.25 GHz
Capacity	
CCITT Rec. G.703	2,048, 2 x 2,048, 4 x 2,048, 16 x 2,048, 8,448, and 34,368 Mbit/s
Interface	
PCM Voice Channel Capacity	Per CCITT Rec. G.703 (Unbalanced, 75-Ohm)
CCITT Rec. G.703	30, 60, 120, or 480
Modulation Type	MSK (Minimum Shift Keying)
Input/Output Connector	BNC Connectors per G.703 or 25-pair Connectors
RF Connector	UBR-140 (UG-419/V) or PDR-120

ENVIRONMENTAL

Temperature	
RF Unit/Antenna	-30°C to 55°C
Modem	0°C to +40°C
Relative Humidity	
RF Unit/Antenna	Up to 100%
Modem	95% at +40°C
Altitude	Up to 4,500 m/15,000 ft

TRANSMITTER

Power Output (at RF Unit antenna port)	
Standard	+13 dBm (13 mW)
With High-Power Amplifier	+23 dBm (126 mW)
Frequency Stability	±0.002%
Optional High Stability	±0.0008%

RECEIVER

Type	Dual Conversion
Sensitivity (10^{-6} BER at RF Unit antenna port)	
1 x 2.048 Mbit/s	-87.0 dBm
2 x 2.048 Mbit/s	-84.5 dBm
4 x 2.048 Mbit/s	-82.0 dBm
1 x 8.448 Mbit/s	-82.0 dBm
16 x 2.048 Mbit/s	-76.0 dBm
1 x 34.368 Mbit/s	-76.0 dBm
Unfaded BER	10^{-10} or better
Maximum Input Signal Level	
10^{-6} BER	-15 dBm

SYSTEM GAIN (Guaranteed value at RF Unit antenna port, excluding antenna, 10^{-6} BER)

Non-Protected

	<u>Standard Power</u>	<u>High Power</u>
1 x 2.048 Mbit/s	98.0 dB	108.0 dB
2 x 2.048 Mbit/s	95.5 dB	105.5 dB
4 x 2.048 Mbit/s	93.0 dB	103.0 dB
1 x 8.448 Mbit/s	93.0 dB	103.0 dB
16 x 2.048 Mbit/s	87.0 dB	97.0 dB
1 x 34.368 Mbit/s	87.0 dB	97.0 dB

Additional branching losses for MHSB configuration are as follows:

	<u>Transmitter</u>	<u>Receiver (A/B)</u>
MHSB Transmitter and Receiver (unequal loss coupler)	1 dB	2/12 dB
MHSB Transmitter and Receiver (equal loss hybrid)	1 dB	4.5/4.5 dB

POWER REQUIREMENTS

Source	-48 VDC, positive ground
Allowable Input Range	-41 VDC to -56 VDC

Optional Power Sources: ± 12 -32 VDC. Includes 30-60 minutes internal battery backup.

Power Consumption (Modem and RF Unit)

	Standard Power	High Power
Non-Protected (Typical)		
2 Mbit/s - 8 Mbit/s	40 Watts	50 Watts
16 x 2 Mbit/s and 34 Mbit/s	45 Watts	55 Watts
Monitored Hot-Standby		
2 Mbit/s - 8 Mbit/s	95 Watts	115 Watts
16 x 2 Mbit/s and 34 Mbit/s	105 Watts	125 Watts

MECHANICAL**Non-Protected (Typical)****Dimensions (H x W x D)**

Modem	88 x 425 x 396 mm (3.5 x 17.0 x 15.2 in.)
RF Unit	330 x 254 x 127 mm (13.0 x 10.0 x 5.0 in.)

Weight

Modem	8.4 kg (18.5 lbs)
RF Unit	10.0 kg (22 lbs)

Monitored Hot-Standby**Dimensions (H x W x D)**

Modem	88 x 425 x 396 mm (3.5 x 17.0 x 15.2 in.)
RF Unit	508 x 330 x 130 mm (20.0 x 13.0 x 5.0 in.)

Weight

Modem	8.4 kg (18.5 lbs)
RF Unit	14.5 kg (38 lbs)

ORDERWIRE AND DATA PORT

Orderwire	Voice Frequency (300-3400 Hz)
Data Port	0 to 9600 bps, Asynchronous RS-232C

Specifications provided apply to equipment connected back-to-back, unless otherwise specified.

Data subject to change without notice.

Personality Card and DMC Net are trademarks of DMC.

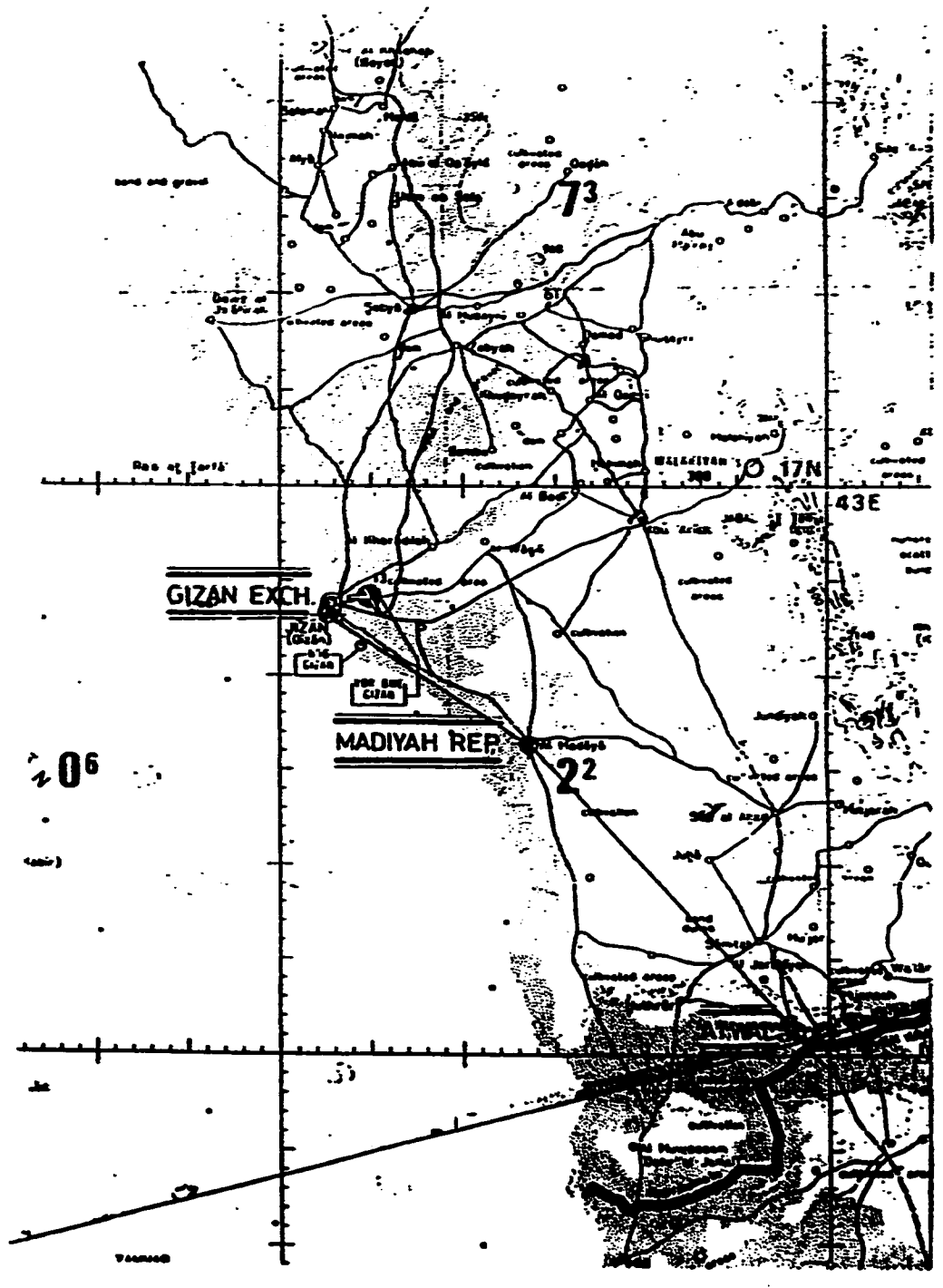


Figure (8-1) Map of site location of Jizan path

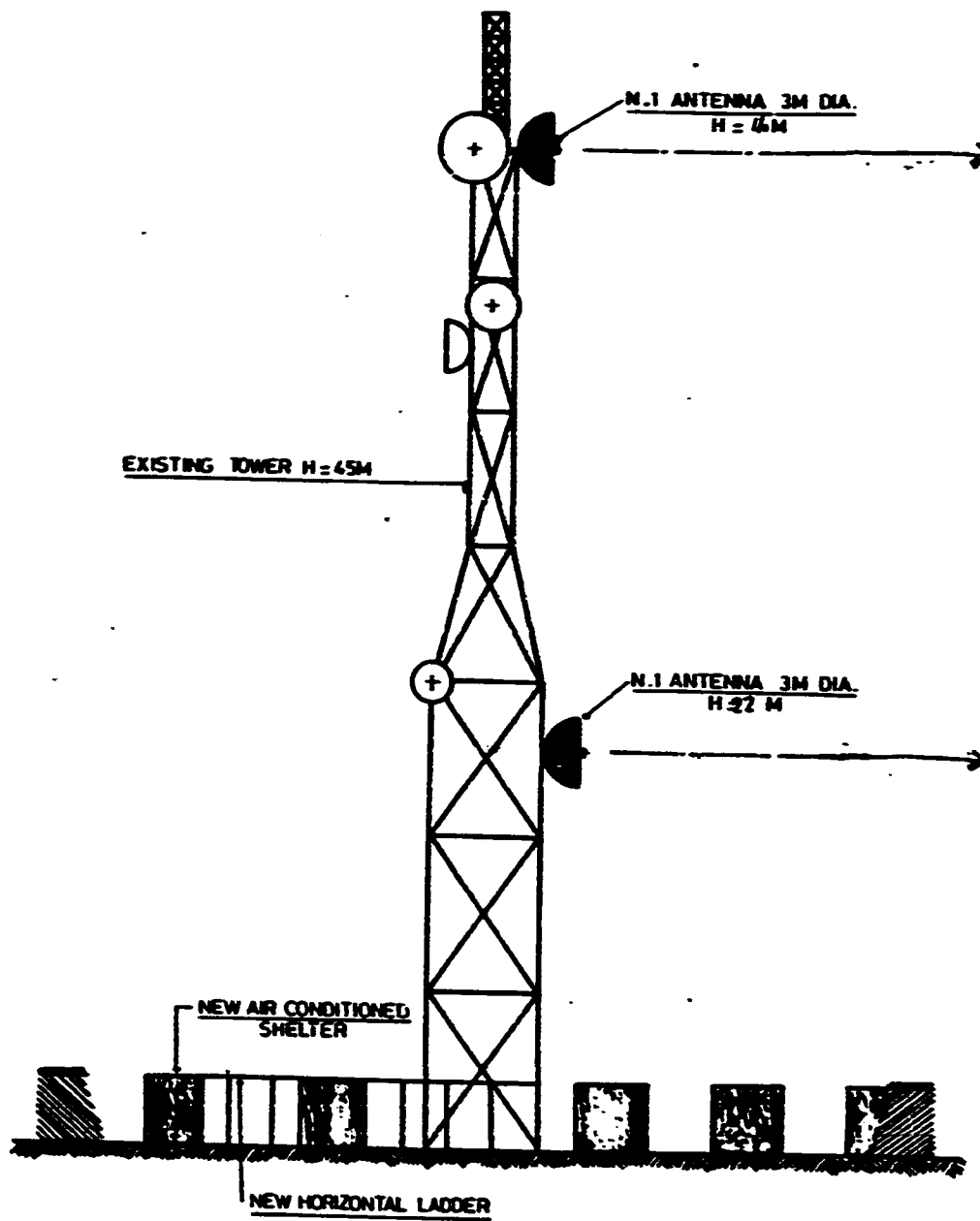


Figure (8-2): The communication tower at Jizan site.

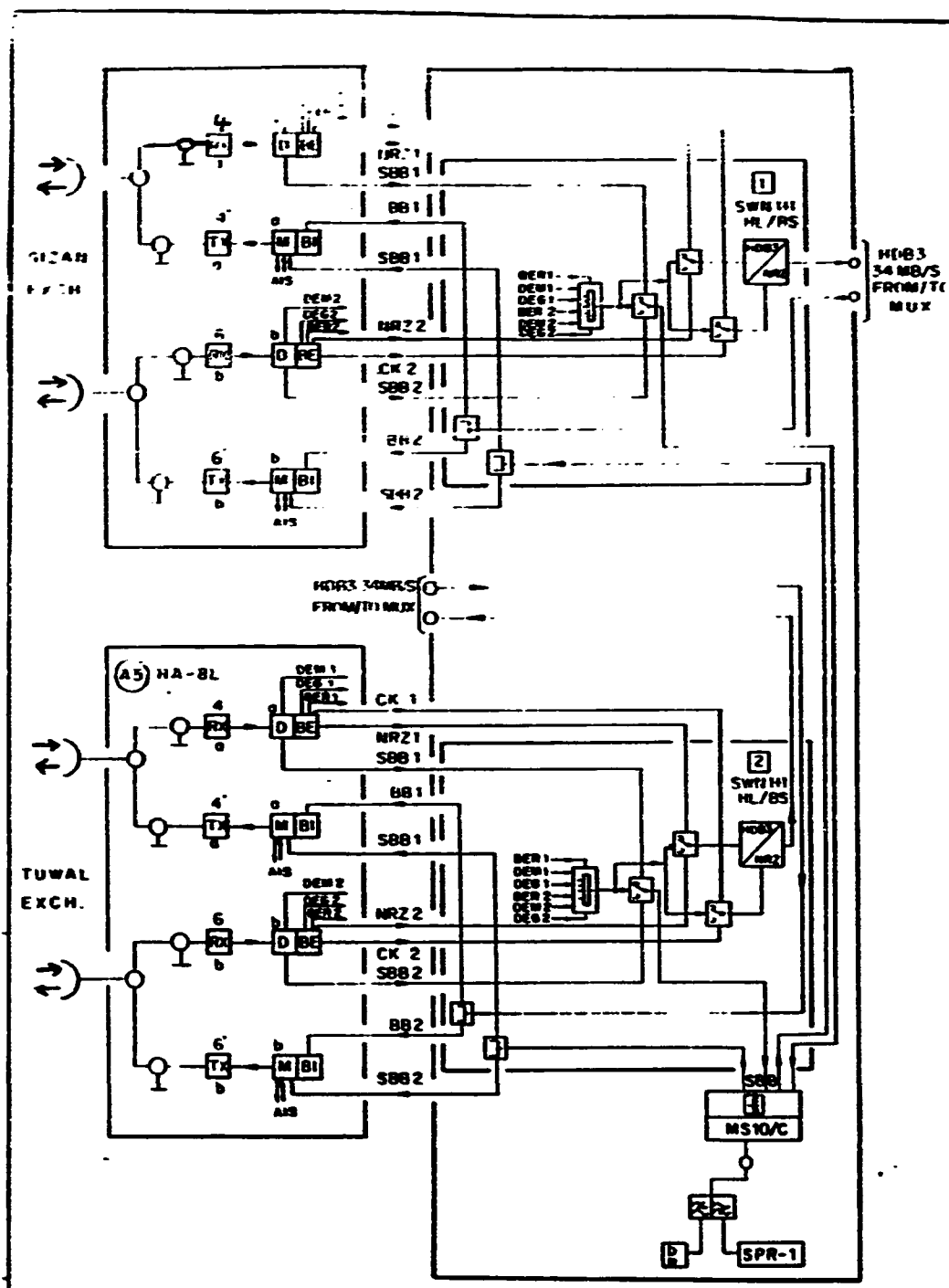


Figure (8-3): Madaiya repeater block diagram.

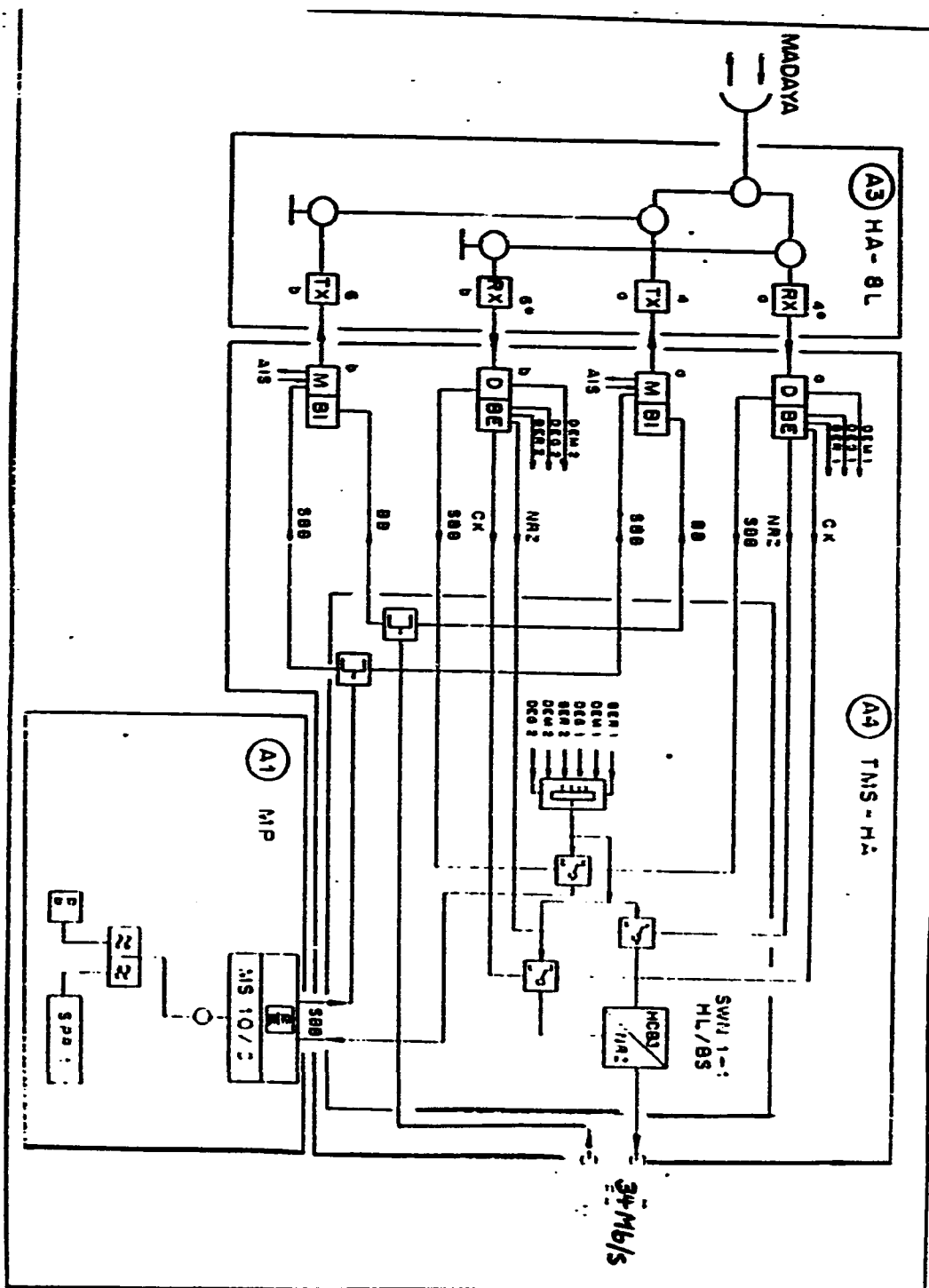


Figure (B-4): The block digrame of Jizan site.

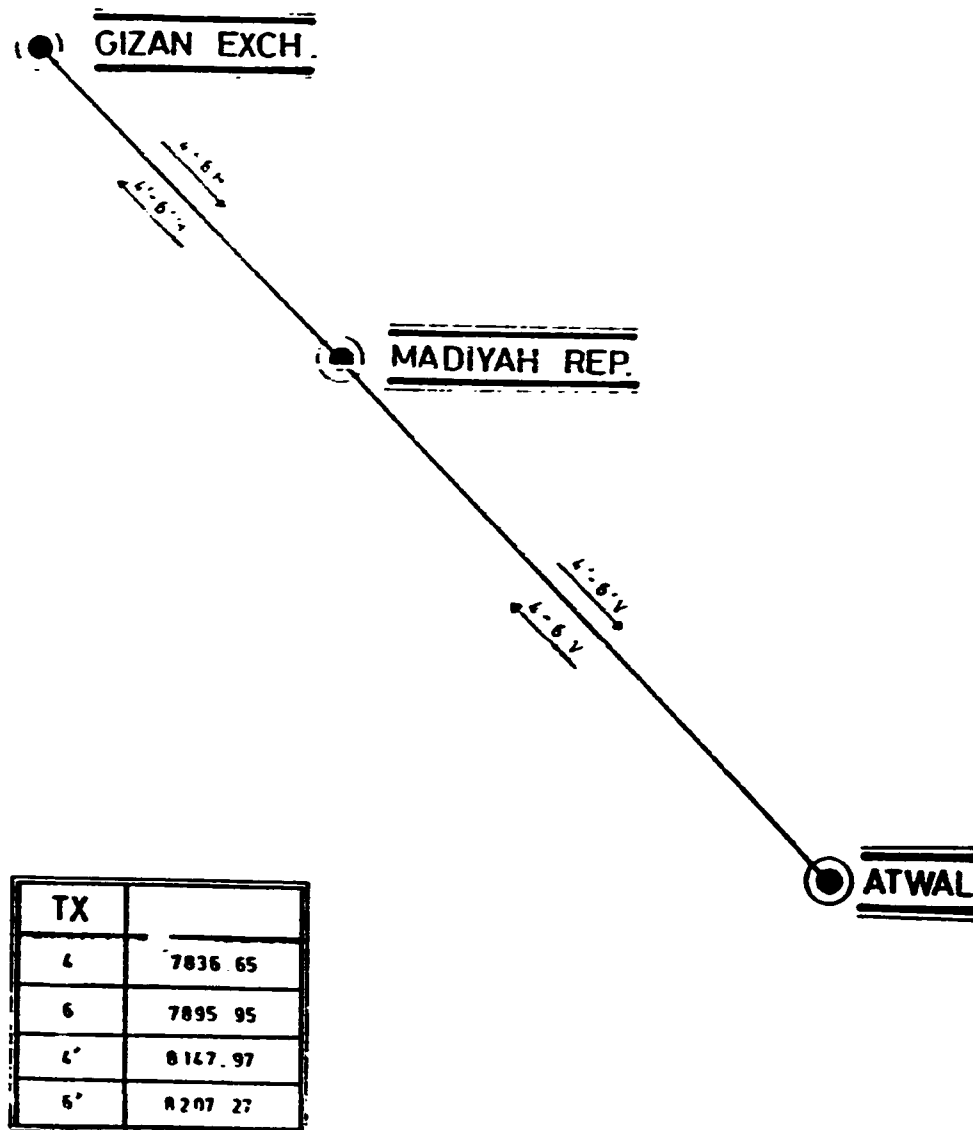


Figure (8-5): The frequency allocation plan of Jizan link.

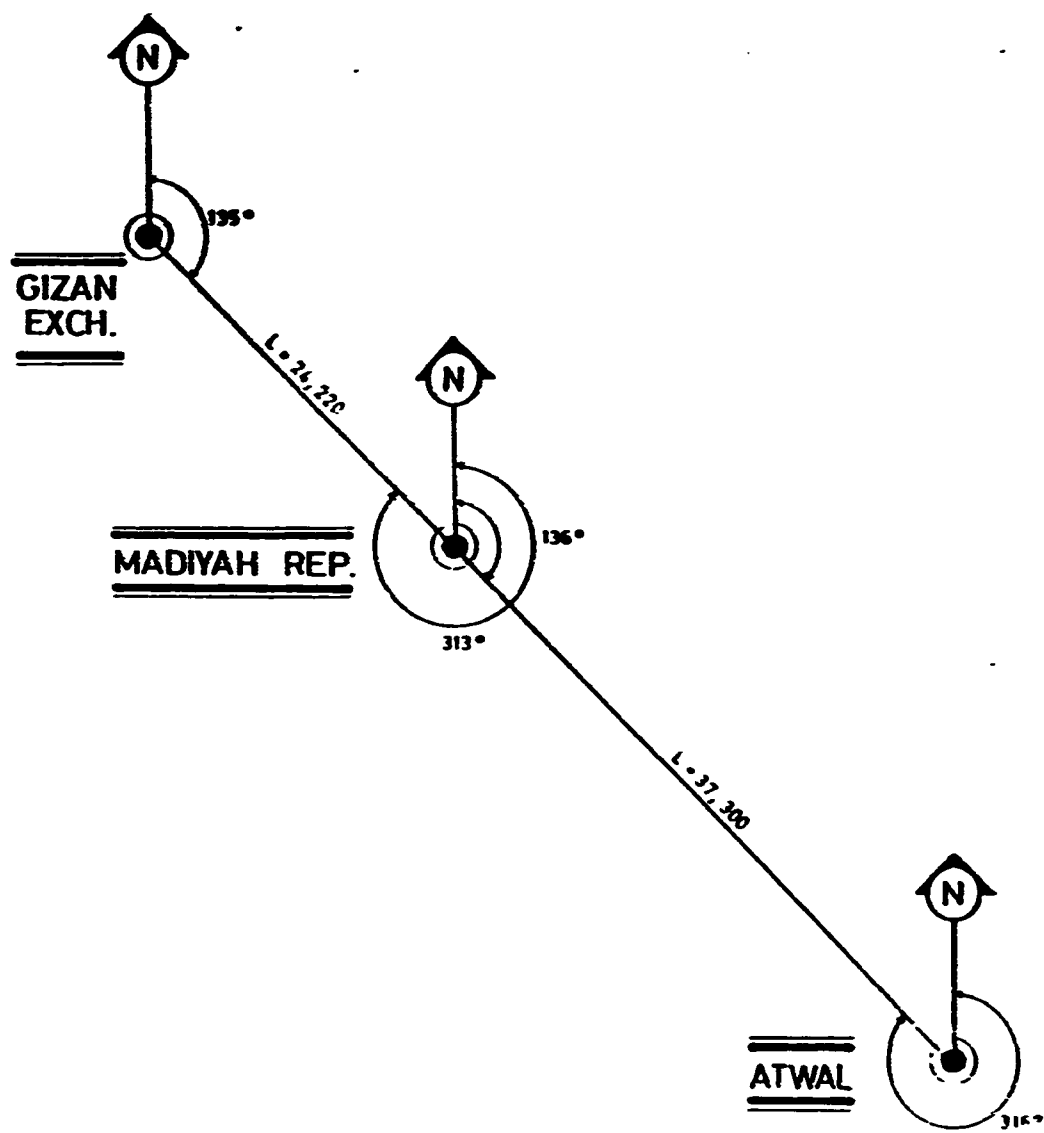


Figure (8-6): The layout Map of Jizan path.

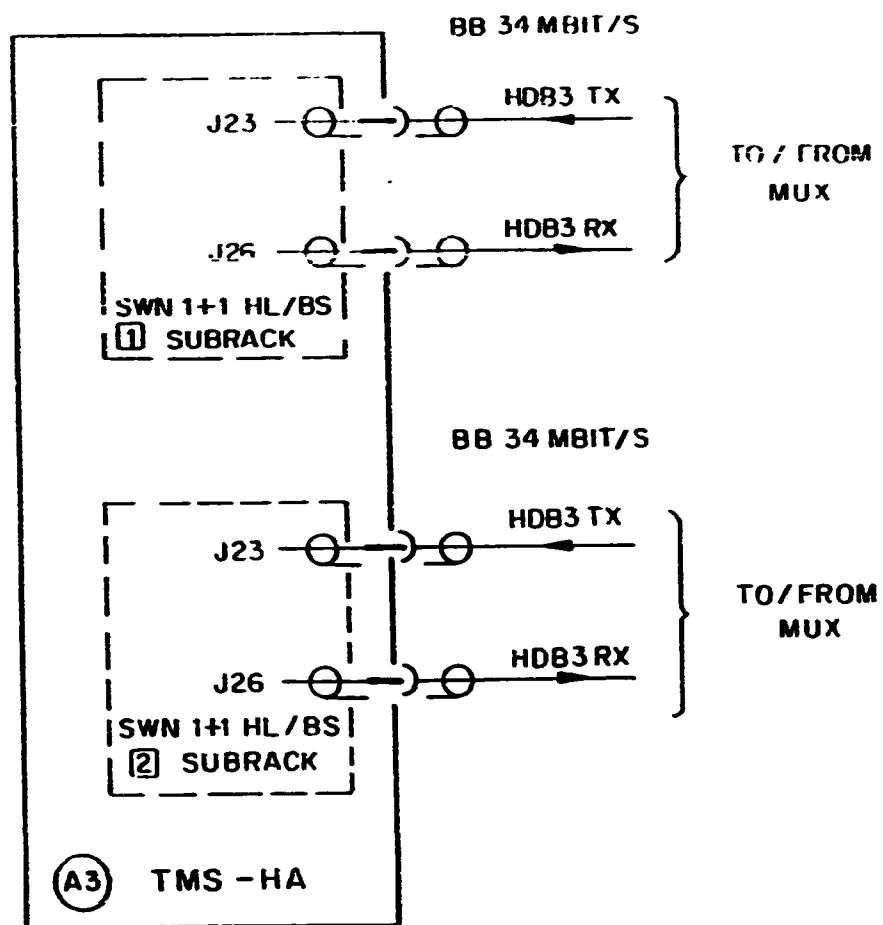


Figure (8-7): The block diagram of the Modem system connection to the switching equipments.

REFERENCES AND BIBLIOGRAPHY

1. Abel, N., "Statistics of multipath fading and rain attenuation on terrestrial radio link operating in the 7 to 15 GHz range," *IEE Conf. Publ.*, No. 195, Part 2, pp. 64-67, Nov. 1978.
2. Al-Baroudi, Uthman A. , " Performance of fractionally spaced equalizer under frequency selective fading," *M. Sc. Thesis* , King Fahd University of Petroleum and Minerals, Aug. 1990.
3. Al-Bidnah, S. A. , " Microwave communication system design in Saudi Arabia," *M. Sc. Thesis* , King Saud University, 1979.
4. Al-Semari, Saud, " Performance of TCM with concatenated codes over fading channels," *M. Sc. Thesis*, King Fahd University of Petroleum and Minerals, June, 1992.
5. Al Shahrani, Ali, "Engineering aspects of the microwave network in Saudi Arabia," *Project submitted in partial fulfillment for the degree of B. Sc.* King Saud Uinversity, Dec. 1984.
6. Anderson, D. W. , Bareber, S. G. and Patel, R. N., "The effects of selective fading on digital radio," *IEEE Tran. Comm.* , vol. COM-27, 3, pp. 1870-1876, Dec. 1979
7. Barber, S., " Cofrequency cross-polarized operation of 91 Mb/s digital radio," *IEEE International Conf. on Comm.* , vol. 3, Session 46, pp. 6.1-6.6, June, 1981.
8. Barnett , W. T. " Microwave line-of-sight propagation with and without frequency diversity," *BSTJ* , vol.49,8, pp.1827-1871, Oct. 1970.
9. Barnett , W. T. " Multipath propagation at 4, 6, and 11 GHz," *BSTJ* , vol. 51, 2, pp.321-361, Feb. 1972.
10. Bell, J. , " Propagation measurements at 3, 6, and 11 GHz over a line-of-sight radio path," *Proc. IEE*, vol. 114 , 5, pp.545-549, 1967.
11. Bello, P., and B. D. Nelin, " The effect of frequency selective fading on the binary error probabilities of incoherent and differentially coherent matched filter receivers," *IEEE Trans. Commun. Syst.* , vol. CS - 11, pp. 170-186, June, 1963.

12. Bello, P. A. and B. D. Nelin, " Predetection diversity combining with selectively fading channels," *IRE Trans. Commun. Syst.* , vol.CS-10, pp. 32-42, Mar. 1962.
13. Biyari, K. H. and Lindsey W. C., " Binary communication through noisy, non Gaussain channels , " *IEEE Tran. Inform. Theory*, 1993.
14. Bullington, K. , "Radio propagation fundamentals," *Bell Syst. Tech. J.*, May. 1957.
15. Bullington, K. , " Phase and amplitude variation in multipath fading of microwave signals, " *BSTJ* , vol.50, 6, pp.2039-2053. July-Aug. 1971.
16. Bundrock, A. J. and Murphy, J. V. " a board-band 11 GHz radio propagation experiment, " *IEEE Tran. Ant. Prop.* , vol. AP-32, 5, pp. 449-455, 1984.
17. Bultitude, R. J. C. , " Measurements, characterization and modeling of indoor 800 / 900 MHz radio channels for digital communications," *IEEE Commun. Mag.*, vol. 25,No. 6, pp. 5-12, June, 1987.
18. Bultitude, R.J. C., "Measured characteristics of 800/900 MHz fading radio channels with high angel propagation through moderately dense foliage," *IEEE Selected Area Commun.* , vol. SAC-5, No. 2, Feb. 1978.
19. Campbell, J. C. , "Digital radio outage prediction with space diversity," *Electron. Lett.* , Vol. 19 , 23, pp. 1003-1004, Nov. 1983.
20. Campbell, J. C., and Coutts, R. P. , "Outage prediction of digital radio systems," *Electron. Lett.*, vol. 18, 25 -26, pp. 1071-1072, Dec. 1982.
21. Chu, T. S. , " The Effects of sandstorm on microwave propagation," *BSTJ* , vol. 58, 2, pp. 549-555, 1979.
22. Crane, R. K., "Prediction of attenuation by rain," *IEEE Trans. Comm.*, vol. COM-28, 9, pp. 1717-1733, 1980.
23. Crane, R. K. , " Propagation phenomena affecting communication satellite communication systems operating in the centimeter and millimeter wavelength bands," *Proc. IEEE*, vol. 59,2, pp. 173-188, Feb. 1971.
24. Carwford, A. , " selective fading of microwave," *BSTJ*, vol. XXXI, 1, pp. 68-90, 1952.

25. Carwford, A. B. , and Sharpless, W. M. , " further observations of the angle-of-arrival of microwave ,"
Proc. IRE, vol. 34, 11, pp. 845-848, Nov. 1946.
26. Crombie, D. , " The prediction of multipath fading on terrestrial microwave links at frequencies of 11 GHz and greater," *AGARD Symposium*, pp. 123-165, Oct. 1983.
27. Damosso, E., De Padova, S., Failli, R., and Lingua, A.,
" Experimental results on the effects of selective fadings on 70 Mb/s, 7 PSK digital radio ,"
Proc. IEEE Global Telecommunications Conference, Nov. 1982.
28. Daniel, M. J. , " Multipath time delay spread in the digital portable radio environment," *IEEE Commun. Mag.*,
vol. 25, No.6, pp. 5-12, June, 1987.
29. Dixon and Massey, F. Jr. , *Introduction to Statistical Analysis*. New York, McGraw-Hill, Third Ed., 1969.
30. Doble, J. E. , " Predictions of multipath delays and frequency selective fading of digital links in the UK,"
IEE Digest, vol. 62 , 1979.
31. Dougherty, H. T., and Hartman, W. J. , " Performance of 400 Mb/s system over a line-of-sight path, " *IEEE Tran. Comm.* , vol. COM-25, 4, Apr. 1977.
32. Emshwiller, M. , " Characterization of the performance of PSK digital radio transmission in the presence of multipath fading," *IEEE International Conf. on Comm.*,
Conf. Record 47.3/1-6, June, 1978.
33. Fedi, F. , " Normalization procedures and prediction techniques for rain attenuation on terrestrial and Earth space radio links, " *IEE Conf. Publ. No. 195. IEE Second international Conf. on Ant. and Prop.* , Apr. 1981.
34. Freeman, L. R., *Telecommunication System Engineering*. WILEY Series In Telecommunications, second Ed. 1989.
35. Garcia-Lopez, J. A., and Casares-Giner, V. , " Optimum antenna separation for space diversity in L.O.S radio link over flat ground," *Electron. Lett.* , vol. 16, 18,
pp. 717-718, Aug. 1980.
36. Gardina, M. , and Vigants, A. , " Measured multipath dispersion of amplitude and delay at 6 GHz in a 30 MHz bandwidth," *IEEE International Conf. on Comm.* , vol. 3,
Session 46, pp. 1433-1437, May, 1984.

37. Giger, A. J. , " Effects of multipath propagation on digital radio, " *IEEE Tran. Comm.*, vol. COM-29, 9, pp. 1345-1352, Sep. 1981.
38. Giloi, H. G. , " Diffraction phenomena during multipath fading, " *AGARD Conf. Proc. No.269*, pp.32.1-32.14, 1979.
39. Giloi, H. G. , " A study of field-strength profiles caused by multipath fading, " *IEEE Trans. Ant. Prop.*, vol. AP-33, 12, pp. 1378-1385, Dec. 1985.
40. Goldhirsh, J. , " A parameter review and assessment of attenuation and back-scatter properties associated with dust storms over desert regions in the frequency range of 1 to 10 GHz, " *IEEE Trans. Ant. Prop.*, vol. AP-30, 6, pp. 1121-1127, 1982.
41. Greenstein, L. J. , " A multipath fading channel model for terrestrial digital radio systems, " *IEEE Tran. Comm.*, vol. COM-26, 8, pp. 1247-1250, Aug. 1978.
42. Harden, B. N. , "Propagation studies and the development of terrestrial microwave radio-relay systems above 10 GHz in the United kingdom, " *IEE Conf. Publ. 98, conf. on Prop. of radio waves at Frequencies above 10 GHz*, 1973.
43. Hewitt, M. T. , and Norbury , J. R. , " Correlation of fading on spaced microwave paths at 2 - 37 GHz, " *IEE Conf. Publ. 98*, pp. 250-255, 1973.
44. Ikegami, F. , Akiyama, T. , Aoyagi, S. , and Yoshida , H. , " Variation of radio refraction in the lower atmosphere, " *IEEE Trans. Ant. Prop.*, vol AP-16, 3, March, 1986.
45. Inoue, T. , " Propagation characteristics on a line-of-sight oversea path in Japan, " *IEEE Trans. Ant. Prop.*, vol. AP-22, 4, pp. 557-565, 1974.
46. Jakes, W. C. Jr. , "An approximate method to estimate an upper bound on the effect of multipath delay distortion on digital transmission , " *IEEE Trans. Comm.*, vol. CSM-27, 1, pp. 76-81, Jan. 1979.
47. Komaki, S. , Horikawa, I. , Morita, K. , and Okamoto, Y. , " Characteristics of a high-capacity 16 QAM digital radio system in multipath fading, " *IEEE Trans. Comm.*, vol. COM-27, 12, pp. 1854-1861, 1979.
48. Lin, S. H. , "Statistical behaviour of a fading signal,"

BSTJ, vol. 50, 10, pp. 3211-3270, Dec. 1971.

49. Lin, S. H., "Impact of microwave depolarization during multipath fading on digital radio performance, " *BSTJ*, vol.56, pp. 645-674, 1977.
50. Lindsey, W. C. , "Error probabilities for rician fading multichannel reception of binary and N-ary signals ,"
IEEE Trans. Inform. Theory , vol. IT - 10, pp. 339-350, Oct. 1964.
51. Liniger, M., " One year results of sweep measurments of a radio link," *IEEE International Conf. on COMM.* , vol. 2, Session C2, pp. 2.3.1 - 2.3.5, June, 1983.
52. Martin, L., "Statistical results on selective fadings,"
IEEE International Conf. on COMM. , vol.3, Session-7B, pp. 5.1-5.5 , June, 1982a.
53. Martin, L., " Computing method of outage time for high bit rate digital radiolink," *IEEE International Conf. on COMM.* , vol. 3, Session - 7B, pp. 6.1 - 6.5 , June, 1982b.
54. Martin, L. , " Phase distortions of multipath transfer functions, " *IEEE International Conf. on COMM.*, vol. 3, Session 46, pp. 1437-1441, 1984 .
55. Martin, L. A. , Campbell, J. C. , and Coutts, R. P. ,
" Results of a 16 QAM 140 Mb / s digital radio field experiment," *IEEE International Conf. on COMM.*, vol. 3, Session F2, pp. 2.2.7 - 2.2.8, 1983.
56. Meadows, R. W. , lindgren, R. E. , and Samuel, J. C. ,
"Measurements of multipath propagation over a line-of-sight radio link at 4 GHz using frequency-sweep technique," *Proc. IEE*, vol. 113,1, pp. 41-61, 1966.
57. Medhurst, " Rainfall attenuation of centimeter waves: comparison of theory and measurement , " *IEEE Trans. Antenna spropa.* , July. 1965.
58. Metzger, and Rolf , V. " An analysis of the sensitivity of digital modulation techniques to frequency-selective fading," *IEEE Trans. Commun. Syst.*, vol. COM-33, NO. 9, pp. 986-992, Sep. 1985.
59. Morita, K., " Perdiction of Rayleigh fading occurence robability of line-of-sight microwave links, " *Rev. Elec. Comm. Labs.*, vol. 20, 7-8, pp. 589-598, July-Aug. 1970.

60. Morita, K. , " Prediction of equivalent Rayleigh fading occurrence rate on line-of-sight reflected wave path," *Rev. Elec. Comm. Labs.*, vol.25, 3-4, pp. 329-335, 1977.
61. Morita, K. , Hosoya, Y. , and Akeyama, A. , " Some experimental results on 20 GHz band rain attenuation and depolarization, " *Proc. IEEE / G-AP International Symp.*, pp. 285-288, Aug. 1973.
62. Medhurst, " Rainfall attenuation of centimeter waves: comparison of theory and measurement , " *IEEE Trans. Antenna spropa.* , July. 1965.
63. Metzger, and Rolf , V. " An analysis of the sensitivity of digital modulation techniques to frequency-selective fading," *IEEE Trans. Commun. Syst.*, vol. COM-33, NO. 9, pp. 986-992, Sep. 1985.
64. Nakagami, M. , *The M-distribution A general formula of intensity distribution of fading in Statistical Methods in Radio Wave propagation*, W. c. Hoffman, Ed. New York : Pergamon, 1960.
65. Ott, R. H., and Thompson, M. C. Jr. , " Characteristics of a radio link in the 55 to 65 Ghz range. *IEEE Trans. Ant. Prop.*, vol. AP-24, 6, pp. 873-877.
66. Panter, *Communication Systems Design*, New York, McGraw-Hill, 1972.
67. Paul. j. , " Uncoded and Coded Performance of MFSK and DPSK in Nakagami Fading Channels," *IEEE Trans. Commun.*, vol. 40, pp.487-493, March. 1992.
68. Pierce, J. N. , "Error Probability of a Certain Spread Channel, " *IEEE Trans. Commun. syst.* , vol. CS - 12 , pp. 120 - 122, March. 1964.
69. Proakis, J. G. , *Digital Communications* . New York : McGraw Hill, 1983.
70. Ramadan, M., " Availability prediction of 8 PSK digital microwave system during multipath propagation, " *IEEE Trans. Comm.* , vol. CSM-27, 12, pp. 1862 - 1869, Dec. 1979.
71. Rice, S. O. , " Statistical properties of a sin wave plus random noise, " *Bell Syst. Tech. J.* , vol. 27 , pp.109-157, Jan. 1948.
72. Rooryck, M., "Validity of two-path model for calculating

quality of digital radio links; determination of model form measurements on analogue links," *Electron. Lett.*, vol. 15, 24, pp. 783-784, 1979.

73. Ryu, T. , " A stepped square 256 QAM for radio system," *IEEE International Conference on Communication*, 1986, pp. 1477-1481.
74. Rue, O., " Intermodulation distortion owing to multipath propagation over FM-FDM microwave links, " *Proc. IEE*, vol. 118, 12, pp. 1687-1690, Dec. 1971.
75. Rummeler, W. D., " A multipath channel model for line-of-sight digital radio systems," *IEEE International Conf. on Comm.*, vol. 3, Session 47, pp. 5.1-5.4, 1978.
76. Rummeler, W. D. , " Extensions of the multipath fading channel model," *IEEE International Conf. on Comm.*, vol. 2, Session 32, pp. 2.1-2.5, June, 1979.
77. Rummeler, W. D. , " A statistical model of multipath fading on a space diversity radio channel, " *BSTJ* , vol. 61, pp. 2185-2219, Nov. 1982.
78. Sasaki, O. , and Akiyama, T. , " Multipath delay characteristics on line-of-sight radio system. *IEEE Trans. Comm.*, vol. COM-27, 12, pp. 1876-1886, 1979.
79. Schiavone, J. A., " Prediction of positive refractivity gradient for line-of-sight microwave radio path," *BSTJ* vol. 60, 6, pp. 803-822, July-Aug. 1981.
80. Segal, B., " Spatial correlation of intense precipitation with reference to the design of terrestrial microwave radio-relay networks," *IEE Conf. Publ.No.219*, Apr.1983.
81. Smith, D. R. , and Cormack, J. J. , " Measurements and characterization of a multipath fading channel, " *IEEE International Conf. on Comm.*, Paper 7B.4, June, 1982.
82. Stein, S. "Fading channel issues in system engineering," *IEEE Select. Area. Commun.* , vol. SAC - 5, NO. 2 , pp. 68 - 89, Feb. 1987.
83. Turin, G. L. , " Communication through noisy, random - multipath channels, " *IRE Convention Record*, vol. 4 , pp.154-166, Mar. 1956.
84. White, R. , *Engineering Considerations For Microwave Communications Systems*, Get Lenkurt, 1970.